Ebubekir KESKİNKILIÇ

A Master's Thesis

AGU 2023

INVESTIGATION AND IMPROVEMENT OF THE SMOOTH MODE TRANSITION TECHNIQUE FOR QUASI-SINGLE-STAGE FOUR-SWITCH BUCK-BOOST INVERTER

A THESIS
SUBMITTED TO THE DEPARTMENT OF ELECTRICAL AND COMPUTER ENGINEERING
AND THE GRADUATE SCHOOL OF ENGINEERING AND SCIENCE
OF ABDULLAH GUL UNIVERSITY
IN PARTIAL FULFILLMENT OF THE REQUIREMENTS
FOR THE DEGREE OF
MASTER OF SCIENCE

By
Ebubekir KESKİNKILIÇ
August 2023

INVESTIGATION AND IMPROVEMENT OF THE SMOOTH MODE TRANSITION TECHNIQUE FOR QUASI-SINGLE-STAGE FOUR-SWITCH BUCK-BOOST INVERTER

A THESIS
SUBMITTED TO THE DEPARTMENT OF ELECTRICAL AND COMPUTER ENGINEERING
AND THE GRADUATE SCHOOL OF ENGINEERING AND SCIENCE OF ABDULLAH GUL UNIVERSITY
IN PARTIAL FULFILLMENT OF THE REQUIREMENTS
FOR THE DEGREE OF
MASTER OF SCIENCE

By
Ebubekir KESKİNKILIÇ
August 2023

SCIENTIFIC ETHICS COMPLIANCE

I hereby declare that all information in this document has been obtained in accordance with academic rules and ethical conduct. I also declare that, as required by these rules and conduct, I have fully cited and referenced all materials and results that are not original to this work.

Name-Surname: Ebubekir KESKİNKILIÇ
Signature :

REGULATORY COMPLIANCE

M.Sc. thesis titled “Investigation and improvement of the smooth mode transition technique for quasi-single-stage four-switch buck-boost inverter” has been prepared in accordance with the Thesis Writing Guidelines of the Abdullah Gül University, Graduate School of Engineering & Science.

Prepared By	Advisor
Ebubekir KESKİNKILIÇ	Asst. Prof. Dr. Burak TEKGÜN

Head of the Electrical and Computer Engineering Program

Assoc. Prof. Dr. Zafer AYDIN

ACCEPTANCE AND APPROVAL

M.Sc. thesis titled “Investigation and improvement of the smooth mode transition technique for quasi-single-stage four-switch buck-boost inverter**”** and prepared by Ebubekir KESKİNKILIÇ has been accepted by the jury in the Electrical and Computer Engineering Graduate Program at Abdullah Gül University, Graduate School of Engineering & Science.

16/08/2023

(Thesis Defense Exam Date)

JURY:

Advisor : Asst. Prof. Dr. Burak TEKGÜN ……..…….

Member : Prof. Dr. İrfan ALAN ……..…….

Member : Assoc. Prof. Dr. Ali Rıfat BOYNUEĞRİ ……..…….

APPROVAL:

The acceptance of this M.Sc. thesis has been approved by the decision of the Abdullah Gül University, Graduate School of Engineering & Science, Executive Board dated ….. /….. / …….. and numbered ……..……. .

…….. /…….. / ……..

(Date)

Graduate School Dean
Prof. Dr. İrfan ALAN

ABSTRACT

INVESTIGATION AND IMPROVEMENT OF THE SMOOTH MODE TRANSITION TECHNIQUE FOR QUASI-SINGLE-STAGE FOUR-SWITCH BUCK-BOOST INVERTER

Ebubekir KESKİNKILIÇ
M.Sc. in Electrical and Computer Engineering
Advisor: Asst. Prof. Dr. Burak TEKGÜN

August 2023

In recent decades, given the world's inevitable energy scarcity, increasing energy demand and green energy concerns, high efficiency energy conversion has become more important and attractive than ever, and researchers have directed their interest to energy-efficient converters. Inverters are a commonly utilized type of converter, which can be classified into two categories: single and two-stage inverters. Considering the inherent drawbacks of traditional inverters, a quasi-single-stage inverter (QSSI) has emerged. The QSSI uses a DC-DC converter to shape the rectified version of the desired AC waveform in the first stage and, in the second stage, it switches only once to alternate the polarity. It stands forward in terms of efficiency, control simplicity, and system stability. Among QSSI, a non-inverting buck-boost converter has drawn attention due to its capability to perform both step-up and down modes and its bidirectional power transfer feature.

In the first stage of the QSS non-inverting buck-boost converter; smooth transitions between the buck and boost modes and efficient conversion cannot be achieved by the traditional two-mode control method when the output voltage level is close to the input voltage level due to various limitations, non-idealities, and disturbances. Many methods have been applied and studied in the literature to minimize or eliminate the effects of the region which is called the “dead zone”. In this thesis study, further efficiency and THD improvement for the QSSI is targeted by employing a four-mode control method. The study incorporates a comparative study of the dead zone effects on inverter systems, which have not been previously documented in the literature. Moreover, it places a priority on optimizing efficiency and minimizing distortion in various applications—ranging from motor control and solar energy systems to grid-tied wind turbines and switched-mode power supplies—by comparing existing methods with open-loop voltage control. In conclusion, the theoretical results are verified with experimental studies.

Keywords: Non-inverting buck-boost converter, quasi-single-stage operation, dead zone elimination method, four-mode control, low THD inverter.

ÖZET
YARI-TEK-AŞAMALI DÖRT-ANAHTARLI ALÇALTICI-YÜKSELTİCİ EVİRİCİ İÇİN PÜRÜZSÜZ MOD GEÇİŞ TEKNİĞİNİN İNCELENMESİ VE GELİŞTİRİLMESİ

Ebubekir KESKİNKILIÇ
Elektrik ve Bilgisayar Mühendisliği Anabilim Dalı Yüksek Lisans
Tez Yöneticisi: Dr. Öğr. Üyesi Burak TEKGÜN

Ağustos 2023

Son yıllarda, dünyanın kaçınılmaz enerji kıtlığı, artan enerji talebi ve yeşil enerji kaygıları dikkate alındığında, yüksek verimli enerji dönüşümü her zamankinden daha önemli ve çekici hale geldi ve araştırmacılar ilgilerini enerji verimli dönüştürücülere yönelttiler. Eviriciler, enerji dönüşümünde yaygın olarak kullanılan bir dönüştürücü türüdür ve tek ve iki kademeli evirici olarak iki kategoriye ayrılabilir. Geleneksel eviricilerin doğasından gelen dezavantajları hesaba katılarak, yarı-tek aşamalı evirici (YTAE) ortaya çıkmıştır. YTAE, ilk aşamada doğrultulmuş AC dalgayı şekillendirmek için DC-DC dönüştürücü kullanır ve ikinci aşamada sadece bir kez anahtarlayarak polariteyi değiştirir. Verimlilik, kontrol basitliği ve sistem kararlılığı açısından öne çıkar. YTAE'ler içinde hem yükseltme hem de alçaltma modlarını gerçekleştirme yeteneği ve çift yönlü güç transfer özelliği nedeniyle, terslemeyen alçaltıcı-yükseltici dönüştürücü ilgi çekmektedir. YTA terslemeyen alçaltıcı-yükseltici dönüştürücünün ilk aşamasında, çıkış gerilim seviyesi giriş gerilim seviyesine yakın olduğu yerlerde, pals doluluk oranı sınırlamaları, ideal olmayan durumlar ve aktif ve pasif bileşenlerdeki çeşitli bozukluklardan kaynaklı geleneksel iki-mod kontrol yöntemiyle pürüzsüz geçiş ve verimli dönüşüm sağlanamaz. "Ölü bölge" olarak adlandırılan bu kısmın etkilerini en aza indirmek ya da ortadan kaldırmak için literatürde birçok yöntem uygulanmış ve incelenmiştir. Bu tez çalışmasında, YTAE için daha yüksek verimlilik ve düşük THD iyileştirmesi, dört-mod kontrol yöntemi kullanılarak hedeflenmektedir. Çalışma, daha önce literatürde belgelenmemiş olan evirici sistemlerindeki ölü bölge etkilerinin karşılaştırmalı bir çalışmasını içerir. Ayrıca, mevcut yöntemleri açık-çevrim gerilim kontrolü ile karşılaştırarak, motor kontrolünden güneş enerjisi sistemlerine, şebekeye bağlı rüzgâr türbinlerinden anahtarlamalı güç kaynaklarına kadar çeşitli uygulamalarda verimliliği optimize etmeyi ve bozulmayı en aza indirmeyi öncelikli bir konu olarak ele alır. Sonuç kısmında, deneysel çalışmalar ile ortaya koyulan teorik sonuçlar doğrulanır.

Anahtar kelimeler: Terslemeyen alçaltıcı-yükseltici dönüştürücü, yarı-tek-aşamalı çalışma, ölü bölge eleme metodu, dört modlu kontrol tekniği, düşük THD evirici.

Acknowledgments

I am deeply grateful to everyone for their invaluable assistance and unwavering support, which have greatly promoted my thesis's success.

I would like to sincerely express my thanks to my principal advisor, Asst. Prof. Dr. Burak TEKGÜN, for providing exceptional inspiration, encouragement, and guidance throughout my entire graduate studies at Abdullah Gül University. His guidance helps me explore and realize my potential in electrical engineering, especially in power electronics.

In addition to my principal advisor, I am thankful to the other members of my M.Sc. supervisory committee: Assoc. Prof. Dr. Ali Rıfat BOYNUEĞRİ who contributed significantly to my knowledge of electrical and electrical engineering concepts during my undergraduate studies and Prof. Dr. İrfan ALAN who has generously imparted his extensive experience to me, sharing valuable insights that will undoubtedly benefit both my research and career. Their suggestions and directions have been crucial to developing my thesis and success in my research and dissertation. My heartfelt thanks go to my coworkers at Abdullah Gül University for their precious assistance during my research assistantship with both their technical and psychological guidance in my career and to my friends who have always been like brothers to me, who stood by me in my difficult period and happiness.

I am grateful for the financial support provided by "TÜBİTAK 1001- The Scientific and Technological Research Projects Funding Program" for my M.Sc. thesis.

Lastly, nevertheless certainly not of the least importance, I would like to extend my profound appreciation and affection to my loving family members. My father and mother Ahmet and Ümmügülsüm played crucial roles throughout my twenty-seven-year journey, along with my beloved wife Nisa who always believed in me more than I did, and my brothers Ömer and Yusuf who provided me with unwavering support. Without the love and support of my family, I would not be the person I am today, and this work would not have been possible. I wholeheartedly dedicate this thesis to them.

"To the tomorrows

where we learn more than yesterday"

TABLE OF CONTENTS

LIST OF FIGURES

LIST OF TABLES

LIST OF ABBREVIATIONS

AC	Alternative Current
DC	Direct Current
VSI	Voltage Source Inverter
CSI	Current Source Inverter
MOSFET	Metal Oxide Semiconductor Field Effect Transistor
IGBT	Insulated Gate Bipolar Transistor
BJT	Bipolar Junction Transistor
PF	Power Factor
THD	Total Harmonic Distortion
QSS	Quasi-Single-Stage
QSSI	Quasi-Single-Stage Inverter
PWM	Pulse Width Modulation
CCM	Continuous Conduction Mode
DCM	Discontinuous Conduction Mode
FSBB	Four-Switch Buck-Boost
RMS	Root Mean Square
ESR	Equivalent Series Resistance
SiC	Silicon Carbide
EMI	Electromagnetic Interference
DSP	Digital Signal Processor
MCU	Microcontroller Unit
FFT	Fast Fourier Transform

To my loving family

Chapter 1

Introduction

The world's energy consumption increases every decade by around 50% from the previous one, and according to the IEA's 2020 report, approximately 70% of the total electricity consumption of around 25000 TWh is from fossil-based sources [1]. Over the past few years, there has been a rising demand for sustainable, non-polluting, and high-efficiency energy sources due to the increasing energy demand and the depletion of fossil fuels. Resources such as photovoltaic, wind energy, and geothermal energy, which are called renewable energy sources, have attracted the great attention of researchers. Some of these sources require additional converters to transform generated DC energy to AC-powered applications in uses like uninterruptible power supplies (UPS), active power filters, adjustable speed AC motor drives, and running AC devices from an electric vehicle's battery. In this regard, DC-AC type converters which are called inverters come to help: they can be used to transform a DC input voltage into an AC output voltage, higher or lower than the input, keeping the power constant with desired fixed or variable frequency output.

Essentially, there are various types of power inverters designed for different applications. They could be roughly categorized into numerous classifications based on the output AC voltage phase (single, three, etc.,) and the number of DC to AC conversion process stages (single, two, and multi-stage). From another viewpoint, they can be categorized as voltage-based (voltage source inverter, or VSI) or current-based (current source inverter, or CSI), or whether they are galvanically isolated or non-isolated.[2]. Each type in these categories can use controlled turn-on and turn-off devices (e.g., FETs, IGBTs, BJTs, etc.).

When selecting the appropriate inverter for a specific application, it is crucial to carefully examine the advantages and disadvantages of each category in accordance with the desired system outputs. For example, in motor drive applications, it is essential to

ensure that the phase number of the inverter matches that of the motor. Single-stage inverters are preferred for their simplicity and low cost, however, they suffer from output voltage ripple because of the difference between the constant DC input power and the instantaneous variable AC output power. On the other hand, while two-stage inverters can reduce output voltage ripple and improve dynamic response, their efficiency is lower, and the cost and system complexities are higher due to the need for energy processing twice [3,4]. Consequently, they may not be suitable for low-power applications. Since the isolated inverter has issues with isolation transformers, transformerless inverters have gained greater interest thanks to their potential for high performance, low loss, and compact size [5,6]. While the traditional CSI output voltage is always greater than the input, the traditional VSI output voltage is lower than the input. The VSI is more commonly preferred because of its straightforward design, bidirectional power flow capability, high power density, and adaptability to variable input-output conditions due to the inherently wide fluctuation of the renewable energy resource output voltage [7–9].

The bidirectionality of inverters is a significant feature that compensates for slow system dynamics effects in both fuel cell backup sources and grid-connected renewable energy applications while maintaining high-efficiency levels. However, although this feature is crucial when the system converts power back to DC power, some inverters can have problems such as control complexity and stability. Therefore, despite selecting an inverter while considering its drawbacks and superiorities, continuous improvements and developments in this field remain necessary, owing to the fact that no chosen inverter can be deemed an ideal power converter.

1.1 Motivation and Objectives

In many applications that utilize battery-powered systems or renewable energy sources, it is necessary to transform the electrical energy produced by one or more power electronic converters. DC-DC converters and inverters are extensively preferred types of converters to adapt the energy produced to satisfy the demands of the consumer with interfacing sources and loads. Buck-boost or step-up type converters within these power electronic converters are particularly chosen for systems, such as PV systems, wind generators, and multi-input systems [10–12], to perform functions such as voltage balancing between the load and source, bidirectional energy flow for energy storage devices or maximum power point tracking operation.

A voltage converter capable of both stepping up and stepping down the voltage is selected for use in these systems. Frequently preferred buck-boost converter topologies, such as the classical buck-boost, Ćuk, flyback, and SEPIC, are used when the input voltage varies widely and overlaps with the output voltage, or in cases there is constant input voltage, but the output needs to be adjusted within a desired range. However, these traditional converters have drawbacks such as extra inductor and capacitor requirements in Ćuk, flyback, and SEPIC, which may make the converter bulky and less efficient. Additionally, the output polarization is inverted in flyback, classical buck-boost, and Ćuk, requiring additional effort to obtain normal outputs. The non-inverting buck-boost converter has an advantage over other converters as it can achieve both step-up and step-down conversions with just a single inductor, capacitor, and four power switches. This reduces the count of additional passive components, circuit area, and conduction loss, resulting in more efficient buck-boost conversion with a smaller size and lower cost. Additionally, the converter produces an output voltage with the same polarization as the input voltage, and it can be controlled by two independent duty cycles. This implies that various values for both duty cycles may be utilized for the same operating point, making it a versatile and flexible option for power electronic conversion.

Although the non-inverting buck-boost converter has the aforementioned advantages and is more suitable for applications requiring high performance and adaptability, it also has inherent disadvantages. Since all four switches are activated and deactivated simultaneously in buck-boost operation within a single switching period, this can lead to high losses and result in low-efficiency operation. Thus, the buck-boost operation is not suitable when high-efficiency operation is required. Further to this, the non-inverting buck-boost converter faces a major challenge in terms of discontinuity that occurs during the operating mode transition between step-down and step-up. This is mainly due to the maximum and minimum constraints of the duty ratios, non-ideal situations that are unavoidable, and various disturbance effects that stem from switching signal and layout-based interferences. To put it in a different way, operating in step-down and step-up modes, especially at the point where the converter output voltage is close to the input voltage, the switch duty cycle cannot be quite close to one and zero, respectively. This situation causes discontinuity, resulting in the creation of subharmonics, output voltage ripple, poor regulation, and uncontrolled oscillation.

In systems where an AC output is desired from a DC input, the non-inverting buck-boost converter can be combined with an H-bridge inverter to achieve this. The H-bridge inverter features a simple structure that allows for power flow in both directions, enabling bidirectional operation of the entire system with a non-unity power factor (PF). However, owing to the association between the input and output voltage during inverter operation, a situation arises where the output and input voltages become equal twice within each half-period. Considering this situation, it is not practical to control this system solely through the buck-boost method for efficiency reasons, and the step-down and step-up operations cannot be directly applied to it on account of the discontinuity that arises. Therefore, in order to function efficiently and ensure a stable output voltage across the entire input voltage range, the converter must be carefully controlled. It is necessary to develop high-efficiency control techniques for this converter that address the stability problems caused by this discontinuity and utilize methods for avoiding it.

After presenting the reasons behind the work being undertaken, the summary of the research objectives is presented in the following manner:

- Investigate and identify the dead zone issue caused by the commonly used step-down and step-up which is referred to as the two-mode control method and develop an applicable model to simulate and examine the proposed buck-boost inverter’s electrical behavior. To verify the effects of a dead zone under a two-mode modulation scheme experimentally.
- The non-inverting buck-boost converter's discontinuity issue has been addressed through various modulation techniques. The single, modified-two, three, and four-mode control schemes are derived to avoid the discontinuity and compared with traditional two-mode modulation schemes.
- Previous studies have primarily focused on addressing the dead zone issue in DC systems, without devoting attention to investigating and enhancing DC-AC applications. Nonetheless, since the output AC signal is subjected to discontinuity every quarter cycle, it is more susceptible to performance degradation than DC systems. Therefore, this study focuses on inverter operation and investigates techniques for avoiding the discontinuity that diminishes the performance in the non-inverting buck-boost topologies.

- In current control-based systems, such as motor control, solar inverters, wind turbines, and switched power supplies, a reference current profile is generated based on the desired torque and speed, desired output power, turbine movement, and required output current. This reference current is then utilized to establish a reference voltage using appropriate control algorithms. This approach maintains efficiency while ensuring an accurate response to changes in the desired output value. The objective of this study is to design an open-loop voltage controller that can efficiently be used for current-controlled systems for generating reference voltages, with a focus on optimizing efficiency and minimizing distortion.
- In order to conduct an objective assessment of the efficiency of different modulation approaches, the fluctuation rate and mean value of the inductor current have been investigated. The four-mode modulation scheme showed outstanding performance compared to both traditional and derived methods. The aim is to identify and select a method that is the most efficient and least distorted among these methods for the inverter application.

1.2 Thesis Outline

The following is an outline of how the remaining content of this thesis will be structured.

In Chapter 2, various existing methods for avoiding the “dead zone” are introduced based on the specific application. The strengths and weaknesses of these methods are then described with respect to efficiency, control complexity, and figure of merit. Among these methods, the most suitable topology is selected for use in the adopted non-inverting buck-boost inverter.

In Chapter 3, the circuit analysis and operation principle of the buck-boost-based inverter topology are given in order to understand and design appropriately a control system for a converter. To comprehensively analyze the behavior of the inverter, the H-bridge part of the system which is responsible to convert DC to AC is also explained in-depth in addition to the non-inverting buck-boost topology analysis. The appropriate selection of inductor and capacitor is discussed, as well as the use of the converter with a conventional control structure. At the end of this section, the total loss calculation of

switches and other passive components for an inverter system is explained theoretically, together with an efficiency statement.

In Chapter 4, the origin of the dead zone, which occurs when the input and output voltages are quantitatively close to each other, is discussed along with various methods to eliminate it. Since the converter inherently allows for control in three different modes, various combinations that could provide proper outcomes and achieve the intended purpose are included in the comparison. In addition to getting rid of the dead zone, the study also involves an analysis of the inductor current performance, covering both its average and ripple value, to determine the outstanding performance among the modes.

In Chapter 5, the simulation and experimental results of all scrutinized modulation methods are presented. The five aforementioned schemes are implemented in computer simulations and hardware as examples to compare modulation schemes from the perspective of their functionality, losses, and total harmonic distortion (THD).

In conclusion, Chapter 6 summarizes the work presented, provides the conclusions drawn, and directions for future research are suggested.

Chapter 2

Literature Review

2.1 Introduction

The objective of this chapter is to conduct a thorough review of the existing literature that has been published on the dead zone avoiding technique. Current studies have revealed numerous solutions aimed at completely eliminating the dead zone problem for the non-inverting buck-boost DC-DC converter. These solutions range from the straightforward approach of directly injecting the buck-boost mode to the inclusion of four different control modes, as well as solutions involving hysteresis band control or adaptive control. Therefore, techniques for avoiding this discontinuity in the non-inverting buck-boost are investigated, and the method that is the most efficient and least distorted is chosen for the application.

2.2 Inverter Topologies for AC Signal Generation

The development of power electronics systems, driven by their fast-dynamic response, has led to the emergence of a two-stage buck-boost DC-AC inverter that is starting to draw the attention of researchers. The first stage typically includes a buck-boost or step-up converter, while the second stage includes an H-bridge inverter [13–15]. However, various disadvantages are beginning to emerge such as active and passive losses, reduced efficiency, increased cost, and system size as a result of complex control, two-stage power processing, and increased number of switches. Therefore, several single-stage buck-boost inverters have been developed to maximize efficiency and minimize size. In [16,17], the full bridge inverter as known as the H-bridge inverter is used with sinusoidal pulse width modulation (SPWM) to obtain AC sine output without any transformer usage. Since they are unity PF inverters, they only transform the power in one direction, furthermore, these types of inverters suffer from the common mode leakage current with poor utilization of the inductors caused significantly reducing the efficiency.

Flyback inverter which is an isolated VSI type inverter is used in [18], although it has completely solved the leakage current problem, the transfer function complicates the control due to the right half plane zero. Z-source inverter [19] is another single-stage type inverter, however, It is not a good option owing to the high input-to-output voltage ratio, as it only operates at unity power factor (PF) and requires more passive components. In [20], H6 and H8 single-stage full-bridge non-isolated inverters are proposed, but the need for more active switches and passive components decreases overall system efficiency.

Based on the shortcomings of the aforementioned inverters, a combination of a transformerless voltage source and step-up and step-down capability for the variable output voltage of the inverter is proposed [21]. This inverter comprises a buck-boost DC-DC converter that generates a rectified sine wave, coupled with an unfolding H-bridge inverter. In terms of the light load performance of the proposed converter, the THD of the output signal is not acceptable, and it lacks the ability to handle reactive power flow operation when the PF deviates from unity, despite the simplicity and clarity of this technique. Otherwise, the output capacitor cannot be discharged in order to regulate the voltage's negative rate of change. Unfortunately, this converter inherently has handicaps in terms of efficiency due to four active switches operating within one switching cycle. In fact, both ensuring efficient power conversion and constant output voltage across the full input voltage range is critical, and achieving this requires precise control of the converter throughout each cycle.

Strictly speaking, this inverter does not belong to either the single or two-stage inverter families, requiring it to be classified as a quasi-single-stage (QSS) type inverter. The QSS power converters have single-stage power processing qualification with a simple pulse width modulation (PWM) control, reliability, and high efficiency without the requirement of the DC-link low pass filter [22]. In [23], a similar structure was used, and the positive and negative output voltage generation was performed separately as in the previous work. Although filter inductors in the power loop have the advantage of minimum voltage drop at any time, it suffers from unsymmetrical output current when the DC input voltages are not equal.

The combination of a non-inverting topology with an unfolding H-bridge allows for bidirectional power flow and enables high-performance operation in non-unity power factor scenarios [24]. The DC-DC part of the inverter can be operated in step-down or step-up mode when the output voltage is lower or higher than the input voltage to generate

rectified sine wave transmission to the H-bridge. However, when operating in the step-down together with the step-up state, referred to as two-mode control in this thesis, proper operation and a smooth transition between states cannot be attained when the input voltage reaches the output voltage. In [25], the region between step-down and step-up modes was not examined in detail, despite the converter was worked in the three-mode control which is buck-boost mode injected among them. The sophisticated method proposed in [26] for low voltage unidirectional converter application. The discontinuity in the transition region caused by duty cycle limitations and its unacceptable increasing output voltage ripple is investigated in [27], as a further analysis, a control method is proposed at the expense of efficiency reduction [28]. This discontinuity called the "dead zone", is a major problem that arises from inevitable non-ideal situations and various disturbances in passive and active components, which cause poor regulation and instability near the equilibrium voltage level [29].

2.3 Dead Zone Mitigation Techniques

The non-inverting synchronous buck-boost inverter is capable of both stepping up and stepping down the output voltage, thanks to its transformerless voltage conversion feature. This makes it an appropriate candidate for implementations where the input of the converter tends to vary widely and overlaps with the output signal or where the input signal is considered constant, but the output signal needs to vary within a desired range. For instance, highly precise position control systems or variable voltage and frequency-controlled motor drive applications.

The converter steps-down the input voltage as a pure buck when the output voltage is adequately lower compared to the input and steps-up the input voltage as a pure boost when the output voltage is adequately higher compared to the input [30]. This control structure requires additional intervention in mode transition due to the mitigation requirement caused by the degradation of the dead zone. In [31], the converter is employed in only buck-boost operation to prevent transition issues. By utilizing this method, it is possible to remove the operational dead zone that causes interruption during mode transitions. This can prevent negative impacts such as subharmonics, higher output voltage ripple, and insufficient regulation. Nevertheless, the power conversion efficiency of this method is considerably decreased because it requires the continuous operation of four switches in the buck-boost mode. The control strategy used in [32] is called *"Dead*

Zone Avoidance and Minimization (DZAM)", which is based on a nonlinear state machine model. This strategy provides fast and accurate control of the converter while avoiding the drawbacks of the dead zone, such as subharmonics and higher output voltage ripple. However, implementing this technique in analog control systems can be challenging. Another approach for the two-mode control strategy is proposed in [33], the operational mode is determined by the correlation between the observed inductor current and the hysteresis band, rather than the correlation between the input and output voltage. The control strategy has advantages in power conversion due to its ability to use two conventional modes, however, it suffers from poor performance in terms of ripple during mode transitions, as well as the complexity of the control logic and compensation techniques required to achieve a smooth transition. In [34], a method called *"Interleaved Modulation with Duty Cycle Offset (IMDO)"* is described and compared it both synchronization and existing interleaved modulation techniques. The offered control technique involves assigning a phase differential duty cycle to the step-down and step-up switches. However, it suffers from average inductor current and ripple as compared with step-down and step-up states. In [35], a control technique for non-inverting buck-boost DC-DC converters is introduced that can operate within either step-down or step-up states. The converter's operating mode is established by an adaptive-window-based mode selector, which produces proper signals to drive the four power transistors correspondingly. However, this method is primarily applied at low power and has drawn attention due to its computational workload.

There are different solutions in the three-mode control category which includes buck-boost state among step-down and step-up during transition. The suggested method in [36], involves overlapping the step-down and step-up states and holding the duty cycle in both of these states utilizing a hysteresis band. This technique has different hysteresis bands for increasing and decreasing trends of voltage gain. In [37], a four-phase interleaved strategy is used to reduce output voltage ripple and give a smooth mode transition with a 90° phase difference. The method is prosed in [38] based on using both step-down and step-up operations throughout the transition and involves assigning specific duty ratios to each operation in order to ensure that the converter gain function remains continuous. This is achieved even though the duty ratio is constrained, giving the impression that it is not limited. In [39], control is implemented using model predictive mode detection without sensing input and output, rather than designing control loops and

modulators for each switching state separately. The controller in this paper addresses the control issue by framing it as a problem of regulating current with adjustable frequency, rather than voltage regulation. This control consists of inner model predictive current and outer voltage proportional-integral (PI) control. To make a general comment on three-mode-based techniques, the buck-boost mode used in this method causes lower efficiency compared to the other modes, although it eliminates the discontinuity in the transition region. Directly applying the three-mode control without any arrangement for the transition may not guarantee optimal control performance for each mode, especially during mode transitions between step-down, buck-boost, and step-up states. Moreover, the controller complexity increases with the number of operational modes, and some methods require more computational effort, leading to the system operating in discontinuous conduction mode (DCM).

When seeking a more efficient alternative to the three-mode approach, the four-mode technique, which includes additional modes during the transition, becomes a viable option. Two implementations of four mode modulation, which change the beginning of the switching period, expressed as the beginning, middle, and end of the switching period, are examined [40]. The four-mode technique used to eliminate the dead zone includes pure buck and boost, as well as extended buck and boost modes. This paper aims to investigate how the duty cycles of the active switches are related to the converter's power transfer ratio and why the dead zone problem exists in power converters, from a new standpoint. It covers different modulation techniques such as one, two, three, and four-mode modulation, and discusses the source of the dead zone problem in each of them. While the study explains the theoretical effects of the compared modes in detail, it does not provide any simulation or experimental verification. In [41] the four-mode control technique is preferred and the converter is modeled not only for control purposes but also from a different perspective, i.e., as a linear parameter variable. Since the small signal model has some shortcomings, it is modeled as a linear parameter variable rather than the small signal model. In addition to the design based on the linear parameter variable, the paper also proposes a control technique called *"Double-buck-clamping"* that achieves the same performance as the previously proposed extended control technique. The step-down/step-up clamping technique adopted in [42], is similar to the four-mode technique discussed earlier, and the purpose of this is to enable power conversion without any method for the dead zone throughout the conversion spectrum. However, the inherently

stable performance of buck-boost converters has not been taken into account. In [43], four-mode control is proposed by adding *"buck-boost buck"* and *"buck-boost boost"* states to conventional modes, to regulate the converter based on the input-output voltage ratio within a specific hysteresis band. The paper also introduces bootstrap sharing for high-side switches with a wide input voltage range, which enables the switch to remain conducting at all times during step-down and step-up states (for high-voltage applications using NMOS). In situations where the input and output voltages are nearly equal, two additional modes - BB Buck and BB Boost - are included to ensure efficient conversion. In these modes, the traditional switching pattern remains the same, but other fully on or off switches are kept open at 20% or 80% depending on the mode. However, the paper notes that there is a drawback as an unstable inductor current appears in step-up operation when the load current increases to 2A.

The literature contains several methods, apart from the ones mentioned here, that have been widely accepted. While numerous studies have concentrated on the methods for avoiding dead zones in buck-boost converters used in DC-DC applications, no research has been conducted for DC-AC applications that utilize the converter. However, since the output AC signal is exposed to discontinuity every quarter period, it is affected more than the DC system. Therefore, this paper aims to investigate and implement current methods from a new perspective.

2.4 Conclusions

The purpose of this chapter is to discuss well-known techniques to mitigate the discontinuity in the non-inverting buck-boost converter, arranged in order from the techniques requiring the least number of modes to those requiring the most. The chapter concludes by emphasizing the significance of implementing these techniques to enhance the performance of the converter when employed as an inverter.

Chapter 3

Topology and Operation Principle of Four-Switch Buck-Boost Inverter

3.1 Introduction

In order to comprehensively comprehend and properly design a control system for various types of converters, such as inverters, rectifiers, and others, it is necessary to thoroughly understand the converter's behavior across all its aspects. In this chapter, a detailed examination of the non-inverting buck-boost inverter, referred to as the four-switch buck-boost (FSBB) inverter in this thesis, is provided to comprehend its mode of operation. Although the proposed inverter places a few workloads on the H-bridge component, the DC-DC and DC-AC parts are also explained in-depth. In addition to describing the use of the converter with a conventional control structure, the selection of the proper inductor and capacitor is also mentioned at the end of the section.

3.2 Circuit Topology

The adopted inverter system comprises an FSBB DC-DC converter and an unfolding H-bridge inverter. This inverter can also be used as a part of a modular system to reduce the power stress and volume of the system. The modular converter system can be selected two and more separately controlled FSBB inverters which also have bidirectional power flow capability. Since other converters in modular systems have the same structure, an explanation is made over one module converter. Therefore, if this inverter is desired to use for a more phased system, the circuit can be performed modular which means the description hereafter is suitable for both single and modular use.

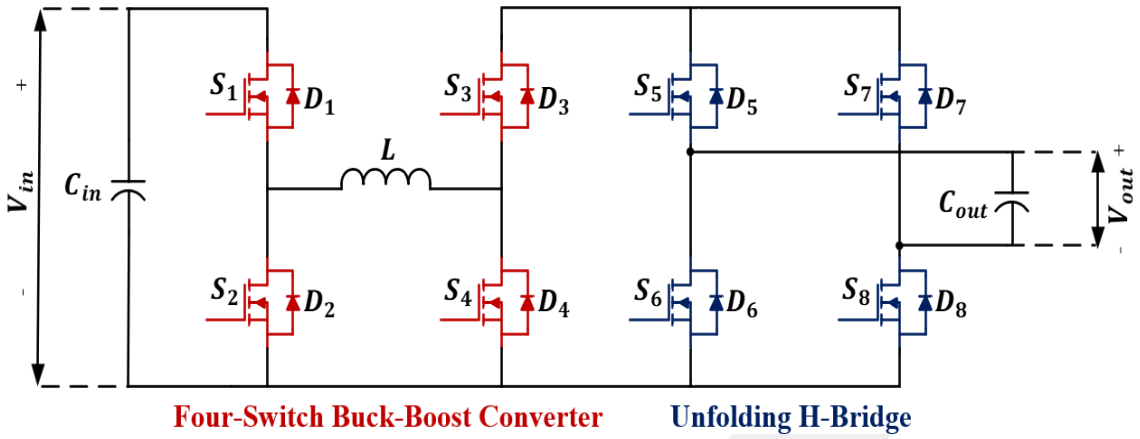

Figure 3.1 The four-switch buck-boost inverter

Fig. 3.1. shows an ideal FSBB inverter circuit. The FSBB inverter is a member of a quasi-single-stage converter which is able to provide step-down and step-up in power processing by means of one simple circuit structure. Although the circuit complexity and cost of the elements on the converter are higher compared to traditional step-down or step-up topologies, quasi-single-stage FSBB inverters are superior to single and two-stage converters in terms of lower input and output harmonics, less voltage stress on a single active element, as well as a wider output voltage and current range. FSBB inverter has inherent advantages such as allowing four-quadrant operation, higher efficiency, and fewer component requirements than other two-stage converters.

In Fig. 3.1, V_{in} and V_{out} are input and output voltages, respectively. The DC-DC part of the adopted inverter comprises four high-frequency switches, S_1~S_4 with four corresponding body diodes, D_1~D_4, to enable step-down and step-up functionality an inductor L is located from middle side of the circuit. One of the two filtering capacitors is at the input and the other is at the output. The switches are synchronously operated in one stage and antiparallel diodes are responsible for creating a current path when switches are turned off [44]. To generate the DC-AC conversion, the unfolding H-bridge converter is connected to the output of the FSBB and is responsible for generating a sine wave by changing the polarity. The unfolding H-bridge converter has four switches that are only switching at the doubled switching frequency and zero crossing of output voltage. Since the task of the H-bridge converter is only to flip the rectified sine output of the DC-DC section, the operation of the inverter and the passive component selection are detailed according to the FSBB DC-DC converter.

3.3 Operation Principle

3.3.1 Four-switch buck-boost DC-DC converter

The FSBB converter can be operated in three traditional modes: step-down (buck), step-up (boost), and buck-boost within a single stage, determined by the input-to-output voltage ratio. To simplify the circuit operation principle, left-side switches are called buck switches, and right-side switches are called boost switches as shown in Fig. 3.2. Both leg switches work with complementary conduction to prevent shoot-through.

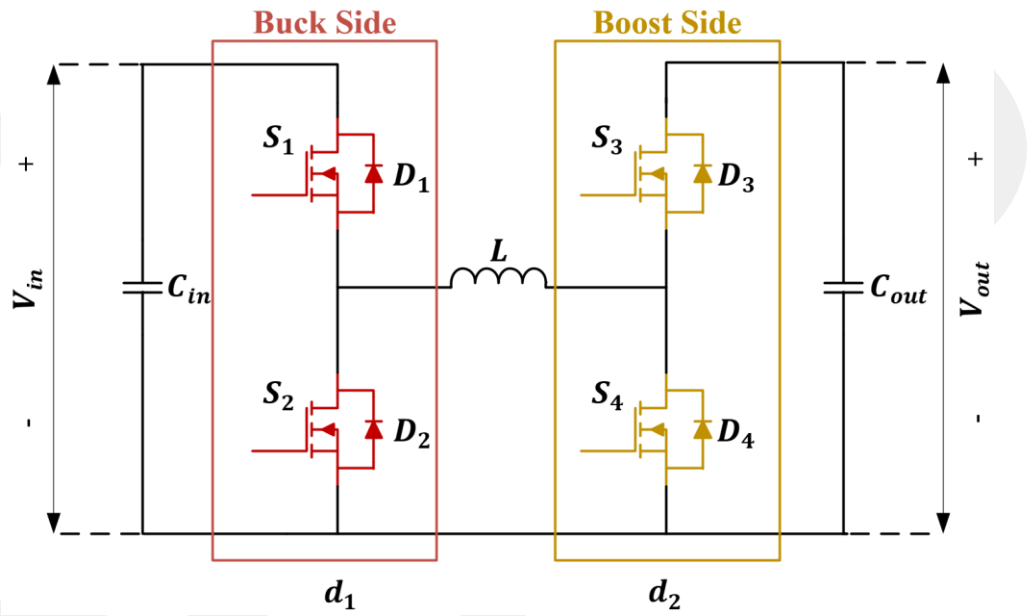

Figure 3.2 The circuit structure of the four-switch buck-boost converter

Considering the ideal case, where the parasitic resistance of the inductor, power switches, and power loss of the passive and active components are neglected, the converter gain is determined by the inductor's voltage-second balance concept. This principle establishes a relation between the input and output voltage, which is also equal to the duty ratio of the buck and boost switches. d_1 is defined as the duty cycle of S_1 switch, and d_2 is defined as the duty cycle of S_4 switch. The voltage gain of the FSBB, M is stated as

$$M = \frac{V_{out}}{V_{in}} = \frac{d_1}{1 - d_2} \tag{3.1}$$

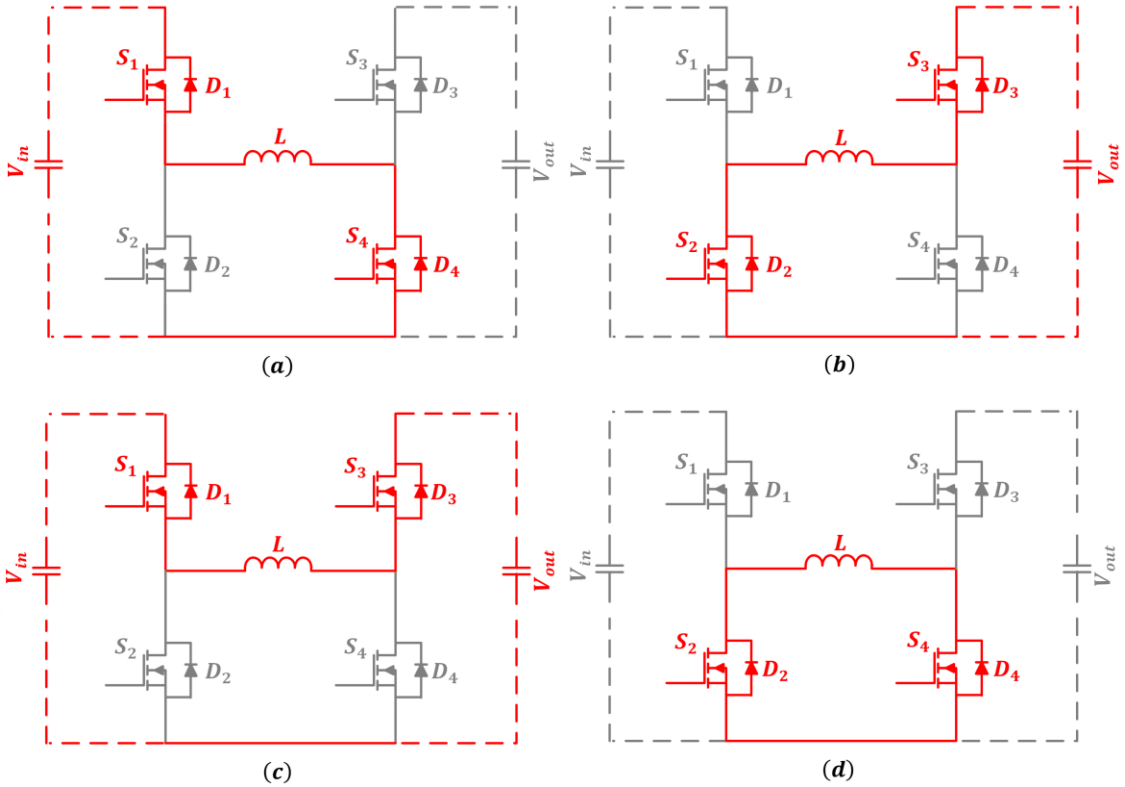

Figure 3.3 FSBB four typical switching modes. (a) Step-up switching, (b) Step-down switching, (c) Bypass, (d) Free-wheeling

The converter output voltage can be adjusted to a desired level relative to the input voltage by controlling the d_1 and d_2 which are duty cycle ratios of the buck and boost switches, which provide independent control over the voltage gain. Therefore, this indicates that the converter can provide two different opportunities to control the voltage gain. As indicated by equation (3.1), there are series combinations of d_1 and d_2 that can be utilized to accomplish the desired voltage gain. As a result, four general switching states plus the current path of the respective state are designated via the red line as depicted in Fig 3.3. Depending on the desired output voltage level and supplied input voltage, various combinations of operating patterns can be developed to improve the converter's performance or obtain a stable output.

The FSBB converter can be employed as the synchronous boost operation in case the output voltage is higher enough compared to the input and the boost operation scheme is performed as a combination of Fig. 3.3(a) and Fig. 3.3(c). Similarly, when the output voltage is lower enough compared to the input and the synchronous buck operation scheme is performed as a combination of Fig. 3.3(b) and Fig. 3.3(c). The FSBB converter can be employed in a buck-boost state depending on whether the output voltage is greater than or less than the input voltage. The switching scheme is performed as a combination

of Fig. 3.3(a) and Fig. 3.3(b). When the stored inductor energy is desired to reduce, in other words, when the converter is operated in a non-energy transferring mode, type switching is performed as in Fig. 3.3(d). Generally, the free-wheeling state is not used in the control of the FSBB converter except in buck-boost operation. The free-wheeling state will not be included in this work control principle. The traditional operation modes corresponding to Fig. 3.3. and their active switching states with a duty cycle in terms of continuous conduction mode (CCM) are listed in Table 3.1.

Table 3.1 Switching mode of the FSBB converter

Modes	S_1	S_2	S_3	S_4	Gain (V_{out}/V_{in})
Boost	ON	OFF	SWITCHING	SWITCHING	$\frac{1}{1-d_2}$
Buck	SWITCHING	SWITCHING	ON	OFF	d_1
Buck-Boost	SWITCHING	SWITCHING	SWITCHING	SWITCHING	$\frac{d_1}{1-d_2}$

3.3.2 Unfolding H-bridge converter

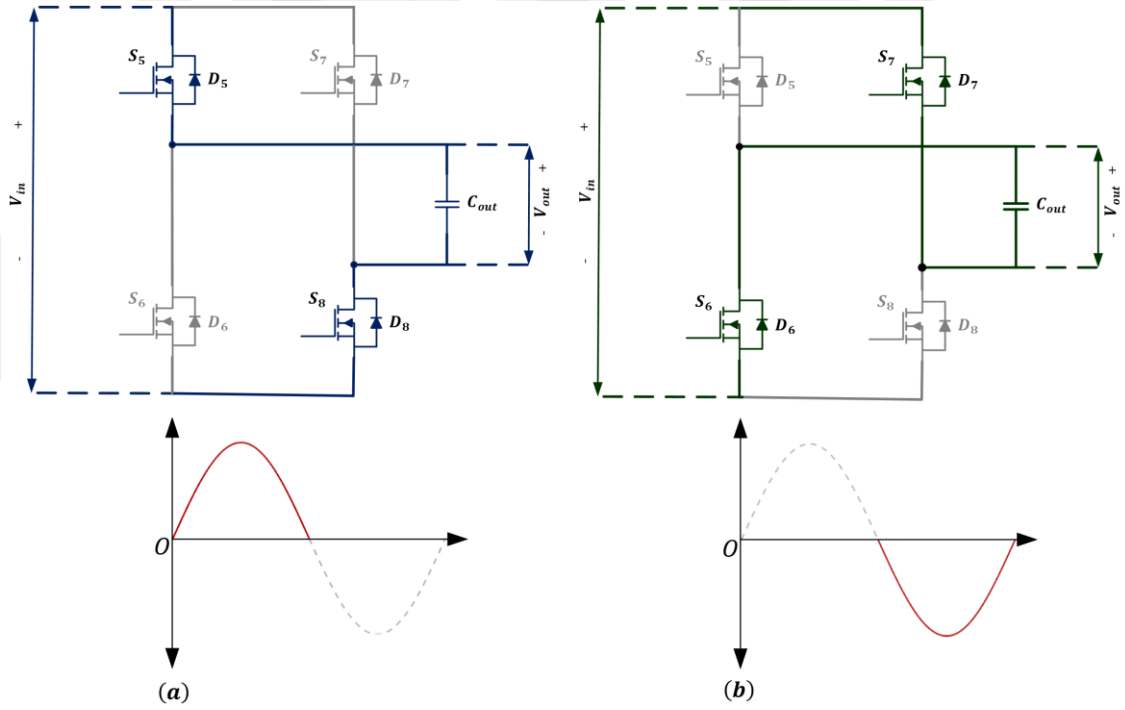

Figure 3.4 Unfolding H-Bridge switching scheme (a) Positive cycle (b) Negative cycle

The purpose of inverters, which are DC-AC converters, is to transform a DC input into an AC output with a preferred amplitude and either a fixed or variable frequency, as

their name implies [45]. Although the output voltage of ideal DC-AC converters should be sinusoidal, in reality, they are not pure sine shape and exhibit some harmonics. In the single-stage inverters or the second stage of the two-stage inverters, the output AC voltage is generally controlled by means of applying the PWM control signals to turn-on and turn-off devices such as MOSFET, IGBT, etc. This can also be referred to as adjusting the inverter's gain, which is stated as the AC output voltage to DC input voltage ratio. On the contrary, an unfolding H-bridge does not need to be switched with the PWM technique due to the way it is used.

The H-bridge inverter, also known as the full-bridge, is a member of the single-phase VSI, and this inverter consists of four choppers [46]. The H-bridge has the ability to rapidly switch the direction of the current applied to the load, usually a motor drive application. The switching scheme and waveforms of the input-to-output signals are depicted in Fig. 3.4. In this figure, the given circuits show the switching operation according to the current direction when the switching occurs, and the waveforms below it show the output form of the rectified sine input voltage according to the relevant switching period. When transistors S_5 and S_8 are turned on simultaneously, Fig. 3.4 (a) depicts that the input voltage appears across the output. If transistors S_6 and S_7 turn on simultaneously, the polarity of the output voltage is inverted as shown in Fig. 3.4 (b). Unlike single and two-stage inverters, the H-bridge switches with twice the output voltage frequency only at zero crossings of the rectified sine wave, rather than switching the entire period. Thus, the system gets rid of large switching losses and provides higher efficiency.

3.4 Inductor and Capacitor Selection

Selecting appropriate values for the shared inductor and capacitor is a key factor for stable converter operation and obtaining low distorted outputs. Each mode has different voltage and current stresses on the passive and active components. For this reason, both inductor and capacitor values must be identified for the specified operating modes and by the particular calculations of these modes. DC-DC converters regulate the output voltage by modulating the duty cycle, which denotes the portion of the switching period through which the switch remains closed. If the fundamental rules of the power electronics are applied to these three modes, the following formula holds for the inductor value in the steady-state operation:

$$L = \begin{cases} \left(\frac{V_{in} - V_{out}}{\Delta_{iL} f_s}\right) d_1, & step-down\ mode \\ \left(\frac{V_{in}}{\Delta_{iL} f_s}\right) d_2, & step-up\ mode \\ \left(\frac{V_{in}}{\Delta_{iL} f_s}\right) d_1, & buck-boost\ mode \end{cases} \quad \textbf{(3.2)}$$

where L is the inductor value, Δ_{iL} is the inductor current ripple, and f_s represents the switching frequency of respective switches. It should not be forgotten that d_2 has the same duty ratio as $d_1$when the converter is operated in buck-boost mode. Thus, the inductor value can be written in terms of both input and output voltage. Similarly, the following formula holds for the output capacitor value for all the above operation:

$$C_{out} = \begin{cases} \frac{1 - d_1}{8L(\Delta V_{out}/V_{out}){f_s}^2}, & step-down\ mode \\ \frac{I_{out} d_2}{\Delta V_{out} f_s}, & step-up\ mode \\ \frac{I_{out} d_1}{\Delta V_{out} f_s}, & buck-boost\ mode \end{cases} \quad \textbf{(3.3)}$$

where C_{out} is the output capacitor value, ΔV_{out} and I_{out} represent the voltage ripple and current value of the converter, respectively. In accordance with the design criteria, the worst-case scenario should be considered in the selection of both the inductor and the output capacitor, in an effort to optimize the system design for reliability and cost-effectiveness.

If the values of the inductor and capacitor are determined using equations (3.2) and (3.3) for a 2-kW peak power level converter that produces a grid output voltage in the range of 0 to a maximum of 325 V, the resulting performance can be demonstrated as shown in Fig. 3.5. The graphs in Fig 3.5 assume a 100% current ripple for the buck, boost, and buck-boost operation using switches at 100 kHz. It should be noted that when designing an FSBB converter, the selection of the inductor and capacitor is based on the maximum or minimum input voltage conditions for each mode [47]. The appropriate passive element should be selected according to the active operating range of the modes.

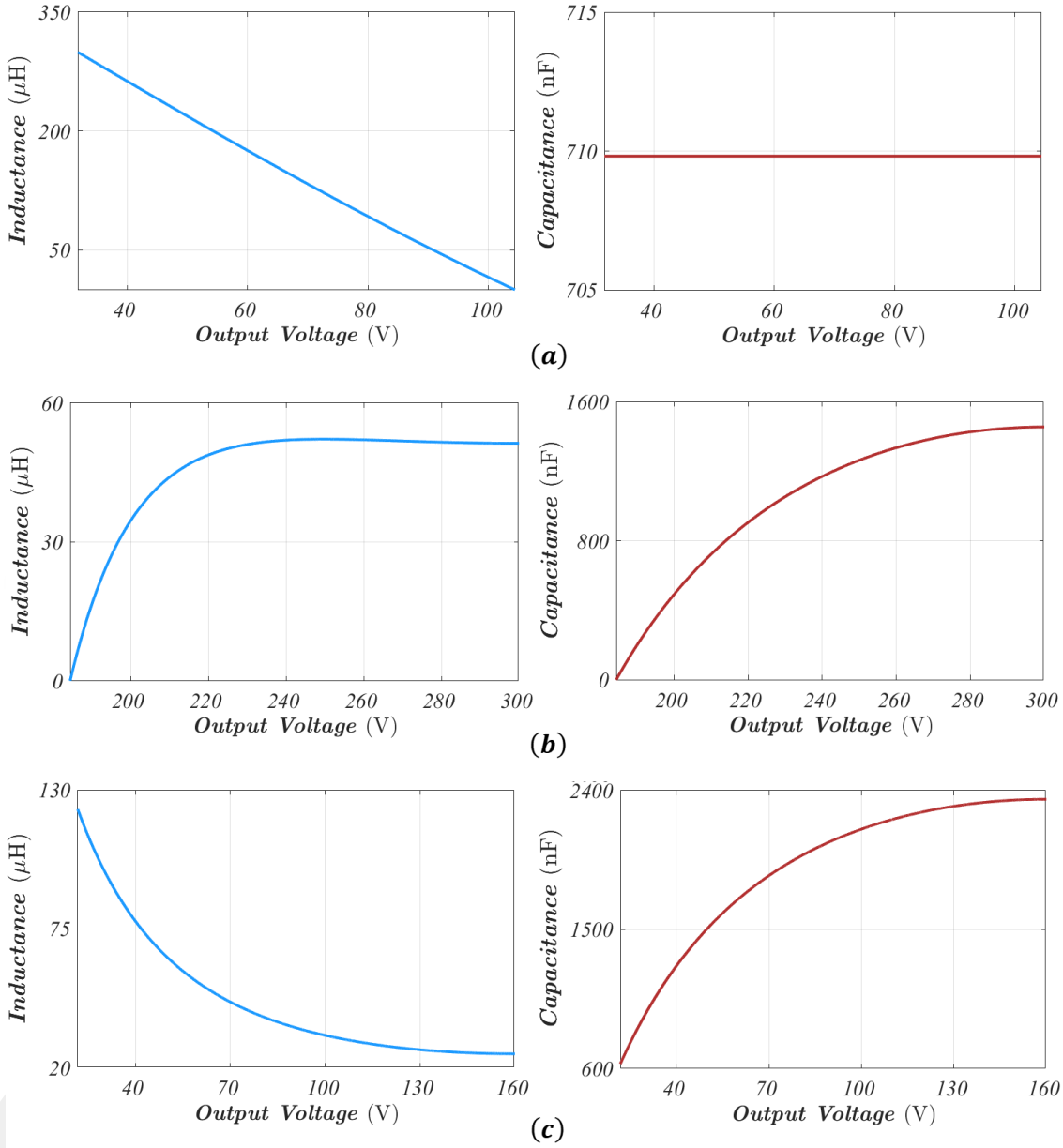

Figure 3.5 Variation of the inductor and capacitor values according to voltage value (a) Step-down (b) Step-up (c) Buck-boost

3.5 Losses

In power electronics applications, losses introduced by passive and active components or semiconductors must be separately considered when calculating efficiency. Passive component losses are derived from the non-ideal approach of modeling the inductor and capacitor with a series resistor. The resistance resulting from the internal losses of a capacitor is known as the equivalent series resistance (ESR), which can be calculated by squaring the current passing through the capacitor and multiplying it by the ESR value of the capacitor.

Semiconductor-based losses can consist of diode and switch losses, depending on the circuit used. These are also divided into conduction and switching losses and analyzed separately. The diodes switching losses occur during the turn-off process, technically called the reverse recovery loss. Since a bidirectional power flow system is proposed in the circuit to be used, diodes are included as body diodes of MOSFETs, and analyses are continued accordingly. To calculate the conduction loss of the body diode, also called the anti-parallel diode, the voltage drop across the diode is as follows [48]

$$U_D = u_{D0} + R_D i_F \tag{3.4}$$

where R_D is internal resistance of the diode and u_{D0} is forward voltage drop. Likewise, the conduction loss on the body diode can be expressed as

$$P_{CD} = u_{D0} i_{Fav} + R_D {i_{Frms}}^2 \tag{3.5}$$

where i_{Fav} is the average diode current and i_{Frms} is the RMS diode current. Diodes' reverse recovery loss, P_{RRD}, is a function of the forward current and higher forward current leads a higher reverse recovery current, i_{RR}, and longer recovering time, t_{RR}. The reverse recovery energy, denoted by the symbol E_{RR}, is obtained by integrally multiplying the reverse recovery current by the diode voltage over the recovery duration.

$$E_{RR} = \int_0^{t_{RR}} i_{RR} V_D dt \tag{3.6}$$

$$P_{RRD} = E_{RR} f_{sw} \tag{3.7}$$

Hence, the total loss on the body diode can be expressed as

$$P_D = P_{CD} + P_{RRD} \tag{3.8}$$

Since the switching time of MOSFETs is limited, there are losses associated with the voltages and currents that the switches need to manage while turning on or off [49]. The increasing time, falling time, switch on/off energy levels, and other information are found in datasheet. Consequently, it is simple to calculate a MOSFET's switching loss by

$$P_{sw} = E_{total} f_{sw} \tag{3.9}$$

where E_{total} is the total switching energy and f_{sw} is the switching frequency. The two main factors that affect switching speed and energy are total gate charge, Q_g, and the on-time resistance of a MOSFET switch, $R_{DS(ON)}$. While the high $R_{DS(ON)}$ causes a high

voltage drop on the switch and, consequently, a high conduction loss, the large Q_g results in slow switching speed and high switching loss. The voltage drop in the semiconductor is stated as follows

$$U_{DS} = R_{DS(ON)} i_D \tag{3.10}$$

where i_D is drain current. The datasheet contains the information necessary to understand how temperature and drain current affect $R_{DS(ON)}$. The following formula is used to determine the MOSFETs average conduction loss

$$P_c = \frac{1}{T_{sw}} \int_0^{T_{sw}} P_c dt = R_{DS(ON)} {i_D}^2{}_{rms} \tag{3.11}$$

Hence, the total power losses of a MOSFET, P_M, and total losses of system, P_{loss}, can be calculated as

$$P_M = P_{sw} + P_c \tag{3.12}$$

$$P_{loss} = P_M + P_D + P_R \tag{3.13}$$

where P_R is the loss caused by passive components. To calculate the efficiency of the system, both the losses caused by passive and active components and the output power are added together, and the ratio of output power to total power losses is determined.

$$\eta = \frac{P_{out}}{P_{out} + P_{loss}} \tag{3.14}$$

3.6 Conclusions

The FSBB inverter, which includes a four-switch buck-boost converter along with an unfolding H-bridge inverter, is discussed in this chapter. The inverter's ability to step-up or step-down voltage and facilitate bidirectional power flow is analyzed. The FSBB converter has the capability of operating with the three traditional modes, which are buck, boost, and buck-boost, separately or in different combinations of these states. In situations where the output voltage is lower than the input, the FSBB converter can be operated in a buck or buck-boost configuration. Similarly, when the output voltage is higher than the input, it can be operated in a boost or buck-boost configuration. The H-bridge stage is responsible for reversing the output polarity of the DC-DC stage at zero-crossing. The procedure for selecting the inductor and capacitor in the FSBB is also described.

Chapter 4

Investigation and Comparison of Mode Transition Techniques

4.1 Introduction

In order to generate a pure sine voltage from DC voltage, inverter systems must be built. Typically, a full-bridge inverter and a boost converter to step-up output voltage are used for battery-powered systems that need a voltage boost. A large inductor in the boost converter and bulky DC bus capacitors directly before three or more switch inverters are included in such a system, which increases the cost and size of the converter [50]. Instead of using two-stage inverters that increase the cost or single-stage inverters that reduce the efficiency, quasi-single-stage inverters are proposed to meet increasing demands while avoiding unavoidable efficiency and cost issues. The FSBB inverter is superior in terms of efficiency and ease of control because the DC-DC part of it switches to produce only rectified sine wave in one period with both its step-up and step-down feature, while the H-bridge part switches this rectified sine at zero crossings. The cycle of generation of 50 Hz one period sine wave by the QSS FSBB inverter using the two-mode control adding the dead zone elimination method is shown in Fig. 4.1. In this graph, the waveforms on the left represents the signals produced or converted by the source or converter on the right of the graph.

It can be clearly shown that the constant pure DC input voltage in Fig. 4.1(a) is converted to rectified sine signal by the FSBB converter. To produce rectified sine wave, initially, the input voltage is stepped down until the output voltage is close to the input as depicted in Fig. 4.1(b) with the black portion of the rectified sine. Thereafter, in the green region, which is the main focus of this paper, the converter transmits the voltage to the step-up part. If the step-up part is performed up to the peak of rectified sine and it is considered as final value, this triplet of buck, transition, boost scheme happens twice and

the reverse of this scheme happens twice to get a period sine wave. Therefore, suitable and stable control structure must be designed for this inverter. However, no further improvement is possible as the H-bridge part of the inverter is switched at zero crossing which means it offers low switching losses due to output grid frequency switching. This H-bridge converter completes its task by only changing the polarity of its input as shown in Fig. 4.1(c). For this reason, it is focused on obtaining higher efficiency and lower THD from the DC-DC part of the inverter.

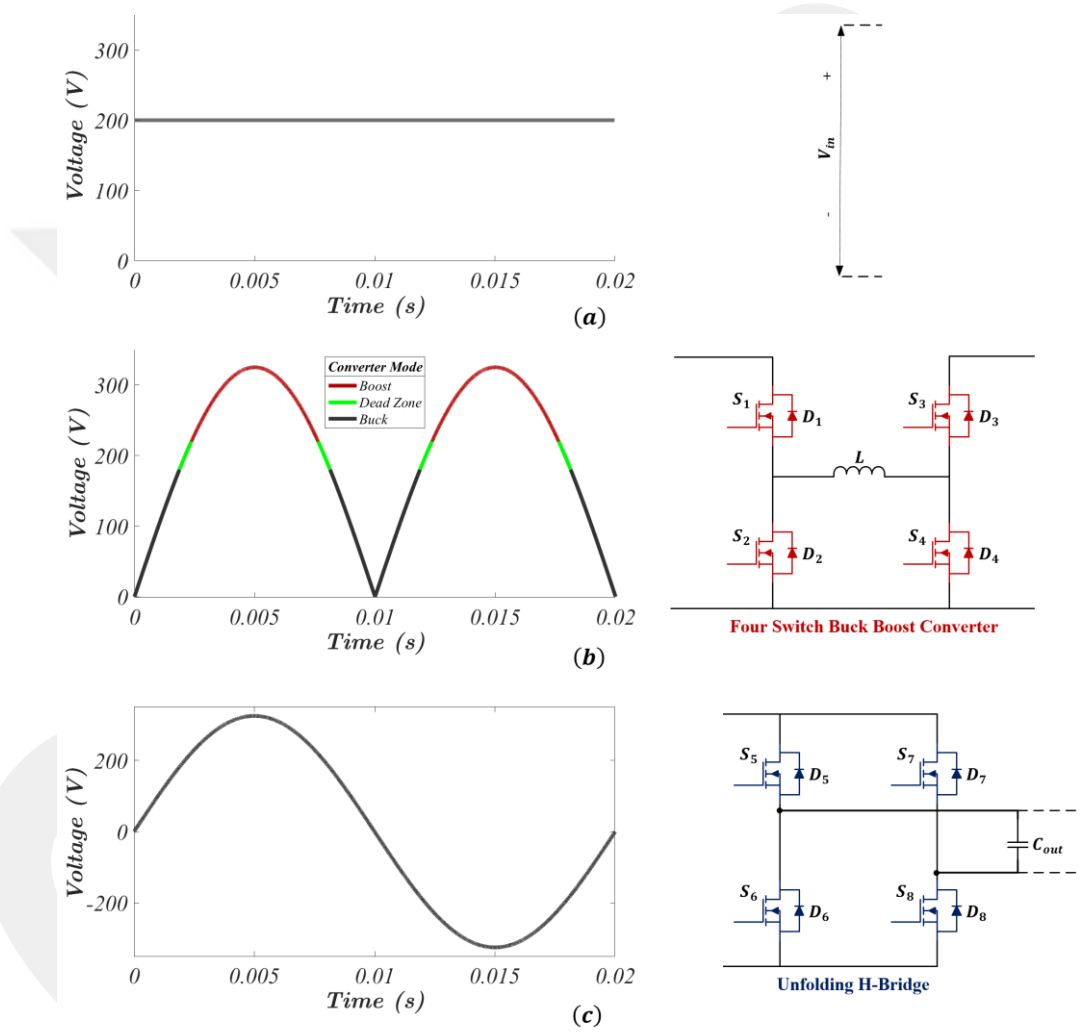

Figure 4.1 Generation of a sine wave by the FSBB inverter system (a) Input signal (b) Rectified sine wave (c) Output signal

Since the FSBB converter can be inherently controlled in three different modes, in order to obtain a desired output with the characteristics, the most appropriate control system should be established by analyzing the modes. The FSBB converter can utilize these modes individually or in combination, depending on the requirements for efficiency and stability. It can be controlled using various techniques. Although some techniques do

not inherently have a transition discontinuity at the input and output voltage equilibrium point than others, efficiency issues can arise due to large inductor current and switching more transistors in a period. In this chapter, the dead zone origin and the different modulation to reduce the impact of the dead zone, in addition to the average current value and current ripple of the inductor according to these modes are examined in detail.

4.2 Origin of the Dead Zone

In the four-switch buck-boost topology, the respective switches' duty cycle must be arranged depending on the performing operation mode of the converter. As shortly pointed out in the prior chapter, there will not be seen any time delay and gap between the transition to the buck/boost to boost/buck mode variation under presuming ideal conditions which are the exception of the inevitable non-idealities, unpredictable switching noises, disturbance of passive and active components and circuit layout. However, considering the actual situation, the mode transitions are not as smooth and continuous as assumed. Switching between buck and boost states in practical situations can result in uncontrollability, even due to the discontinuity caused by gating circuits and switches' switching time delay [51]. Fig. 4.2 shows the comparison of voltage gain and duty cycle value for the ideal and actual case when the converter is employed as buck and boost operation, respectively.

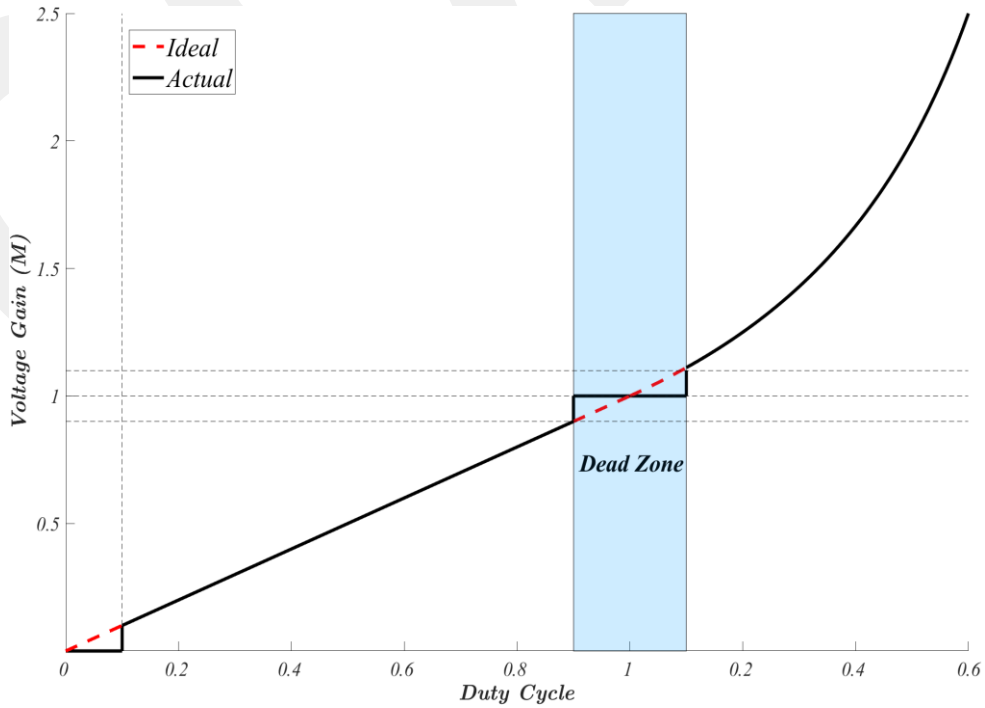

Figure 4.2 Comparison of the ideal and the real case by duty cycle vs voltage gain

In the two-mode modulation method, buck to boost or vice versa, the converter is operated in the corresponding mode until the input voltage and output voltage converge, then the mode is changed to another mode. It is important to note that, as already mentioned, the FSBB converter is capable of bidirectional power transfer. In this figure, the dashed red line represents the ideal situation and overlaps with the actual curve shown in black except for some limiting levels. In the actual situation, the maximum and minimum constraints for the switches' duty ratio are considered and create the points where it diverges from the other curve. It can be seen that the required time delay of switches in the mode transition causes the discontinuity of the actual case curve which may result in a larger output voltage ripple at the duty ratio around 0-10% and 90-100%.

Equation (3.1) can be redefined so that the comparison of the two case differences can be understood more clearly. Let us define a new parameter called δ, which represents the slope of a straight line that describes the operational connection in which buck and boost duty ratios need to be satisfied for the output and input relation.

$$\delta = \frac{1}{M} = \frac{1 - d_2}{d_1} \tag{4.1}$$

It can be seen from formula (4.1) that all values for the slope δ are created by independently varying duty ratios of buck and boost. If the d_1 and d_2 relationship is wanted to be shown graphically, d_1 becomes the abscissa and $1-d_2$ becomes the ordinate. A schematic representation of the two-mode control technique is shown in Fig. 4.3 for both ideal and actual scenarios, respectively. The slope of the dashed red line in Fig. 4.3(a) is 1, at which point the voltage gain is also 1. All possible operation points for both duty ratios are shown within the square, with a dashed line dividing the square into two regions: the orange region represents the buck operation, and the blue region represents the boost operation. When the converter is employed as either the buck or boost operation, $1-d_2$ or d_1 is set at 1, respectively. This approach is referred to as traditional two-mode control, with the objective of achieving higher power conversion efficiency by enabling the converter to operate in each of the two modes separately [37]. When in the boost operation, the slope δ increases from 0 up to 1, while the output voltage is adjusted by controlling d_2. Conversely, for the buck operation, the dashed red diagonal is greater

than 1, and the voltage gain M decreases from 1 while the output voltage is adjusted by controlling d_1.

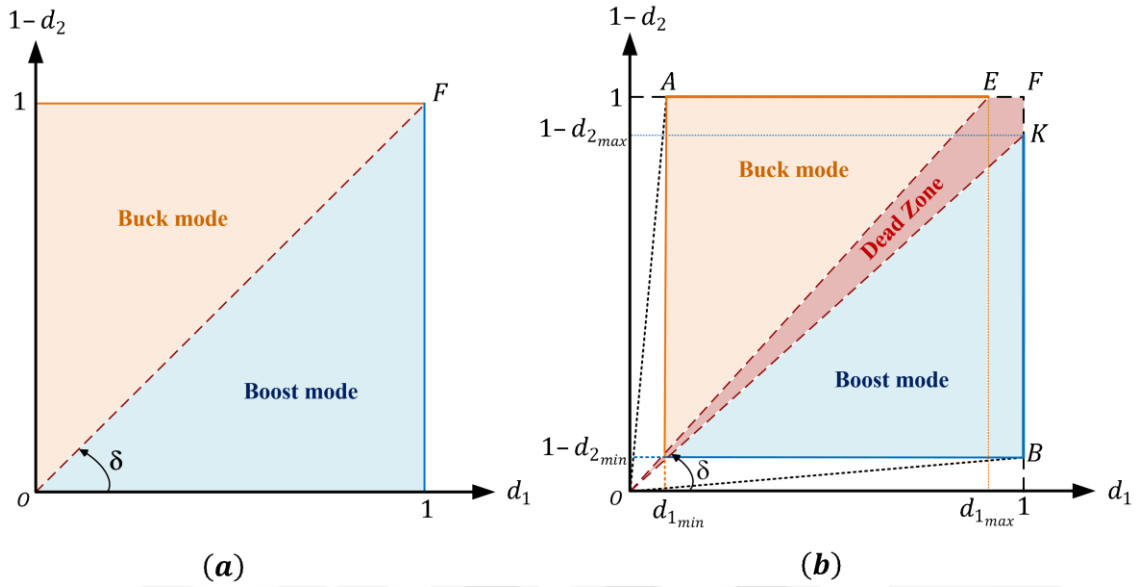

Figure 4.3 Two-mode operation scheme (a) Ideal operation (b) Actual operation

In the ideal case, it can be seen that the converter is employed as in a buck and boost voltage range from zero to voltage equality level with seamless transfer between mode transition. However, in the case of real power design applications, there are some hidden drawbacks inherent in it. This is because there will always be considered maximum and minimum switchable regions of the buck and boost switches due to the aforementioned non-ideal conditions. This means that Fig. 4.3(a) should be replaced with Fig. 4.3 (b) to present a realistic design and to consider all the unavoidable conditions that may be encountered. As can be seen in the differences between the two figures, it is understood that not all combinations given in ideal conditions are valid due to the dead zone region. Owing to the dead zone presence, in addition to buck and boost operations shown in the ideal operation scenario, more or different operating zones may be needed in the actual circuit to eliminate the wigwag between mode transitions. The range of values that duty cycles d_1 and d_2 can take according to switchable values can be expressed as

$$\begin{cases} d_{1_{min}} \le d_1 \le d_{1_{max}} \\ 1-d_{2_{max}} \le 1-d_2 \le 1-d_{2_{min}} \end{cases} \quad \textbf{(4.2)}$$

where $d_{1_{min}}$, $d_{1_{max}}$, $d_{2_{min}}$ and $d_{2_{max}}$ represent the values at which the duty cycle has an upper and lower limit in both the buck and boost operation, respectively. The actual operating scheme is depicted in Fig. 4.3(b), where the buck mode is enclosed by an orange

AOE region, the boost mode within the blue KOB triangle, and the dead zone area between the two modes are within the red OEFK irregular rectangle. The values within the unshaded area between the y-axis and the OA line and between the x-axis and the OB line can be effortlessly prevented and ignored by optimizing the converter specifications. However, the values between the OK and OE are crucial for the operation, as it needs to reach the voltage gain in cases where the output voltage is close to the input [40]. Put another way, under the traditional control, when the buck operation duty cycle is $d_1 > d_{1_{max}}$, and similarly when the boost operation duty cycle is $1-d_2 < 1-d_{2_{min}}$, discontinuity occurs in the active operating area of the converter.

4.3 Dead Zone Elimination Methods

The objective of the following parts is to introduce and examine a number of widely used and straightforward approaches for avoiding dead zones, to establish a strong basis for selecting the best strategy in this thesis. These methods have their superiority and inferiority in terms of switching and active power losses and control circuit complexity and are evaluated with these criteria in mind. The various methods for avoiding dead zones in this thesis are evaluated based on their effectiveness in reducing voltage ripple, level of control complexity, and efficiency. For the sake of fairness, the calculation takes into consideration exclusively the losses associated with hard-switching when comparing the system efficiency, while other losses can be considered equal.

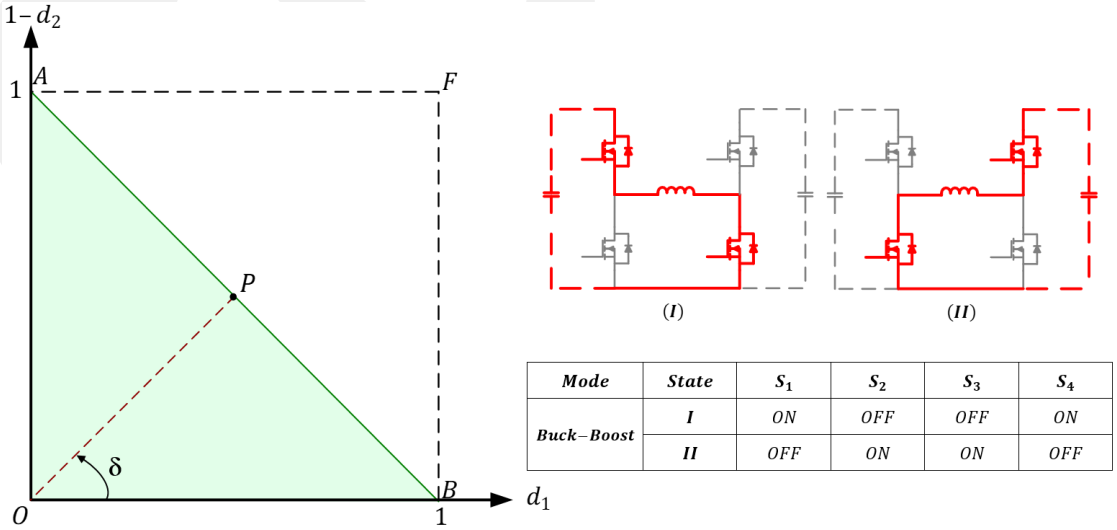

Mode	State	S_1	S_2	S_3	S_4
Buck–Boost	I	ON	OFF	OFF	ON
	II	OFF	ON	ON	OFF

Figure 4.4 Single-mode operation scheme

4.3.1 Single-mode modulation

The first and simplest approach to avoid the dead zone during operation is to use a full buck-boost operation. This approach is referred to as "single-mode modulation" in this thesis, it means that the FSBB converter is operated using one mode to provide the entire voltage conversion ratio while actively using four switches in one period. The duty cycles of both the buck stage, d_1, and the boost stage, d_2, are controlled by a single control signal, which eliminates the need for separate control. This means that both pairs of diagonally located switches, namely S_1, S_4 and S_2 , S_3, are switched ON and OFF simultaneously. Since the switch pairs are given the same duty cycle, the operating area of the voltage gain transforms into the AOB triangle as shown in Fig. 4.4. The slope δ can adjusts to any value between zero and infinity and the desired voltage can be achieved by placing the operating point P on any location of the AB line within the green triangle. The voltage gain formula for the single-mode modulation can be stated as

$$M = \frac{1}{\delta} = \frac{d}{1-d} \tag{4.3}$$

where d represents the common duty cycle signal for switch pairs. It should be noted that the voltage gain is identical to the absolute value traditional buck-boost converter. This mode provides continuous voltage conversion entire voltage range and the common duty cycle D has value in the range [0,1]. Eliminating the dead zone and the gap at the transition means that any additional variations in the voltage fluctuation that may occur when the input-output voltage equality level is also eliminated. Nonetheless, this modulation method has been studied in [52], the converter achieves a maximum efficiency of 72% for low voltage, and as the output voltage increases, the power conversion efficiency decreases inversely. Since four switches are actively switched in a period, raising the switching frequency results in increased switching loss for this mode which will naturally make the efficiency of the converter lower.

4.3.2 Modified two-mode modulation

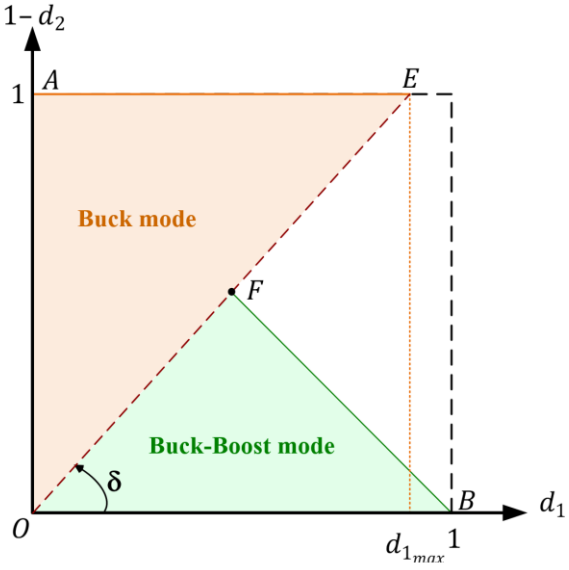

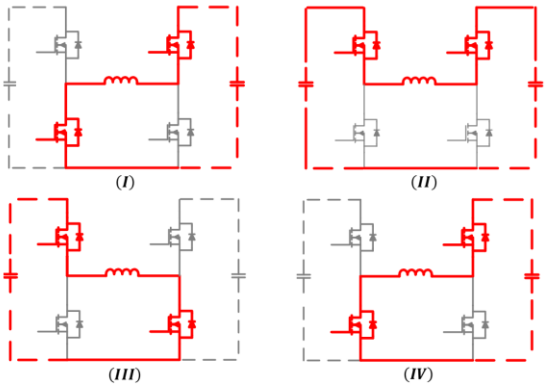

Mode	State	S_1	S_2	S_3	S_4
Buck	I	OFF	ON	ON	OFF
	II	ON	OFF	ON	OFF
Buck−Boost	III	ON	OFF	OFF	ON
	IV	OFF	ON	ON	OFF

Figure 4.5 Modified two-mode operation scheme

The second method to eliminate the dead zone combines the following two states: the buck state which is better in terms of stability and efficiency, and the buck-boost state which eliminates discontinuity [53]. Since the converter functions in both buck and buck-boost operation under this modulation scheme and differs from the traditional two-mode modulation, this approach is referred to as "modified two-mode modulation" in this thesis. In comparison to the single-mode, this modulation performs the buck-boost state after the maximum value of the buck state duty cycle which is almost half of the period instead of the entire voltage conversion range. The buck state is preferred over the buck-boost state as it utilizes only half of the active switches used in a conversion period, resulting in lower switching losses. The range of values for this modulation that duty cycles d_1 and d_2 can take according to switchable values can be stated as

$$\begin{cases} 0 \le d_1 \le d_{1_{max}} \\ \dfrac{d_{1_{max}}}{2} \le \dfrac{d}{1-d} \le 1 \end{cases} \tag{4.4}$$

where d represent the common duty cycle signal for buck-boost operation and $\frac{d_{1_{max}}}{2}$ is found by the relationship between a buck to a buck-boost state transition. For instance, after the buck state is performed up to 90% of the input voltage value to prevent the unavoidable limitation, the buck-boost state takeovers the converter control from that level. Thus, the buck-boost state initial duty cycle should be started around 0.45 to get desired higher output voltage. In this technique, the converter is employed as the buck

operation in cases where the output voltage is adequately lower compared to the input voltage. As the output voltage reaches a value close to the input voltage and needs to be increased, the converter switches to the buck-boost operation as evident from the Fig. 4.5. The buck state operational region is enclosed by an orange AOE triangle, and the buck-boost region by a green FOB triangle.

The improvement of extremely low efficiency is the key benefit of the proposed approach over the single-mode modulation approach. In this scenario, there is no way to restrict the development of extra switching losses outside of the buck operating mode. The remaining discontinuity shown in [36] is another issue; it is the cause of subharmonics and other control-related problems.

4.3.3 Three-mode modulation

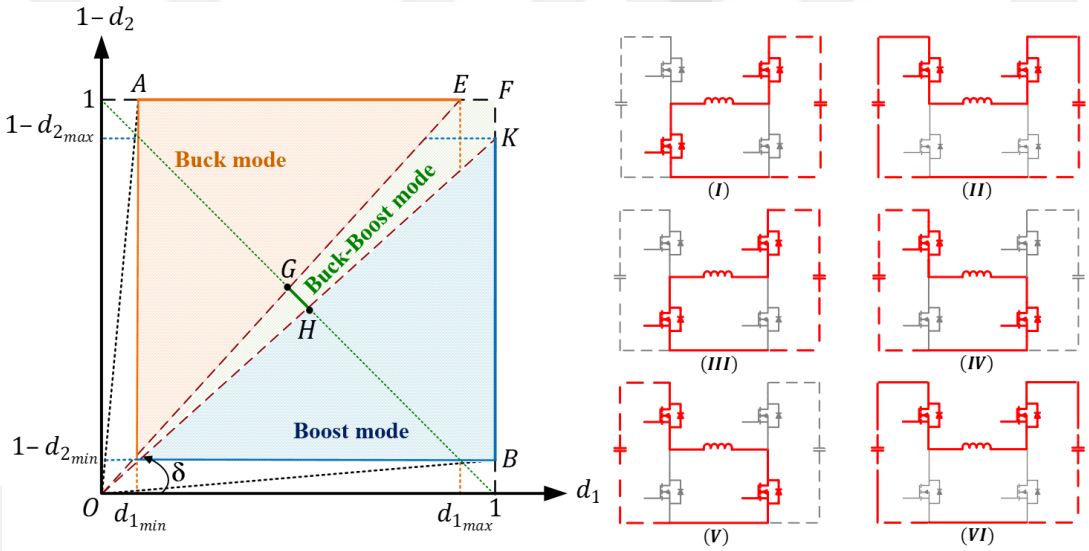

Mode	State	S_1	S_2	S_3	S_4
Buck	I	OFF	ON	ON	OFF
	II	ON	OFF	ON	OFF
Buck–Boost	III	OFF	ON	ON	OFF
	IV	ON	OFF	OFF	ON
Boost	V	ON	OFF	OFF	ON
	VI	ON	OFF	ON	OFF

Figure 4.6 Three-mode operation scheme

Although the modulation techniques mentioned so far have been successful operations in dead zone elimination, a more stable and efficient system will be revealed by getting rid of the drawbacks they have. A technique with low control complexity, eliminating discontinuity and low power loss can be obtained from the combination of traditional, single-mode, and modified-mode controls. This modulation method is

referred to as three-mode modulation [54]. In the three-mode control, which combines the traditional two-mode modulation's high efficiency with the single-mode modulation's dead zone elimination capabilities, the operating modes are established between boost, buck-boost, and buck in accordance with the input and output ratio. This means that the buck-boost operation is only used in a restricted region where the voltage output of the converter is almost equal to the voltage input. The buck and boost states are active throughout the remaining operating region, just like in the conventional two-mode modulation, hence the average system efficiency is higher than with techniques that were discussed before. Thus, in this operating scheme, the entire operating range is filled by the three modes. The range of values for the duty cycles d_1 and d_2 can take for this modulation can be stated as

$$\begin{cases} d_{1_{min}} \leq d_1 \leq d_{1_{max}} \\ d_1 = d_2 \\ 1 - d_{2_{max}} \leq 1 - d_2 \leq 1 - d_{2_{min}} \end{cases} \quad \textbf{(4.5)}$$

As can be seen in equation (4.5), it will be possible to adjust the duty cycles by examining the entire operating area in three parts. All switching regions with their maximum and minimum limitations are separated and the aforementioned dead zone area is eliminated with the green-shaded buck-boost operation as depicted in Fig. 4.6. Three different subsections of the entire operating zone can be used to explore and elaborate on this mode of operation.

4.3.3.1 Pure buck mode

The FSBB performs exclusively in the buck operation if the output voltage is adequately less compared to the input, which indicates that the duty cycle of the buck side switches is between $[d_{1_{min}}, d_{1_{max}}]$ and the boost side duty cycle remains at zero. This operational region is enclosed by an orange AOE triangle as shown in Fig 4.6. In this mode, the boost side switch S_3 is constantly ON while S_4 on the same leg is constantly OFF, which indicates that the output voltage is purely regulated by the duty cycle d_1. Two operating stages occur in this mode. Switch S_1 is turned ON and switch S_2 is turned OFF to avoid a short circuit through the source since it is essential to ensure that the two switches are not on simultaneously. Since the inductor is charged and the current derivative remains constant and positive, the current increases linearly. When the switch S_2 is turned ON and the switch S_1 is turned OFF, the inductor releases its stored energy

to the load. During this time, the inductor's current, I_L, diminishes steadily and uniformly at a negative stable rate.

4.3.3.2 Pure boost mode

The FSBB performs exclusively as the boost operation if the output voltage value is adequately greater compared to the input, which indicates that the boost side switches duty cycle is between [$1-d_{2_{min}}$, $1-d_{2_{max}}$] and the buck side duty cycle remains at one. This operational region is enclosed by a blue KOB triangle as depicted in Fig 4.6. In this operation, the buck side switch S_1 is constantly ON while S_2 on the same leg is constantly OFF, which indicates that the output voltage is purely regulated using the duty cycle d_2. Similarly, two operating stages occur in this mode. If switch S_3 is turned ON and S_4 is turned OFF, the inductor is charged and the I_L is increased linearly at a constant positive rate. Conversely, if switch S_4 is turned ON and S_3 is turned OFF, the inductor releases its stored energy to the load and the I_L diminishes steadily and uniformly at a negative stable rate.

4.3.3.3 Buck-boost mode

The FSBB performs in the buck-boost operation if the output voltage approaches the input voltage, which indicates that a single control signal is used to adjust both the buck and boost side duty cycles by creating a common duty cycle. This operational region is enclosed by a green OEFK irregular rectangle as depicted in Fig 4.6. One of the buck and boost side switches S_1, S_4 are ON/OFF, while S_2 and S_3on the same leg is OFF/ON synchronously which indicates that the output is regulated by the common duty cycle D. During the initial switching stage, the inductor accumulates energy while the source current through S_1, the inductor, S_4, and then back to the input. Switches S_2 and S_3 must be simultaneously turned ON to enable the inductor to discharge its stored energy into the load, with the I_L passing through S_3, load and S_2.

4.3.4 Four-mode modulation

The three-mode modulation method has drawbacks due to the buck-boost operation at the mode transitions. Using this buck-boost state during mode transition doubles the switching-based loss of the FSBB, whereas when operating in the buck or boost state requires only two switches to be activated and deactivated during each cycle [55]. As the input voltage reaches a value close to the output, which is the interval where the duty

cycle in the buck-boost control is close to 50%, the current in the inductor doubles, and the conduction loss increases fourfold compared to the buck or boost operation. In addition, the buck-boost operation not only increases the switching and conduction loss but also increases the output ripple during the transition. In order to eliminate the dead zone more efficiently and compensate for the lack of three-mode control, an approach for achieving four-mode modulation was introduced in [56] by including extra stages. Instead of using variable frequency, as a further analysis, a four-mode technique with fixed frequency is proposed in [57] to accomplish a smooth mode transition between buck and boost. In this technique, the mode transition interval between buck and boost operation is filled with two additional conversion modes. By reducing switching losses and average inductor current, this method has the potential to improve converter performance [58].

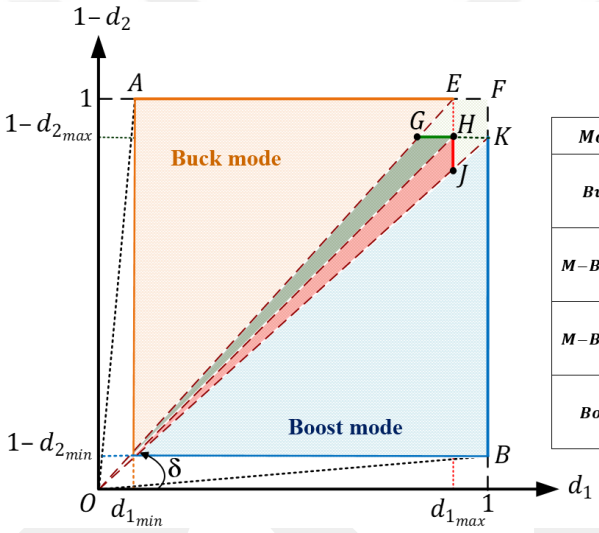

Modified-Buck mode

Modified-Boost mode

Mode	State	S_1	S_2	S_3	S_4
Buck	I	OFF	ON	ON	OFF
	II	ON	OFF	ON	OFF
M−Buck	III	OFF	ON	80%	20%
	IV	ON	OFF		
M−Boost	V	80%	20%	OFF	ON
	VI			ON	OFF
Boost	VII	ON	OFF	OFF	ON
	VIII	ON	OFF	ON	OFF

Figure 4.7 Four-mode operation scheme

This approach consists of the traditional two-mode modulation with simple control and efficiency and an additional two modes that can eliminate the dead zone according to the voltage ratio of the input to the output. In the narrow region, as the input voltage becomes closer to the output, the FSBB operates in these two different modes: modified-buck and modified-boost. Similar to the three-mode approach, the pure buck operation is performed when the converter's input is sufficiently higher compared to the output, and likewise, the pure boost operation is performed when the converter's input is sufficiently lower compared to the output. It maintains optimum efficiency throughout the entire range of operation, except for the dead zone operation, as the buck and boost operations are active throughout the remaining operating region, similar to conventional two-mode

control. The range of values for the duty cycles d_1 and d_2 can take for this modulation can be stated as

$$\begin{cases} d_{1_{min}} \le d_1 \le d_{1_{max}}, & Mode\ I \\ d_1 = \dfrac{v_{out}}{v_{in}}\left(1-d_{2_{fix}}\right), d_2 = d_{2_{fix}}, & Mode\ II \\ d_1 = d_{1_{fix}}, d_2 = 1-\dfrac{v_{in}}{v_{out}}d_{1_{fix}}, & Mode\ III \\ 1-d_{2_{max}} \le 1-d_2 \le 1-d_{2_{min}}, & Mode\ IV \end{cases} \quad \textbf{(4.6)}$$

where $d_{1_{fix}}$ and $d_{2_{fix}}$ are determined constant value for the modified buck and boost state, respectively. These clamped values can be stated as [59]

$$\begin{cases} d_{1_{fix}} = d_{1_{max}}\left(1-d_{2_{min}}\right) \\ d_{2_{fix}} = 1-d_{1_{max}}\left(1-d_{2_{min}}\right) \end{cases} \quad \textbf{(4.7)}$$

In this control technique, $Mode\ I$ and $Mode\ IV$ represent represents the pure buck and pure boost operation, respectively. $Mode\ II$ means the modified-buck and $Mode\ III$ is the modified-boost mode. According to equation (4.6), the $Mode\ I$ and $Mode\ IV$ are operated in similar ranges to the three-mode control, however, the buck duty cycle switches whereas the boost duty cycle is held constant at its minimum rate in the $Mode\ II$, on the other hand, when the converter is operating in the $Mode\ III$, the boost duty cycle switches whereas the buck duty cycle is kept at its maximum rate. Thus, it will be again possible to adjust the duty cycles by examining the entire operating area and all separated switching regions with their maximum and minimum limitations are shown in Fig. 4.7. It is apparent that the operating zones of the buck operation shown with orange and the boost operation shown with blue are exactly the same as the previous control method. The two extra modes are obtained by adding a curved outward line, GHJ, as an extra path in the discontinuity region as depicted with OEFK irregular rectangle.

In Fig. 4.8, the duty cycle characteristics of the four-mode control technique are shown, which display the voltage ratio starting from a point where the output voltage is almost zero and continuing up to a value where the input voltage is several times greater. The FSBB employs as a pure buck to step down the input voltage within its minimum duty cycle to the maximum range. Then, the modified buck and modified boost states are utilized consecutively to ensure a smooth transition to the pure boost. As the buck-only and boost-only modes have already been elaborated in the previous technique, this part will focus only on explaining the two modified modes.

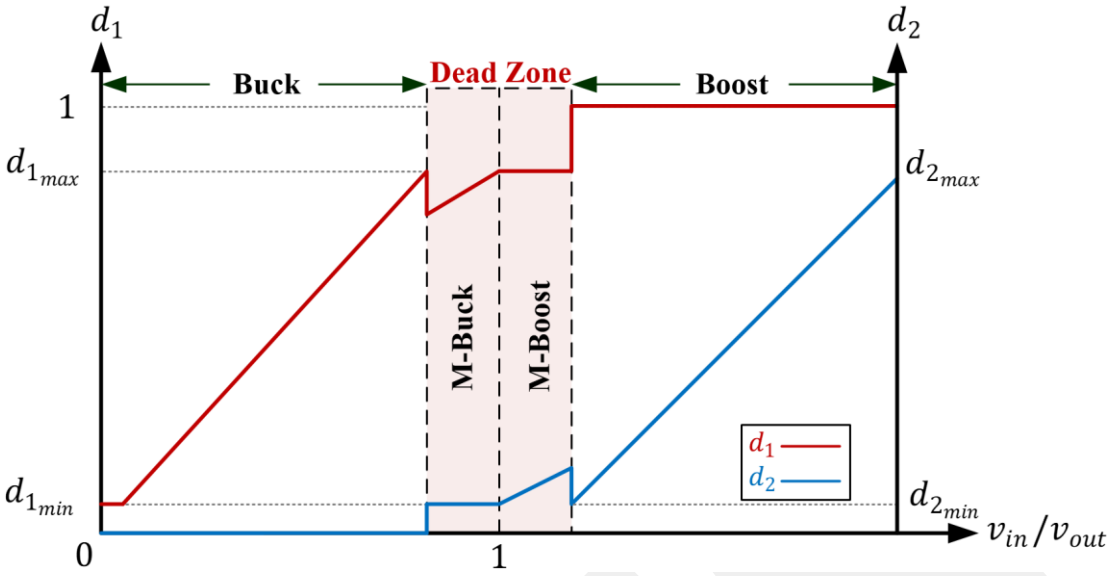

Figure 4.8 Duty cycle characteristic of four-mode modulation

4.3.4.1 Modified-buck mode

The FSBB performs in the modified-buck operation if the output voltage is slightly lower compared to the input and this operational region is enclosed by a green GOH triangle as depicted in Fig 4.7. In this operation, the buck switches duty cycle d_1 is utilized to control the output, whereas the duty cycle of the boost side d_2 is kept constant at the predesigned clamping value [$d_{2_{fix}}$] as depicted in Fig 4.8. To define the switching cycle more precisely, this mode can be studied as four operating stages as shown in Fig 4.9 (a). The boost side switch S_3 always is ON while S_4 on the same leg is always OFF during stage I and stage II, while the buck side switches S_1 and S_2 are ON and OFF consecutively. In the beginning of the mode, the inductor releases its stored energy to the load with S_1 (S_2) is ON (OFF) and then the I_L slightly increases when the S_2 (S_1) is ON (OFF). Throughout the second half of the mode, S_1 (S_2) is ON (OFF) keep unchanged while the S_3 and S_4 are turned ON and OFF consecutively and the I_L increases up to output voltage reaches the input voltage.

4.3.4.2 Modified-boost mode

The FSBB is operating in the modified-boost operation if the output voltage is slightly higher compared to the input and this operational region is enclosed by a red HOJ triangle as depicted in Fig 4.7. In this operation, the boost switches duty cycle d_2 is utilized to control the output, whereas the duty cycle of the buck side d_1 is kept constant at the predesigned clamping value [$d_{1_{fix}}$] as depicted in Fig 4.8. According to Figure

4.9(b), there can be four operating stages in this operation as well. The buck switches S_1 is always ON while S_2 on the same leg is always OFF until the middle of the switching period, while the boost side switches S_3 and S_4 are ON and OFF consecutively. At the beginning of this operation, the inductor is charged and the I_L derivative remains constant and positive, the I_L increases linearly when S_3 (S_4) is ON (OFF). In the second operating stage, the I_L slightly decreases when the S_4 (S_3) is ON (OFF). Throughout stage III and stage IV, S_4 (S_3) is ON (OFF) keep unchanged while the S_1 and S_2 are turned ON and OFF consecutively and the I_L decreases up to output voltage reaches the demanded level.

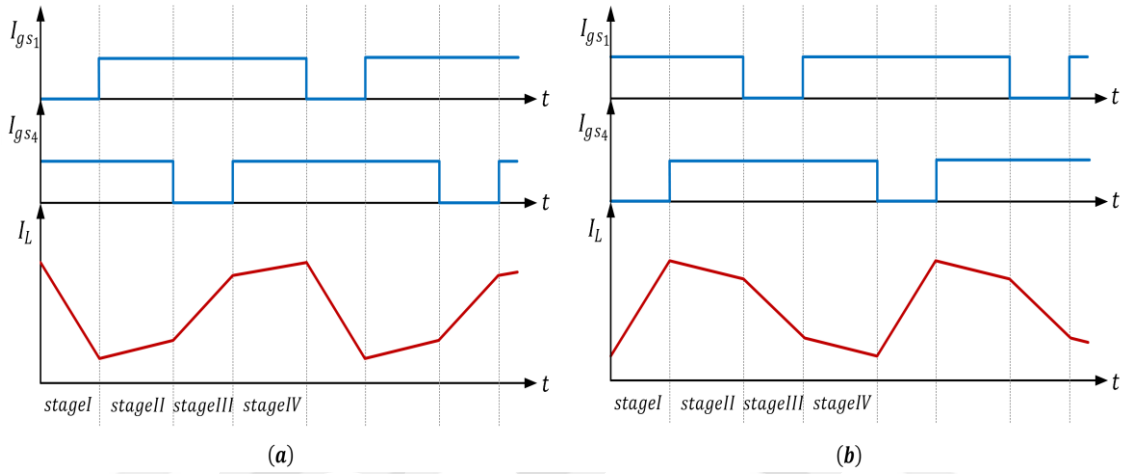

Figure 4.9 Inductor current waveforms (a) Modified-buck (b) Modified-boost

4.4 Inductor Current Performance

It is widely recognized that the converter's efficiency depends on how much power is lost. Since the inductor current is a critical metric for assessing the performance of the power converters, the output voltage fluctuation, the mean, and RMS inductor current values are studied for comparison. Reduced inductor average and RMS values result in fewer conduction losses for the inductor and transistors, which improves efficacy [60]. The control strategies examined in this thesis are the single-mode technique, traditional and modified two-mode technique, three-mode technique, and four-mode technique are compared among themselves in terms of the average value of inductor current and ripple according to the below equations. When the FSBB is operated using single-mode modulation, it is simple to obtain the inductor current's average and ripple as

$$I_{av_1} = \frac{(V_{in} + V_{out})}{V_{in}} I_{out} \tag{4.8}$$

$$\Delta I_{L_1} = \frac{V_{in}V_{out}}{Lf_s(V_{in}+V_{out})} \tag{4.9}$$

where I_{av_1} is average current value of the inductor, ΔI_{L_1} represents the inductor current ripple and I_{out} represents the output current.

When the FSBB is operated using traditional two-mode modulation, the average value $I_{av_{t2}}$ and current ripple $\Delta I_{L_{t2}}$ of an inductor are stated as [61]

$$I_{av_{t2}} = \begin{cases} I_{out}, & V_{out} < V_{in} \\ \dfrac{V_{out}}{V_{in}} I_{out}, & V_{out} > V_{in} \end{cases} \tag{4.10}$$

$$\Delta I_{L_{t2}} = \begin{cases} \dfrac{V_{out}(V_{in}-V_{out})}{Lf_sV_{in}}, & V_{out} < V_{in} \\ \dfrac{V_{in}(V_{out}-V_{in})}{Lf_sV_{out}}, & V_{out} > V_{in} \end{cases} \tag{4.11}$$

When the FSBB is operated using modified two-mode modulation, the average value $I_{av_{m2}}$ and current ripple $\Delta I_{L_{m2}}$ of an inductor are stated as

$$I_{av_{m2}} = \begin{cases} I_{out}, & V_{out} < V_{in} \\ \dfrac{(V_{in}+V_{out})}{V_{in}} I_{out}, & V_{out} \geq V_{in} \end{cases} \tag{4.12}$$

$$\Delta I_{L_{m2}} = \begin{cases} \dfrac{V_{out}(V_{in}-V_{out})}{Lf_sV_{in}}, & V_{out} < V_{in} \\ \dfrac{V_{in}V_{out}}{Lf_s(V_{in}+V_{out})}, & V_{out} \geq V_{in} \end{cases} \tag{4.13}$$

When the FSBB is operated using three-mode modulation, the average value I_{av_3} and current ripple ΔI_{L_3} of an inductor are stated as

$$I_{av_3} = \begin{cases} I_{out}, & V_{out} < V_{in} \\ \dfrac{(V_{in}+V_{out})}{V_{in}} I_{out}, & V_{out} \approx V_{in} \\ \dfrac{V_{out}}{V_{in}} I_{out}, & V_{out} > V_{in} \end{cases} \tag{4.14}$$

$$\Delta I_{L_3} = \begin{cases} \dfrac{V_{out}(V_{in}-V_{out})}{Lf_sV_{in}}, & V_{out} < V_{in} \\ \dfrac{V_{in}(V_{out}-V_{in})}{Lf_sV_{out}}, & V_{out} \approx V_{out} \\ \dfrac{V_{in}(V_{out}-V_{in})}{Lf_sV_{out}}, & V_{out} > V_{in} \end{cases} \tag{4.15}$$

When the FSBB is operated using four-mode modulation, the average value I_{av_4} and current ripple ΔI_{L_4} of an inductor are stated as

$$I_{av_4} = \begin{cases} I_{out}, & V_{out} < V_{fix-buck} \\ \dfrac{I_{out}}{1-d_{2_{min}}}, & V_{fix-buck} < V_{out} < V_{in} \\ \dfrac{V_{out}I_{out}}{1-d_{1_{max}}}, & V_{in} < V_{out} < V_{fix-boost} \\ \dfrac{V_{out}}{V_{in}}I_{out}, & V_{out} > V_{fix-boost} \end{cases} \tag{4.16}$$

$$\Delta I_{L_4} = \begin{cases} \dfrac{V_{out}(V_{in}-V_{out})}{Lf_sV_{in}}, & V_{out} < V_{fix-buck} \\ \dfrac{V_{out}(V_{out}-V_{in}(1-d_{2_{min}}))}{Lf_sV_{in}}, & V_{fix-buck} < V_{out} < V_{in} \\ \dfrac{V_{in}(V_{out}-V_{in}d_{1_{max}})}{Lf_sV_{out}}, & V_{in} < V_{out} < V_{fix-boost} \\ \dfrac{V_{in}(V_{out}-V_{in})}{Lf_sV_{out}}, & V_{out} > V_{fix-boost} \end{cases} \tag{4.17}$$

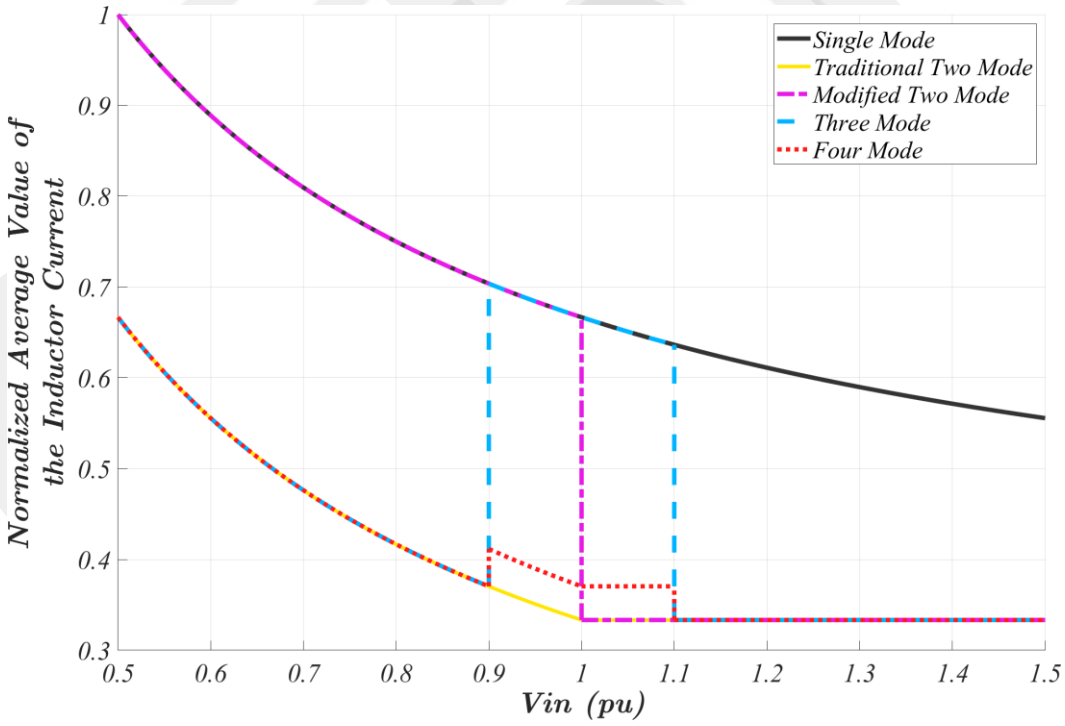

Figure 4.10 Inductor average current value comparison under various techniques

To provide a clear comparison between the aforementioned techniques, inductor current fluctuations and average inductor current value under various techniques are shown in Figs. 4.10 and 4.11, respectively. Since worst-case scenarios will be obtained

by the single-mode modulation scheme, the other modulations are scaled based on the maximum values obtained in the single-mode modulation. The per unit values are used to achieve simpler expression and general parametric results, and the following are the settings of the parameters used to generate the figures: $V_{in} = 0.5\text{–}1.5\,pu, V_{out} = 1\,pu, L = 1\,pu,$ the output power $P_{out} = 1\,pu$ and $f_s = 1\,pu$. The output voltage is considered as unchanging at the unit value, the input voltage varying from half to one and a half of the output. Since it has been reported that the highest and lowest duty ratios of the buck and boost state, respectively, are established with around 10% tolerance [62], $d_{1_{max}} = 0.9$ and $d_{2_{min}} = 0.1$ are taken, then based on equation (4.7), the approximate values of $d_{1_{fix}} = 0.81$ and $d_{2_{min}} = 0.19$ are calculated for the duty cycle constraints employed in this part.

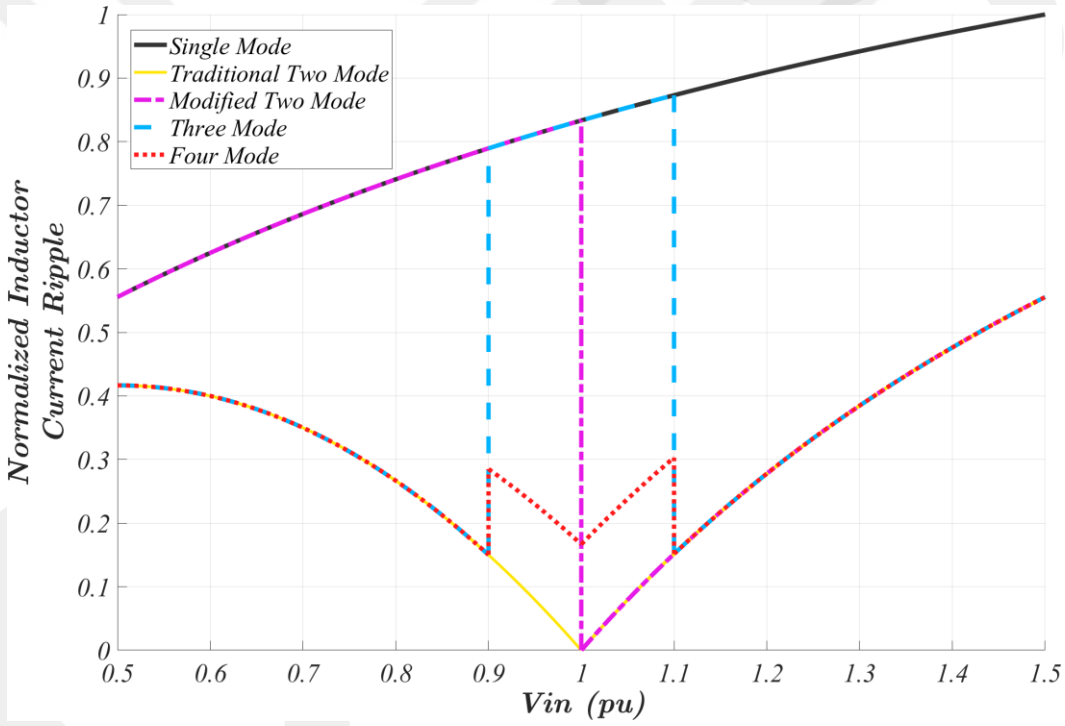

Figure 4.11 Inductor current ripples comparison under various techniques

As evident from Figs. 4.10 and 4.11, the average inductor current value follows a similar pattern to that of the current ripple across the entire input voltage range for all the methods used. Therefore, comparisons can be made with similar interpretations based on both figures. Although the single-mode modulation seems to have a simple control structure and this technique removes discontinuities during transitions and their undesirable effects, it results in a high inductor current fluctuation and RMS value. Since the single-mode approach operates continuously in buck-boost mode, this method is by several lengths the poorest in the sense of system efficiency and this technique is not

usually preferred for implementation. When the output voltage value becomes adequately greater or less compared to the input, the three-mode and four-mode techniques exhibit comparable performance to the traditional two-mode technique and they are superior to the performance achieved with the single-mode method. Whereas, when the output voltage value becomes slightly less compared to the input, the traditional two-mode has the smallest average value and less fluctuation performance despite the operational dead zone. When the output voltage value becomes slightly greater compared to the input, the modified two-mode stands out with the two-mode. Since the modified two-mode has higher switching and conduction loss like single-mode due to buck-boost operation for more than half the time, it is not a good option to use applications where high efficiency is expected. In terms of overall ripple and current performance together with the figure of merit of the dead zone elimination, it is seen that four-mode is superior to three-mode and other modulation techniques. As a result of both average inductor current value and ripple comparisons, choosing and using the four-mode modulation solves the dead zone problem and also eliminates other negative effects.

4.5 Conclusions

The limitations that arise inherently from the circuit when it is employed in traditional two-mode control, which causes a dead zone to appear in a certain range. The control techniques created as combinations of three different modes and their specific operating regions, along with the association between output and input voltages, are examined in detail. In addition to the aim of eliminating the dead zone, efficiency was also a crucial factor when designing the control. Explanations and calculations have been provided for single-mode, modified-two-mode, three-mode, and four-mode techniques, as well as the traditional two-mode control that creates the dead zone. Analyses were made to reveal the real performance of the circuit based on the inductor performance under five different control techniques. The results presented that the four-mode modulation scheme eliminates the dead zone and has superiority in terms of efficiency.

Chapter 5

Results and Discussions

5.1 Introduction

In this chapter, the input and output voltage, power, and switching frequency values for the prototype are determined and the selection criteria for passive components such as inductor capacitors and power switches are selected based on theoretical analysis and other important parameters. The selected parameters and design criteria for the FSBB inverter are presented in Section 5.2. Real-time simulation results are discussed and a comparison of the efficiency of the five discussed modes is mentioned in Section 5.3 In addition, the investigated techniques from the previous sections are experimentally implemented and compared to decide their figure of merits in Section 5.4.

5.2 Design Specifications

To validate and compare the theoretic analysis and demonstrate its effectiveness, a prototype of the adopted inverter is constructed and tested both in a computer environment and the laboratory. The design of the inverter is dependent on various active and passive parameters, such as the inductor (L), input and output capacitor (C_{in} and C_{out}), and the power switches (S_n). Determining values of these components are not straightforward for the selection process and they contain many criteria within themselves. Material selection for the inductor depends on various operating conditions such as maximum power, the maximum current that will flow through it, inductance, exposure voltage, and switching frequency [63]. Even though a perfect material exhibits high saturation, low loss, and linear permeability, none of the existing matter satisfies all these criteria as required simultaneously. The optimal design is achieved through a trade-off between the different parameters, including the inductor's geometric, magnetic properties, physical size, core material, core losses, and saturation current calculations.

When selecting input and output capacitance each design specifically must be considered for the worst-case scenario. The capacitance value and type (ceramic, bulk, etc.,) may vary depending on the intended application. The primary goal of selecting input capacitors is to minimize the voltage overshoot as well as the ripples. Correlatively, output capacitance is a crucial part of the overall feedback system as well as reducing overshoot [64]. If the output capacitance is insufficient, the system responds with a large overshoot, and also high ESR in the output capacitor can result in high ripples. When reflected ripple is a problem, a small (with nano-values) input inductor can be used with careful determination as it will affect the input capacitor selection. Therefore, a suitable output capacitor should be selected based on the design parameters that specify the maximum voltage overshoot and ripples, and it should have sufficient capacitance and a low ESR.

Table 5.1 Parameters of the built converter

Parameter	Type / Value
Input Voltage $\boldsymbol{V_{in}}$ (V)	200 DC
Output Voltage $\boldsymbol{V_{out}}$ (V)	220 RMS
Maximum Output Power $\boldsymbol{P_{out}}$ (W)	2000
Switching Frequency $\boldsymbol{f_{sw}}$ (Hz)	100 k
Inductor $\boldsymbol{L}$ (μH)	40
Capacitors $\boldsymbol{C_{in}, C_{out}}$ (μF)	4
Switches	C3M0065090J
Gate Driver	ADuM4135

For the MOSFET selection, there are certain parameters that should be known such as the drain-source voltage (V_{DS}), the on-state resistance $\left(R_{DS_{ON}}\right)$, the gate-source voltage (V_{GS}), the maximum ambient temperature $\left(T_{A_{max}}\right)$ and the maximum junction temperature $\left(T_{J_{max}}\right)$. Proper switch choice is crucial for the desired operation of the converter, as negligence or oversight in this selection can cause sudden interruptions and breakdowns during operation. Although it is necessary to select a V_{DS} that is sufficiently higher than the maximum operating level to prevent the destruction of the device, choosing more durable MOSFETs may result in large $R_{DS_{ON}}$ which increases switching loss. The V_{GS} should be selected higher than the threshold voltage according to manufacturer datasheet [65]. On the other hand, the temperature-related parameters help in designing the heatsink or calculating the maximum power dissipation in the switch.

Table 5.2 Maximum rating of C3M0065090J SiC MOSFET

Parameter	Value	Unit
Drain-Source Voltage V_{DS}	900	V
Continuous drain current I_D	36	A
On-time resistance $R_{DS(ON)}$	65	mΩ
Turn-On Switching Energy E_{ON}	42	µJ
Turn Off Switching Energy E_{OFF}	6	µJ
Diode Forward Voltage V_{SD}	4.4	V
Total gate charge Q_g	30	nC
Output capacitance C_{oss}	66	pF

According to all criteria and aforementioned calculations, the built converter's specifications and decided parameters are in Table 5.1. Moreover, typical maximum ratings given by the manufacturer of the selected silicon carbide (SiC) technology power switch are listed in Table 5.2. It is a good practice to choose a component's maximum value with 20-25% tolerance. For instance, a value of 60 µF would be acceptable with a margin of 20% above the calculated value of 48 µF. However, since this value is not always available commercially, a capacitor with an upper value of 68µF or 82µF can be accepted.

5.3 Simulation Results

The superiority of the proposed control technique is validated using the FSBB converter with an unfolding H-bridge. A 2-kW inverter system is simulated to demonstrate a comparison of all the aforementioned dead zone mitigation techniques, using the Altair PowerSim (PSIM) simulation tool. PSIM is a robust software tool for simulating electrical environments that empower users by offering a broad range of commonly used components. Furthermore, it allows for fast and easy verification of power circuit designs at every stage of the product design process. To make more precise comparisons, the tool provides loss calculation based on the Eon database with the MOSFET model [66]. The switches used and the remaining parameters are those listed in Table 5.1 and are the same as those utilized in the experimental study.

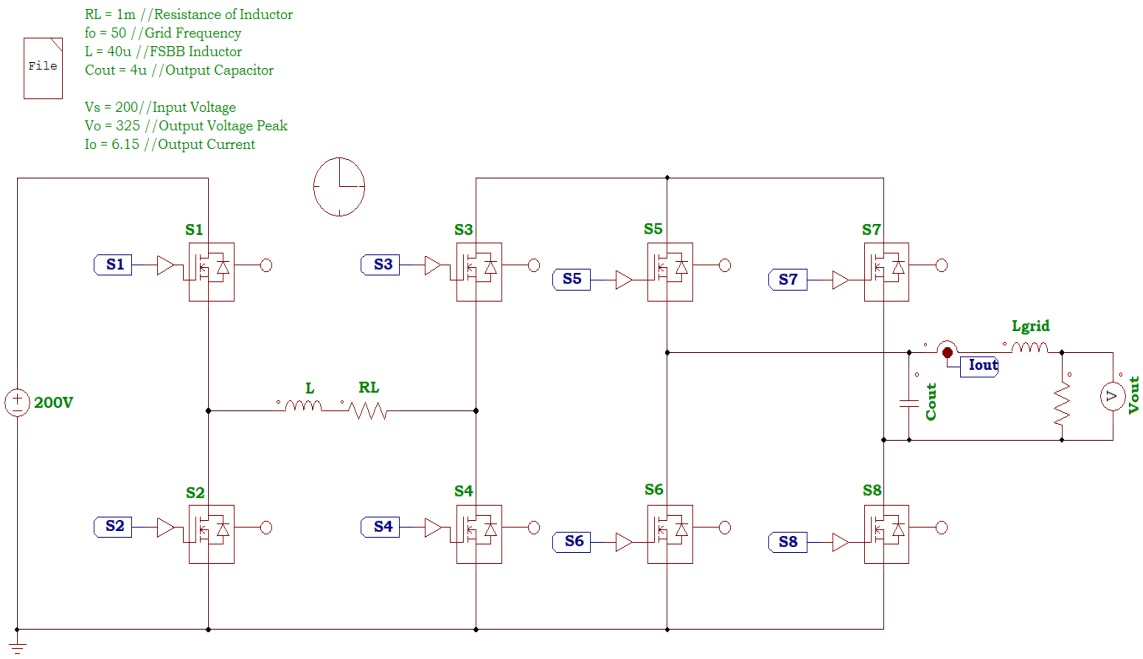

Figure 5.1 Simulation circuit of the FSBB inverter

The FSBB inverter is illustrated in Fig. 5.1 and simulated accordingly. In this circuit, $S_1 - S_4$ belongs to the DC rectified AC production part, which is the FSBB converter, while $S_5 - S_8$ are part of the unfolding H-bridge inverter. To mimic a real test environment, a small resistance (R_L). Additionally, an inductor is placed at the output side to ensure smooth output signals. Since the input source is able to give pure DC in the simulation, there is no need to use an input capacitor.

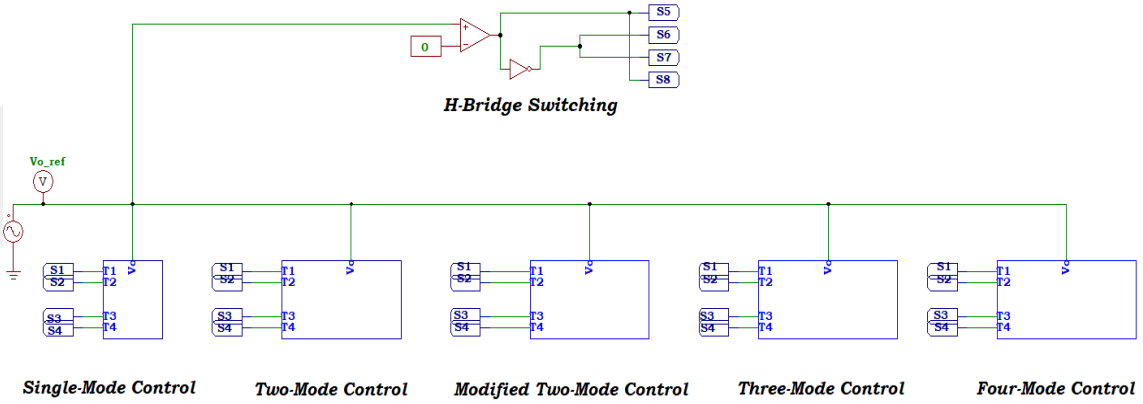

Figure 5.2 Control structure of the FSBB inverter

Fig. 5.2 shows the five different control approaches used to control the FSBB inverter. In order to see the behavior of all modes fairly, modulation schemes are applied sequentially, starting from the single mode, without making any changes in the circuit. The inverter is operated in an open-loop principle with a pure 50 Hz sine wave. As can be seen in the H-bridge control, the MOSFETs are switched only half of the output references period.

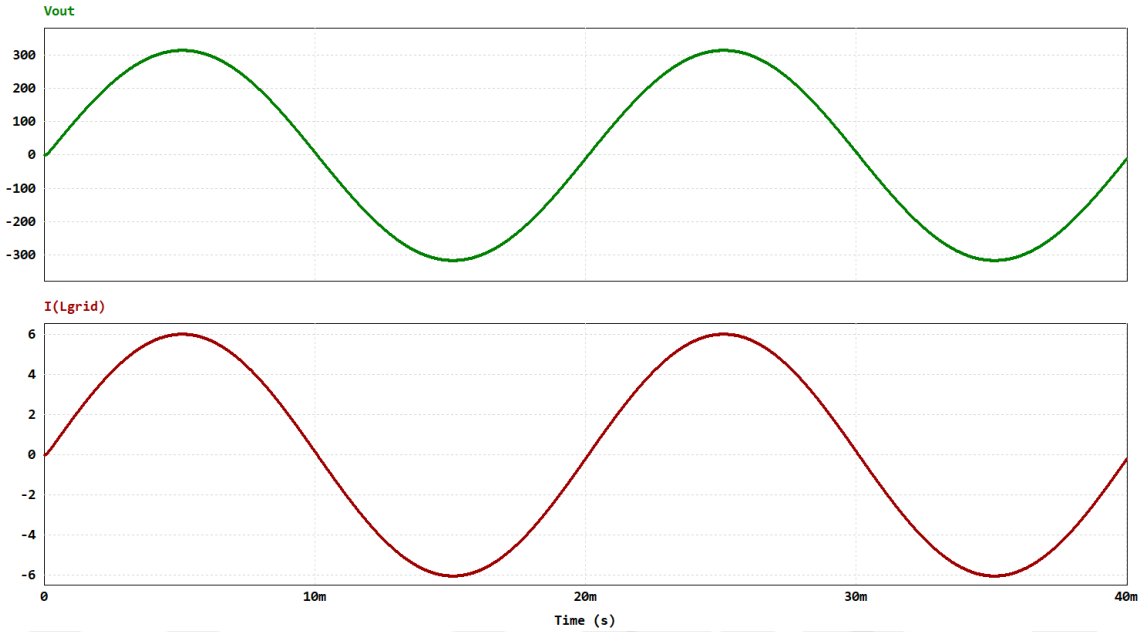

Figure 5.3 The output voltage and current in the single-mode modulation

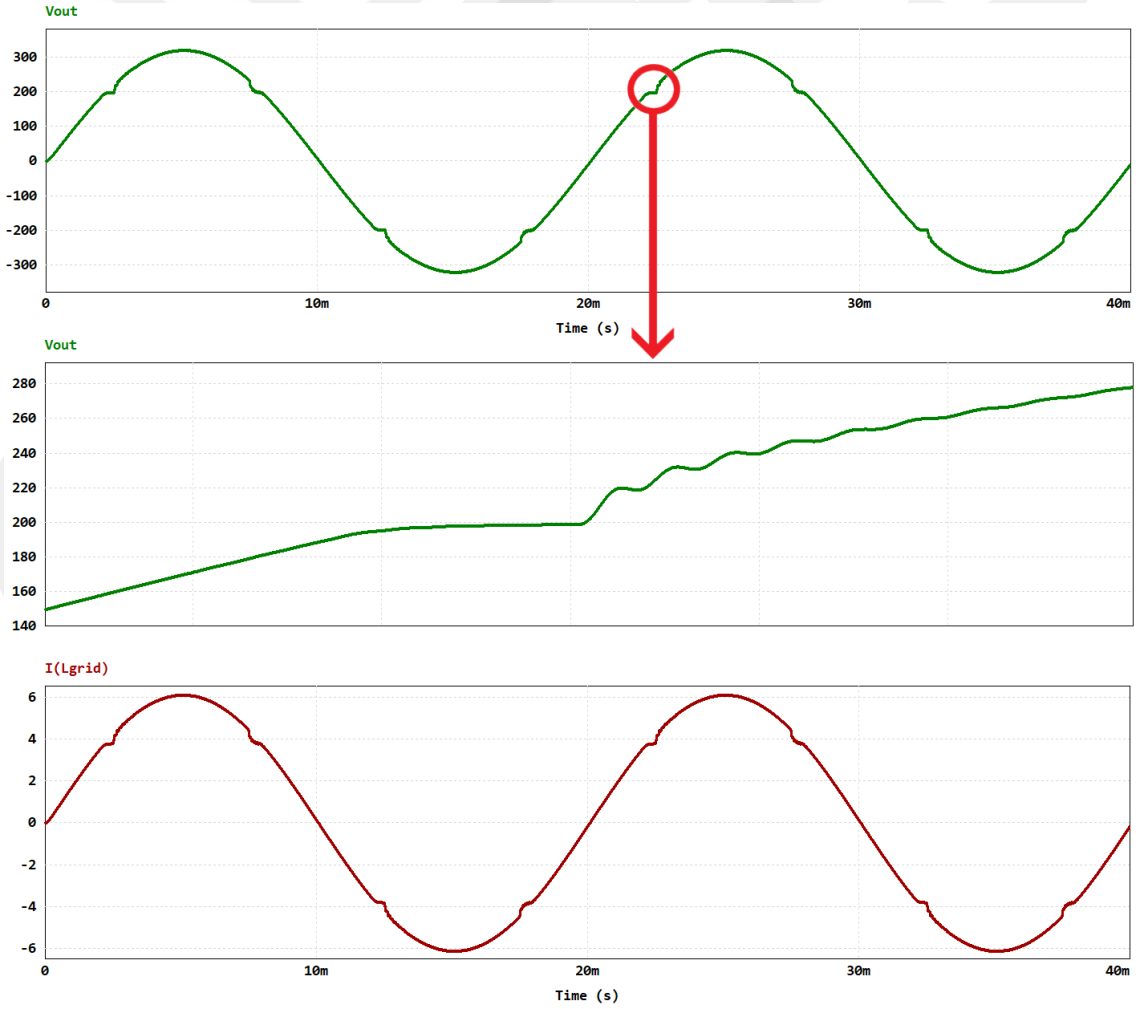

Figure 5.4 The output voltage and current in the two-mode modulation

The output voltage and current waveforms are illustrated in Fig. 5.3 when the inverter is employed using full-period buck-boost operation. The appearance of these results as pure sinuses is exactly as expected and mentioned before. This approach is considered the simplest control method, as it eliminates the dead zone and ensures a desired AC output with a low ripple.

Fig. 5.4 depicts the waveforms of the output voltage and current when utilizing the inverter in conventional buck and boost operations. When the output voltage is below 200V the inverter attempts to function as pure buck, when the output voltage is above 200V the inverter attempts to function as pure boost. However, owing to inevitable switching limitations, the inverter cannot employ either buck or boost operation when the output voltage is approximately at the level of 200V, as shown in the middle graph. This graph depicts the region where the output voltage becomes closer to the input voltage, and a discontinuity occurs around this level. After operating with the buck operation at the maximum duty ratio, the output becomes unstable and oscillates.

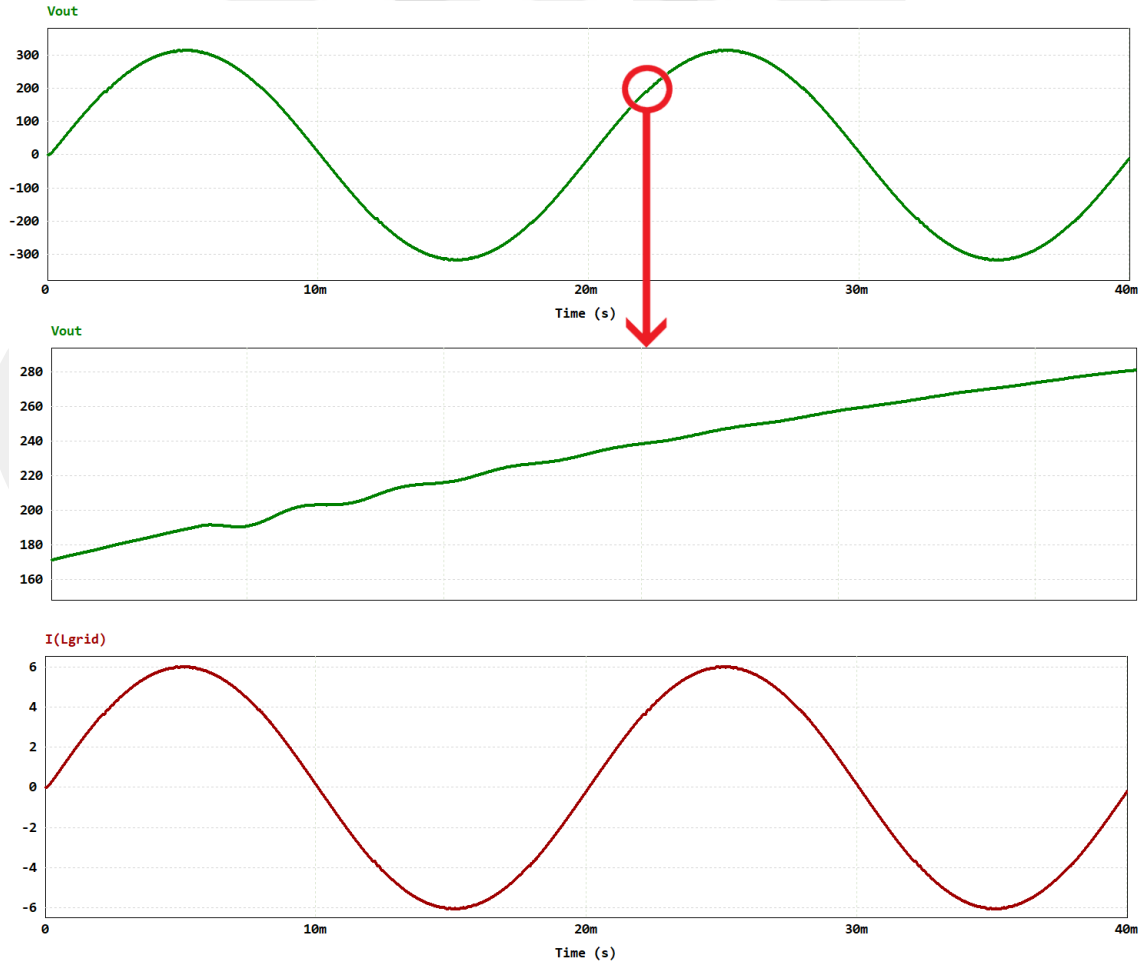

Figure 5.5 The output voltage and current in the modified two-mode modulation

Fig. 5.5 illustrates the waveforms of the output voltage and current when employing the inverter in buck and buck-boost operations. In this control, the buck mode is operated up to the maximum duty cycle level, and then the buck-boost mode is switched. The stability problem, which does not normally occur when the buck-boost mode operates alone, unexpectedly arises in this scheme. The inverter, which runs smoothly in buck operation, switches to buck-boost operation at the level where the output voltage approaches the input. However, ripple occurs due to subharmonics and control.

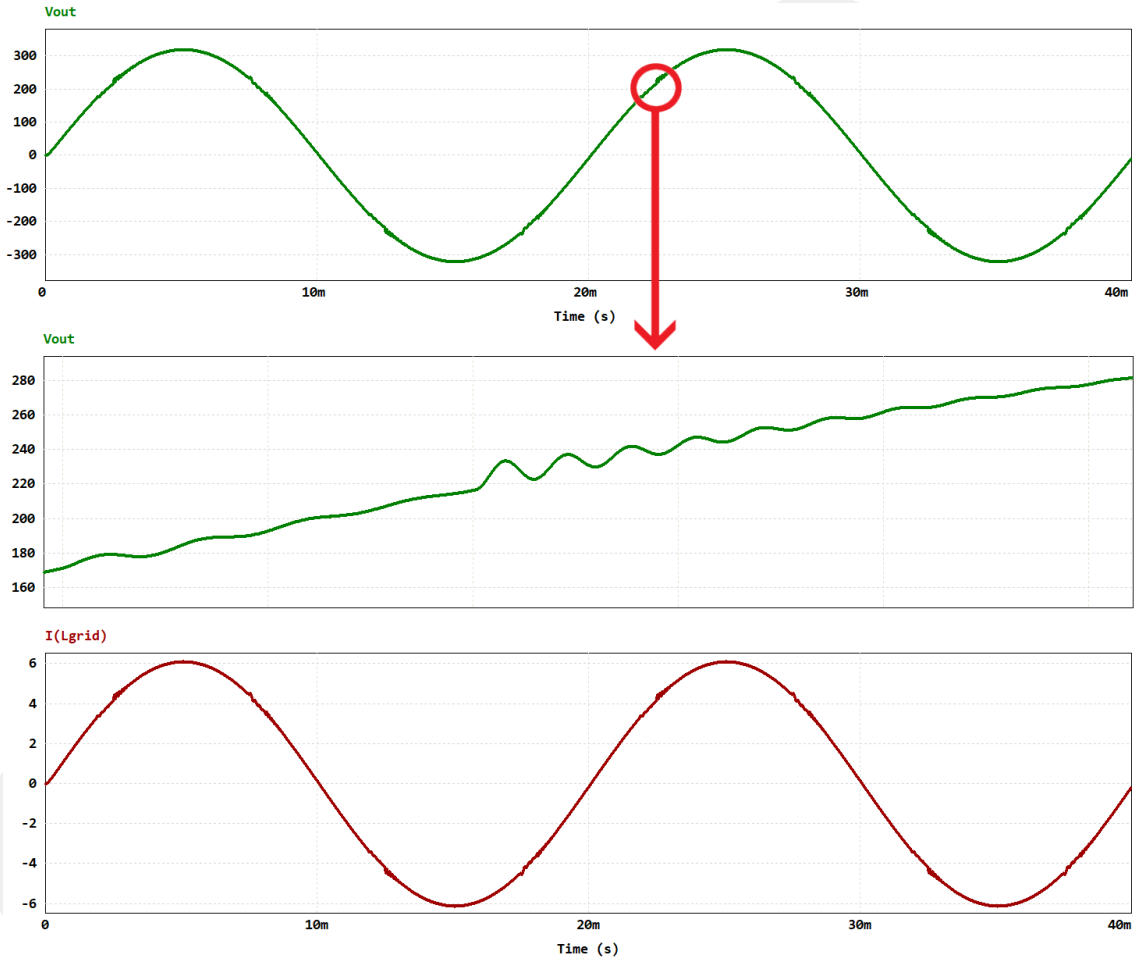

Figure 5.6 The output voltage and current in the three-mode modulation

The waveforms of the output voltage and current when employing the inverter in buck, buck-boost, and boost operations are illustrated in Fig. 5.6. A smoother transition from the dead zone can be expected with buck-boost. Nonetheless, even with minor damage throughout the buck-boost operation, oscillations begin to increase in boost mode and harmonics emerge. Although the lossy buck-boost operation is limited between buck and boost, subharmonics, which stem from the three different mode transitions, negatively affect the output voltage in terms of ripple and harmonic suppression requirements will rise.

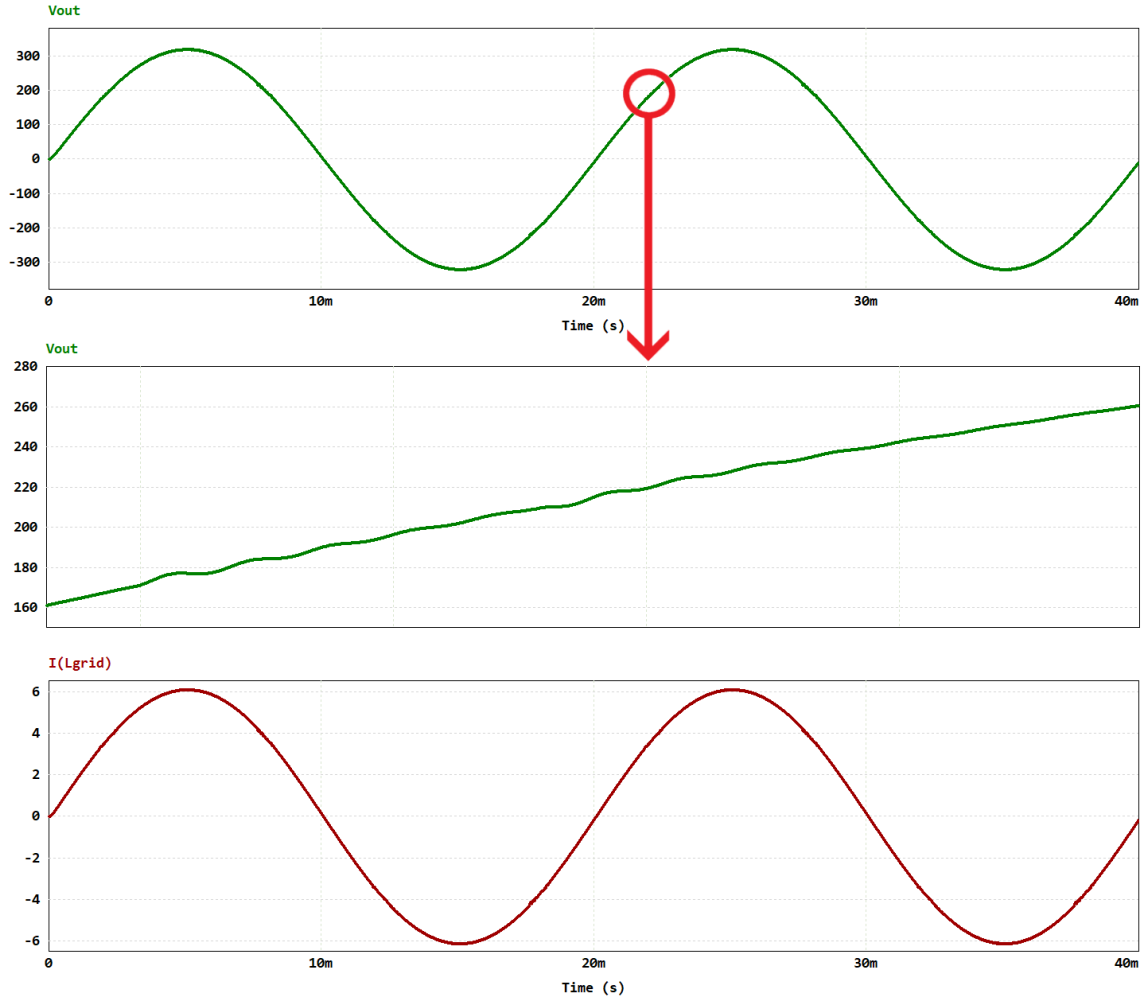

Figure 5.7 The output voltage and current in the four-mode modulation

The waveforms of the output voltage and current when employing the inverter in buck, modified-buck, modified-boost, and boost operations are illustrated in Fig. 5.7. Pure buck and boost modes are used when the output voltage is adequately lower or higher compared to the input, respectively. Modified-buck and modified-boost modes are employed when the output voltage approaches the input, and they are located between buck and boost operations. By avoiding the four-switch operating in buck-boost operation, improved power conversion efficiency can be achieved. It can be clearly observed that this scheme produces a better waveform than other dead zone elimination methods except for the single-mode scheme. By improving the transient response and implementing a closed-loop control design that reduces errors through processing, it may be possible to generate a nearly pure sine wave.

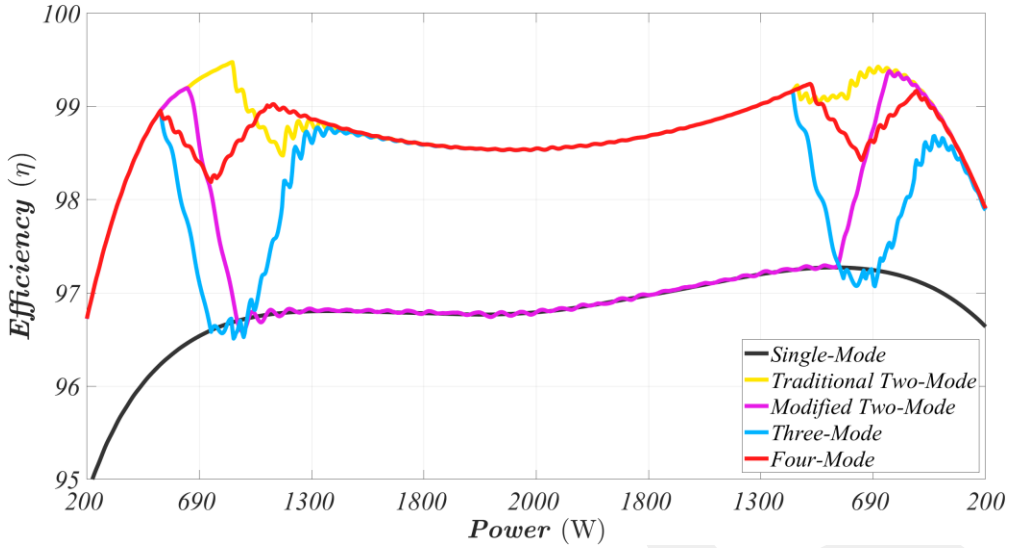

Figure 5.8 Efficiency of the FSBB inverter under five different modes

Fig. 5.8 illustrates the instantaneous power conversion efficiency of five different modes versus output power. While the traditional two-mode achieves a power conversion efficiency of over 99% in buck mode, it is not an ideal control technique due to the dead zone it creates during mode transition. Although the single-mode technique successfully eliminates discontinuity and produces a smooth signal, it results in poor power conversion efficiency, which is a significant drawback. The modified two-mode control method yields better efficiency than the single-mode, but overall efficiency and transition performance remain unsatisfactory. The three-mode control technique performs well in ranges where the output voltage is greater than the input, with a reduction in the discontinuity region and a smooth transition, albeit with lower efficiency due to the buck-boost operation. As opposed to that, by using the four-mode control, an efficiency of over 98% is achieved across the input voltage range for all loading scenarios.

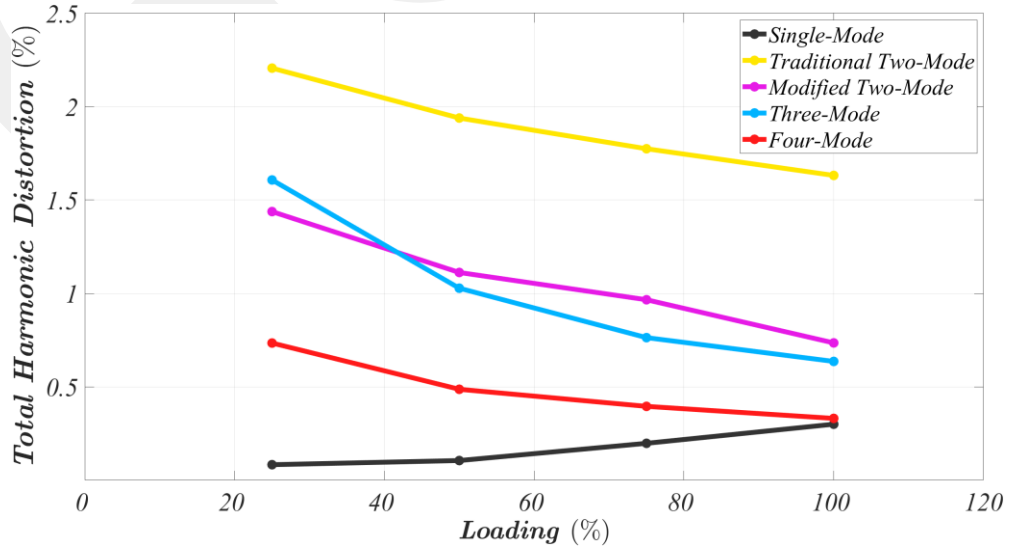

Figure 5.9 THD comparison of the FSBB inverter under five different mode

Fig. 5.9 compares the THD of the four-switch buck-boost inverter under variable load conditions using five different modulation schemes. Among the results of modulation schemes, if the single-mode scheme is excluded as it is the least efficient of the others, then the two-modulation scheme results in twice as much distortion as the scheme with the highest THD. The modified two-mode scheme produces a distortion of 0.75% to 1%, making it a mid-performing scheme among other dead zone mitigation methods. The three-mode modulation scheme produces high harmonics at low loads but has less than 1% distortion at near-full loads. Finally, the four-mode modulation scheme performs best with the highest THD of 0.73% and the lowest of 0.33% under various nonlinear loading conditions. Consequently, the efficiency and harmonic results demonstrate that the FSBB inverter, with the adopted dead zone elimination strategies, can achieve satisfactory efficiency and smooth mode transition with low harmonic distortion.

5.4 Experimental Verifications

A prototype of the four-switch buck-boost converter with an unfolding H-bridge inverter was designed and tested in a laboratory environment. The purpose was to validate both the theoretical and simulation results and to enable a fair comparison of the modulation techniques discussed in Chapter 3 in a real-time implementation. The fabrication of the FSBB inverter was conducted following the specifications provided in Table 5.1, which include a 200 VDC input, 220 VRMS output, and a switching frequency of 100 kHz. The inductor and capacitor values were selected based on the previously calculated values employed in the simulation results and in Chapter 3.4 to meet the design requirements.

The initial step in the prototype fabrication process is designing the schematic cards for the FSBB inverter. Power input connections, voltage indicator, and EMI filter are shown in Fig. 5.10. The EMI filter at the input contains feed capacitors and ferrite inductors to filter out very high-frequency noise in the MHz range. Further in the circuit, a common-mode choke is added to filter high-frequency common-mode noise with high impedance. At the input of the circuit, various capacitors ranging from 10 μF to 1 nF are added to the filter to store energy and filter noise in the kHz range. To minimize connections to the ground, 1 nF and 100 nF capacitors are connected between the positive

and negative terminals and the ground. The small equivalent inductance and resistance of these capacitors play a crucial role in reducing EMI. The circuit utilizes film capacitors that possess these characteristics.

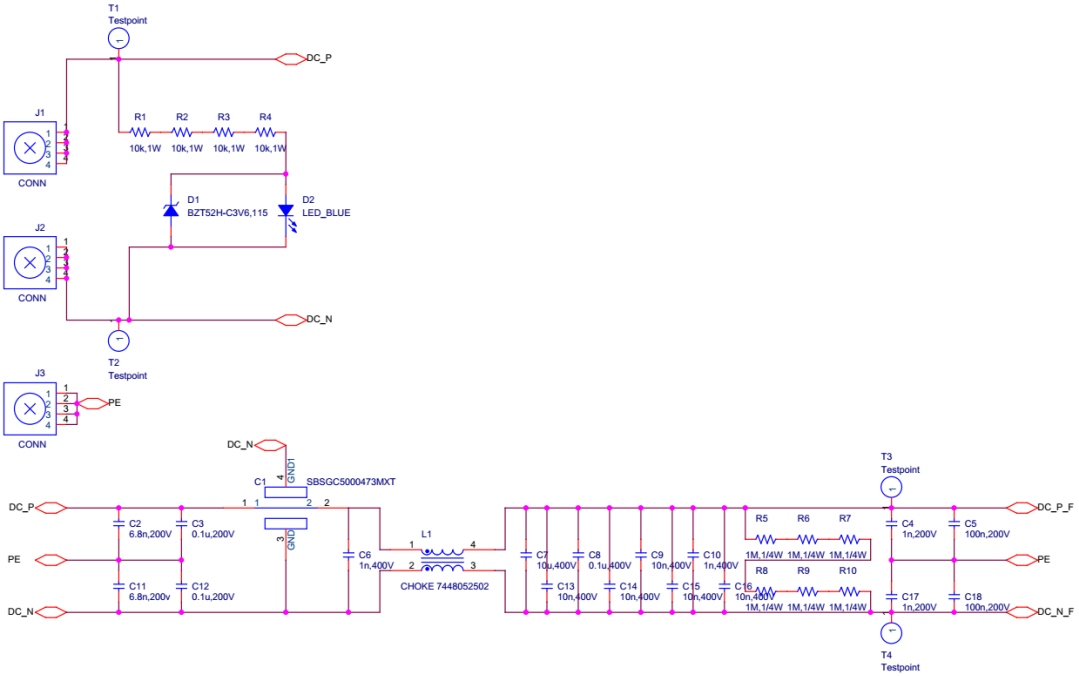

Figure 5.10 Power input connections, voltage indicator, and EMI filter circuit

The bidirectional DC-DC converter circuit and gate driver circuit connector connections can be seen in Fig. 5.11.

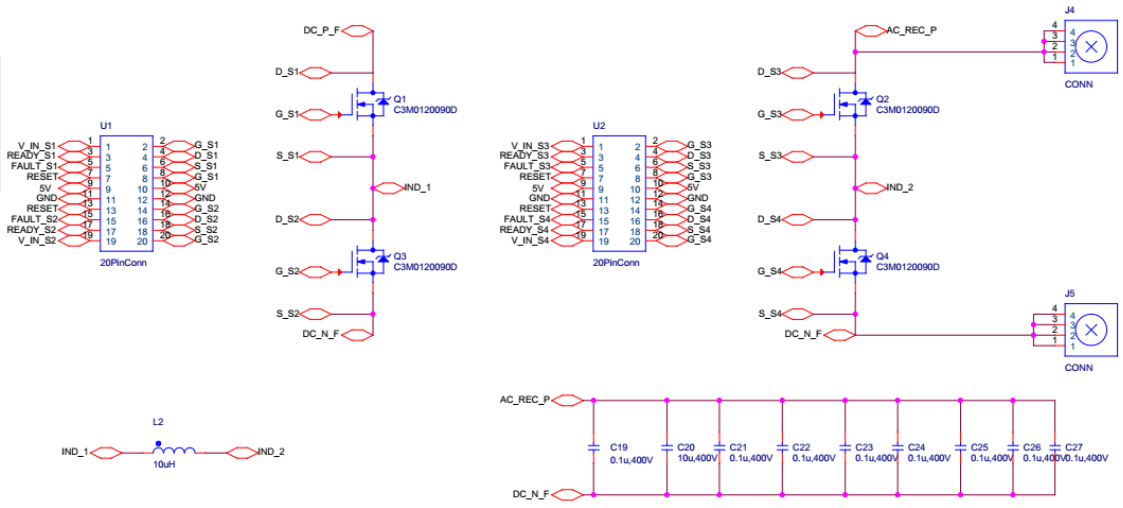

Figure 5.11 Connector connections of the bidirectional DC-DC converter and gate driver circuit

Connector connections of the H-bridge inverter circuit and gate driver circuits, which are connected to the continuation of the DC-DC converter circuit, are shown in Figure 5.12.

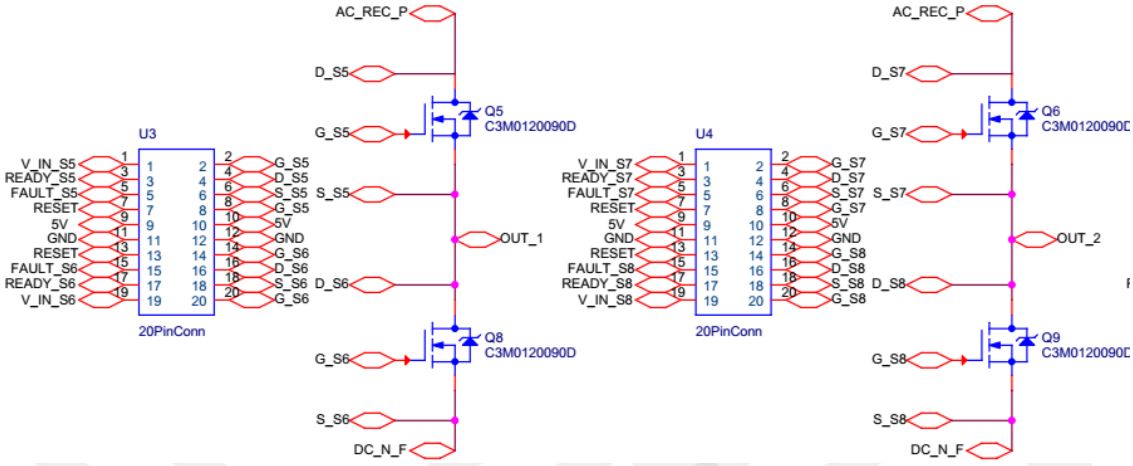

Figure 5.12 Connector connections of the H-bridge inverter and gate driver circuit

In Fig. 5.13, there are voltage divider-based circuits to measure the DC input voltage and a high-precision LV-25P voltage sensor, along with peripheral components, to measure the output voltage of the DC-DC converter. Fig. 5.14 shows current sensors to measure the inverter output current, as well as 5V and 12V power supply input connectors, cooling fan connectors, and the DSP connection connector. Through the DSP connection connector, all gate driver signals (trigger, fault, reset) and analog signals (sensor measurements) are transferred to the control circuit. In order to make the circuit suitable for future projects and have a universal structure, a current sensor is connected to each half-bridge output.

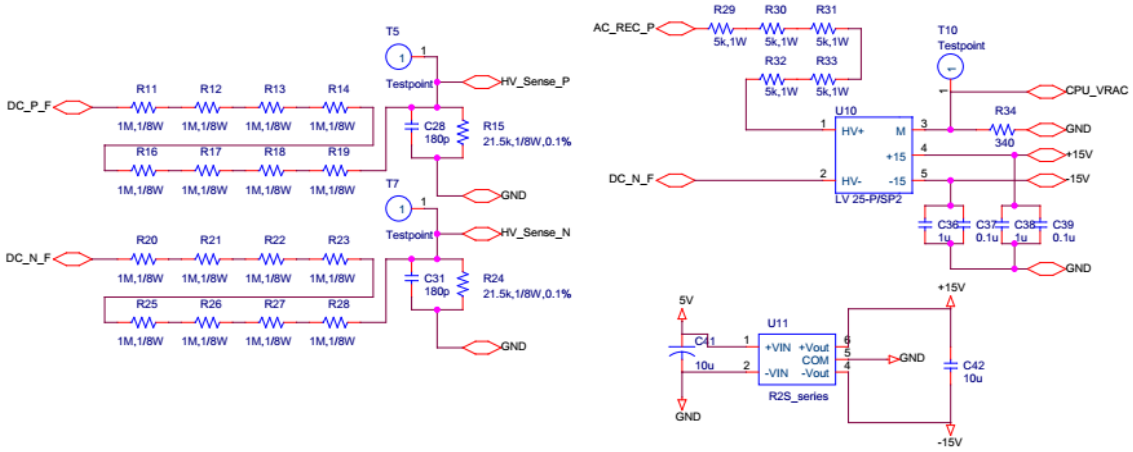

Figure 5.13 Input voltage divider, and a high-precision LV-25P voltage sensor for DC-DC converter and peripheral components

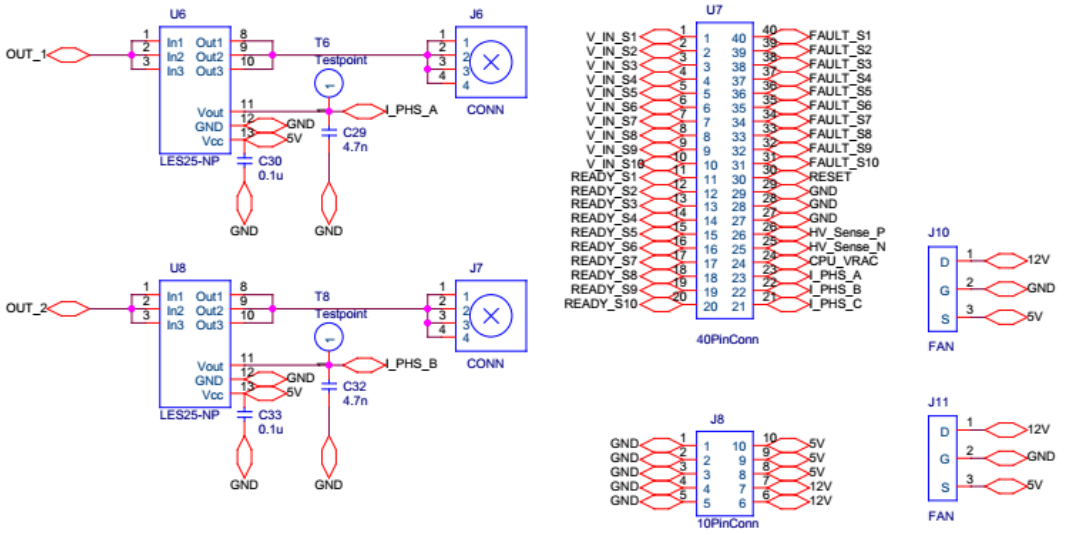

Figure 5.14 Current sensors, 5V and 12V power supply input connections, cooling fan connectors, and DSP interface connectors

At last, the gate driver circuit was developed. Within this circuit, two isolated DC-DC converters were utilized to generate isolated voltages. The gate driver section employed the Infineon 1ED020I12F2 integrated circuit, as depicted in Figure 5.15. This IC provides both optical and galvanic isolation, enabling it to supply currents of up to 3A. Moreover, it includes a short-circuit detection feature known as DeSat. In case of any errors, it generates an error signal, deactivates the outputs, and communicates the issue to the upper unit until a reset command is received.

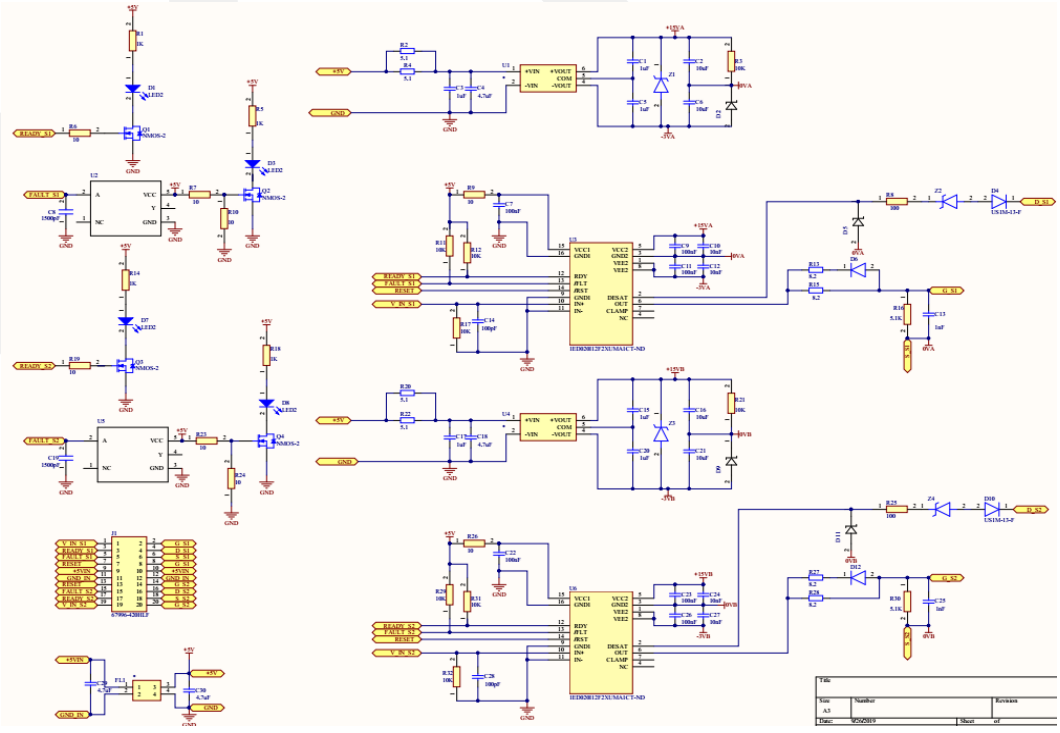

Figure 5.15 Gate driver circuit

After completing the circuit schematics, the power and control circuits were designed as four-layer layouts, while the gate driver circuit was designed as a two-layer layout. Following this, the boards were manufactured, and the components were carefully mounted to create the prototype shown in Fig. 5.16. Additionally, to mitigate fluctuations caused by the power supply, an extra capacitor is placed on the DC supply side. The FSBB DC-DC converter consists of switches on both the buck and boost sides, located at the bottom of the card, each with its gate driver on top. Additionally, there is a green box indicating the inductor placed between the buck and boost legs. Following this, the unfolding H-bridge inverter circuit is present, which switches at the zero points and generates the output by inverting the rectified sinusoidal waveform with respect to each half period.

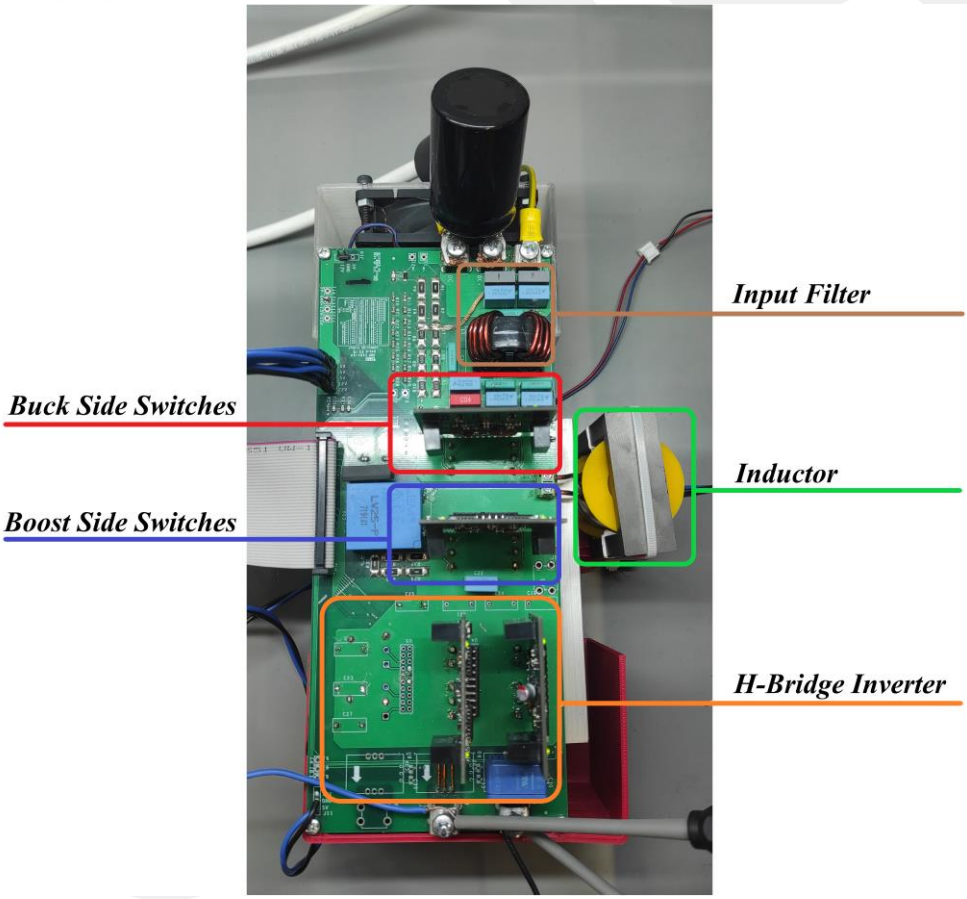

Figure 5.16 Four-switch buck-boost inverter prototype

To ensure a fair and transparent presentation of the results, it is essential to develop a converter capable of stable operation within all modulation techniques. After the meticulous completion of the hardware assembly, meeting these requirements, a Dual-Core microcontroller (MCU) [67] is selected to control the FSBB inverter. The microcontroller is mounted on a compatible docking station that establishes crucial

connections between the microcontroller and the inverter. The implementation of the control procedures for all five modulation techniques was conducted based on the design results derived from both technical analysis and simulation. For each control technique, the control signal is converted into appropriate duty cycles for both the buck and boost legs, utilizing the dual-carrier approach within the Code Composer Studio (CCS) integrated development environment. This environment includes embedded application development and debugging tools, which further enhance the efficiency and accuracy of the conversion process.

When beginning the process of creating the control algorithm, the first step involves configuring the generation of PWM duties. This is a crucial aspect in controlling the switching legs within the converter. The successful implementation of the dual-carrier approach relies on the setup of the enhanced PWM (ePWM) blocks provided by the Support Package in CCS. These blocks are responsible for configuring the event manager of the MCU to generate ePWM waveforms. Specifically, two ePWM blocks are utilized for the DC-DC part of the inverter, with one dedicated to the buck leg and the other to the boost leg. Within the MCU's ePWM unit, there are two channels: channel A manages the high-side switch of the leg, while channel B manages the low-side switch. Subsequently, the H-bridge PWM configuration is implemented in the same manner, and complementary switching is created for each leg of the DC-AC part of the inverter. After configuring the appropriate PWMs for the switches, sufficient dead time must be added to prevent shoot-through. Thus, with a switching frequency of 100 kHz, and a 100 ns dead time applied after both turning on and off of the switches, this results in a 10%-time loss during each switching period. The PWM configurations, dead time adjustments, and open-loop control algorithms for both the DC-DC and DC-AC side switches are customized to suit five different modulation techniques. By adjusting the duty cycle of the switches through the controller interface, the control side is effectively prepared.

Fig. 5.17 shows the general experimental setup with the produced prototype and controller. The setup includes measurement and power supply equipment. The numbers on the visual represent the following components: 1. Texas Instruments TMS320F28379D MCU for controlling the circuit and its docking station with communication ports. 2. FSBB DC-DC converter and H-bridge inverter prototype with integrated cooling equipment. 3. Tektronix Hall Effect current sensor to measure and display the output current on the oscilloscope. 4. Resistive load bank with adjustable

settings for desired output loads. 5. Two types of power generators: AMETEK SGX series DC power supply for supplying up to 8 kW of power and R&S®HMP4000 power supply for 12V fan and 5V card supply. 6. Powertek DP25 differential voltage probe for measuring the output voltage. Lastly, the Tektronix MDO3000 Series oscilloscope is used to display graphs and acquire data over time, allowing the measurement of voltages and currents provided by the circuit during the measurement phase.

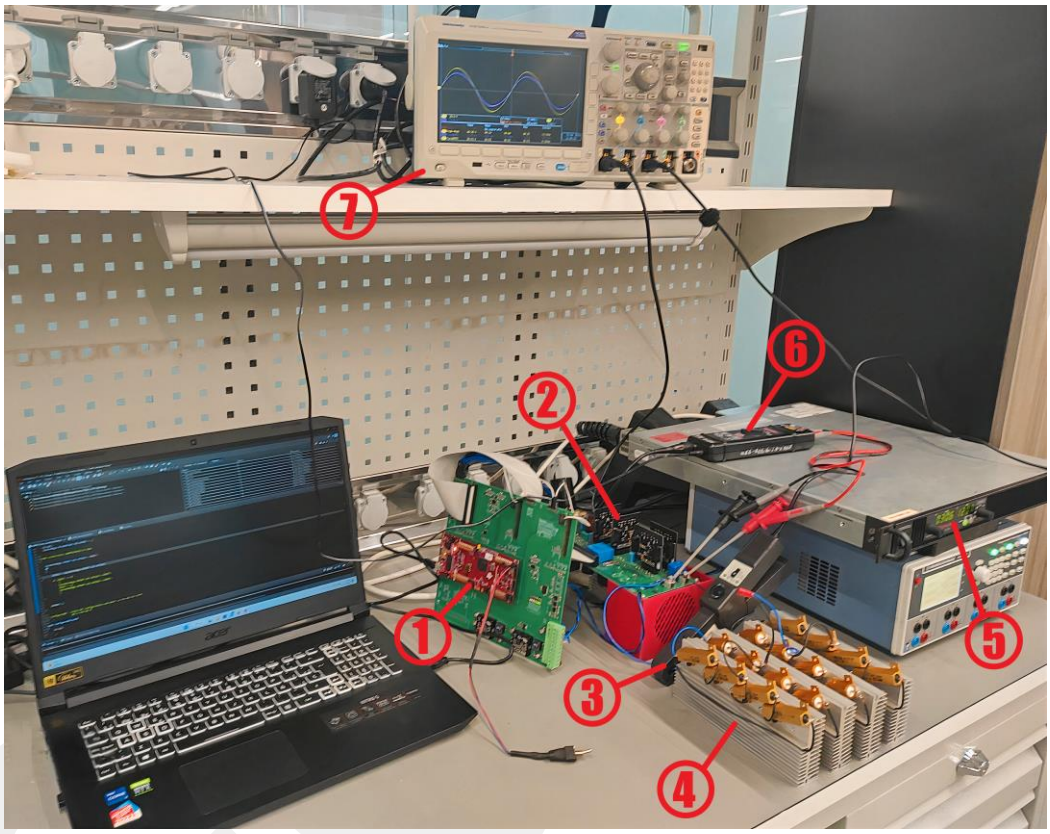

Figure 5.17 Test bench for the experiment 1) MCU with docking station 2) FSBB inverter 3) Current sensor 4) Load 5) DC generator 6) Differential voltage probe 7) Oscilloscope

To observe the behavior of all modes fairly, modulation schemes are sequentially applied, starting from the single mode without any changes in the circuit, identical to the simulation results. The inverter is operated in an open-loop principle for all modes to generate a pure 50 Hz sine wave. The output voltage and current waveforms shown in Fig. 5.18 include a zoomed mode transition when the inverter operates in single-mode, where only the buck-boost mode is active. As anticipated and mentioned earlier, the results exhibit pure sinusoidal waveforms, aligning with the expected behavior. When observing the output voltage's proximity to the input voltage, since there is no mode transition, the voltage continues to increase without any deterioration. This method is

considered the most straightforward control approach since it eliminates the dead zone and ensures a desired AC output with minimal ripple.

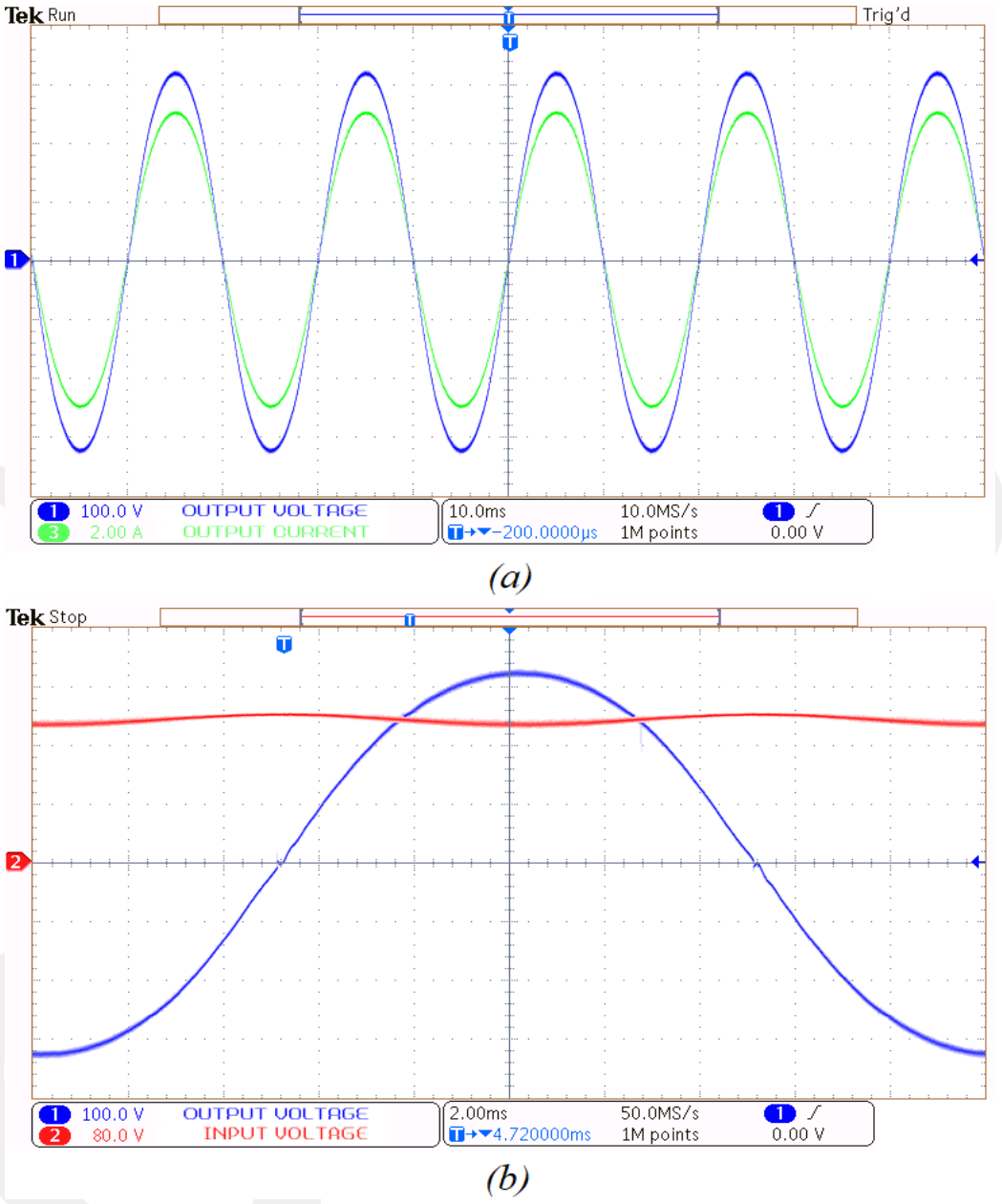

Figure 5.18 Single-mode modulation (a) The output voltage and current (b) Zoomed output and input voltage

Fig. 5.19 shows the output voltage and current waveforms with zoomed mode transition when the inverter is in two-mode, which means buck and boost operations are active. When the output voltage is below 200V, the inverter operates purely as a buck converter. Conversely, when the output voltage exceeds 200V, the inverter endeavors to operate purely as a boost converter. However, due to inherent switching limitations, the inverter cannot effectively operate in either buck or boost mode when the output voltage floats around 200V, as indicated in Fig. 5.19 (b). As the inverter reaches the maximum duty ratio of 90% in buck operation and the minimum duty ratio of 10% in boost operation, the output becomes unstable and discontinuity occurs at this point.

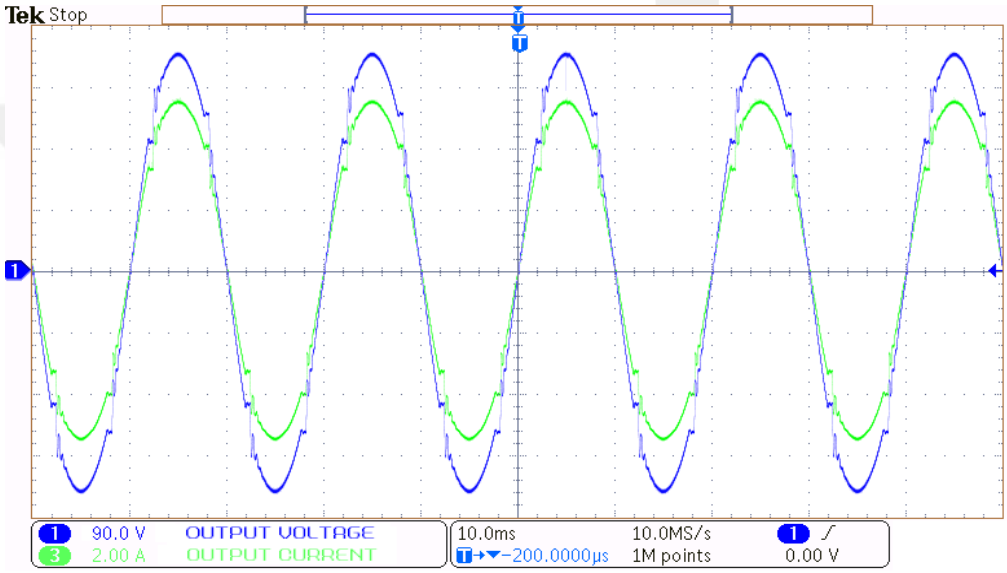

(a)

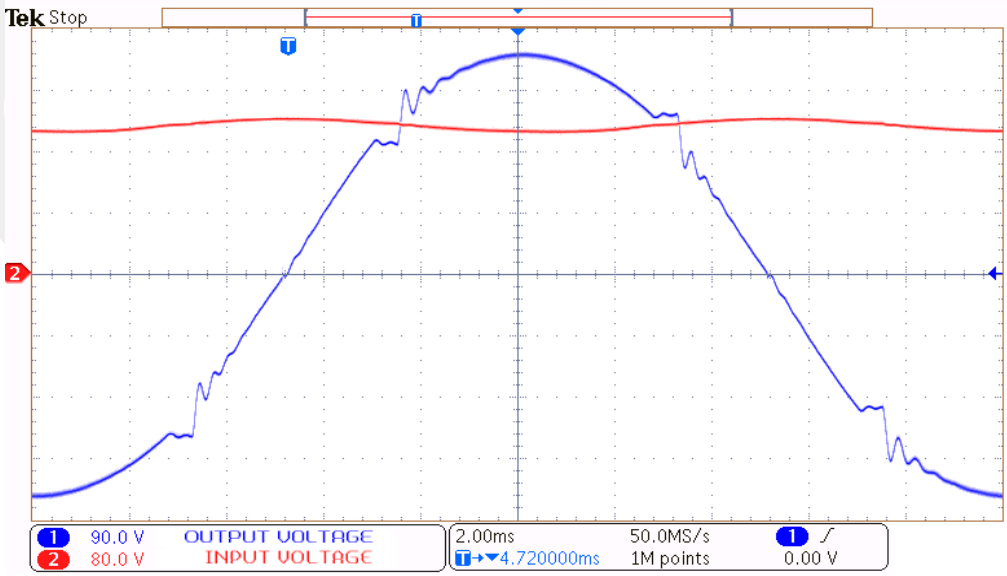

(b)

Figure 5.19 Two-mode modulation (a) The output voltage and current (b) Zoomed output and input voltage

The waveforms of the output voltage and current when the inverter is in modified two-mode, which means the buck and buck-boost operations are active as shown in Fig. 5.20. In this control scheme, the buck mode is operated up to the maximum duty ratio of 0.9, and then the buck-boost mode is switched. The stability issue, which is not typically encountered when the buck-boost mode operates independently, unexpectedly appears in this scheme. Nevertheless, it demonstrates a smoother transition compared to the two-mode operation.

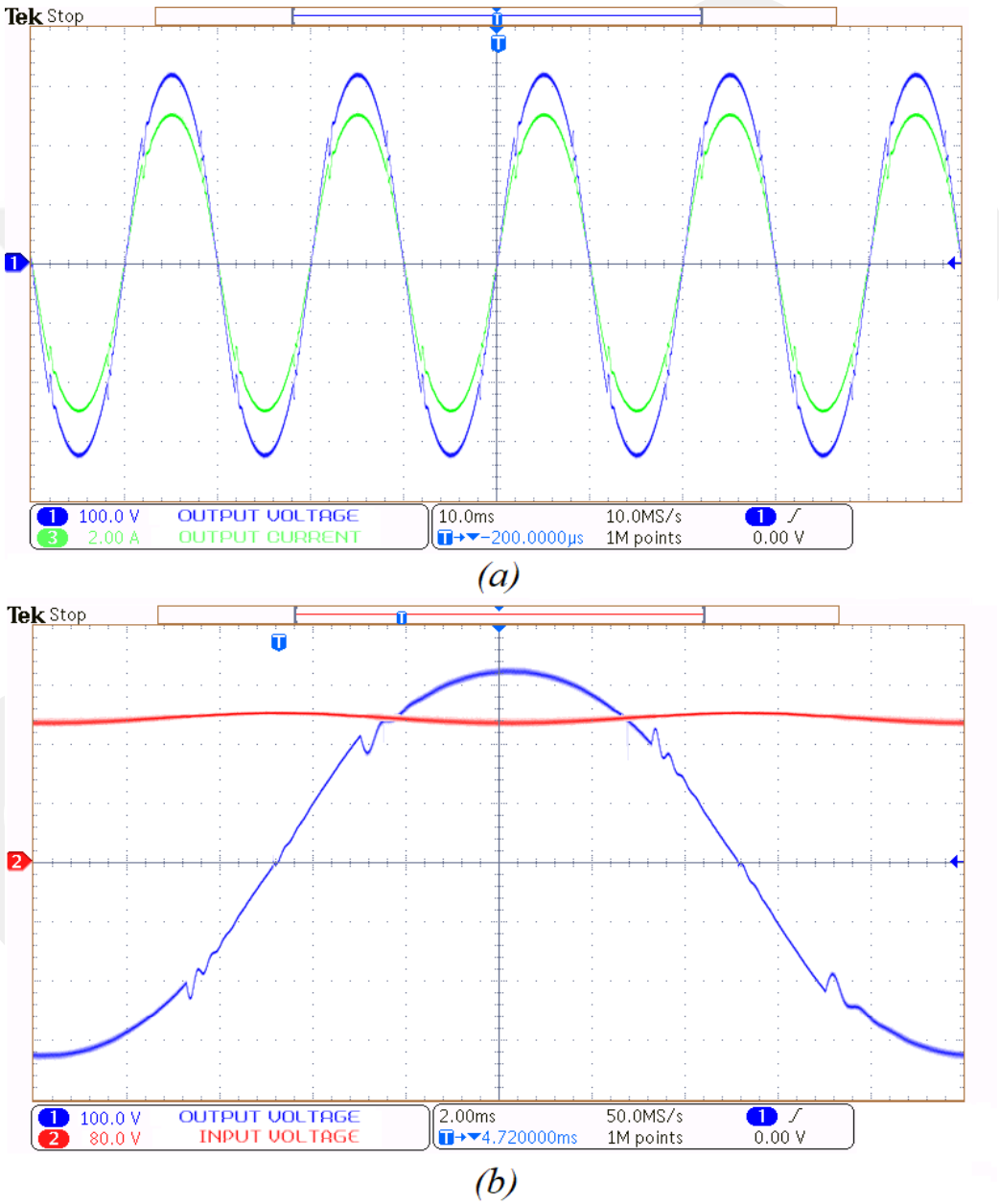

Figure 5.20 Modified two-mode modulation (a) The output voltage and current (b) Zoomed output and input voltage

Fig. 5.21 depicts the output voltage and current waveforms of the inverter operating in three modes: buck, buck-boost, and boost. During the buck-boost operation, even with slight damage, oscillations start to increase in the boost mode, leading to the emergence of harmonics. Although the lossy buck-boost operation is confined between buck and boost, the presence of subharmonics resulting from the three mode transitions negatively impacts the output voltage, leading to higher ripple and increased requirements for harmonic suppression.

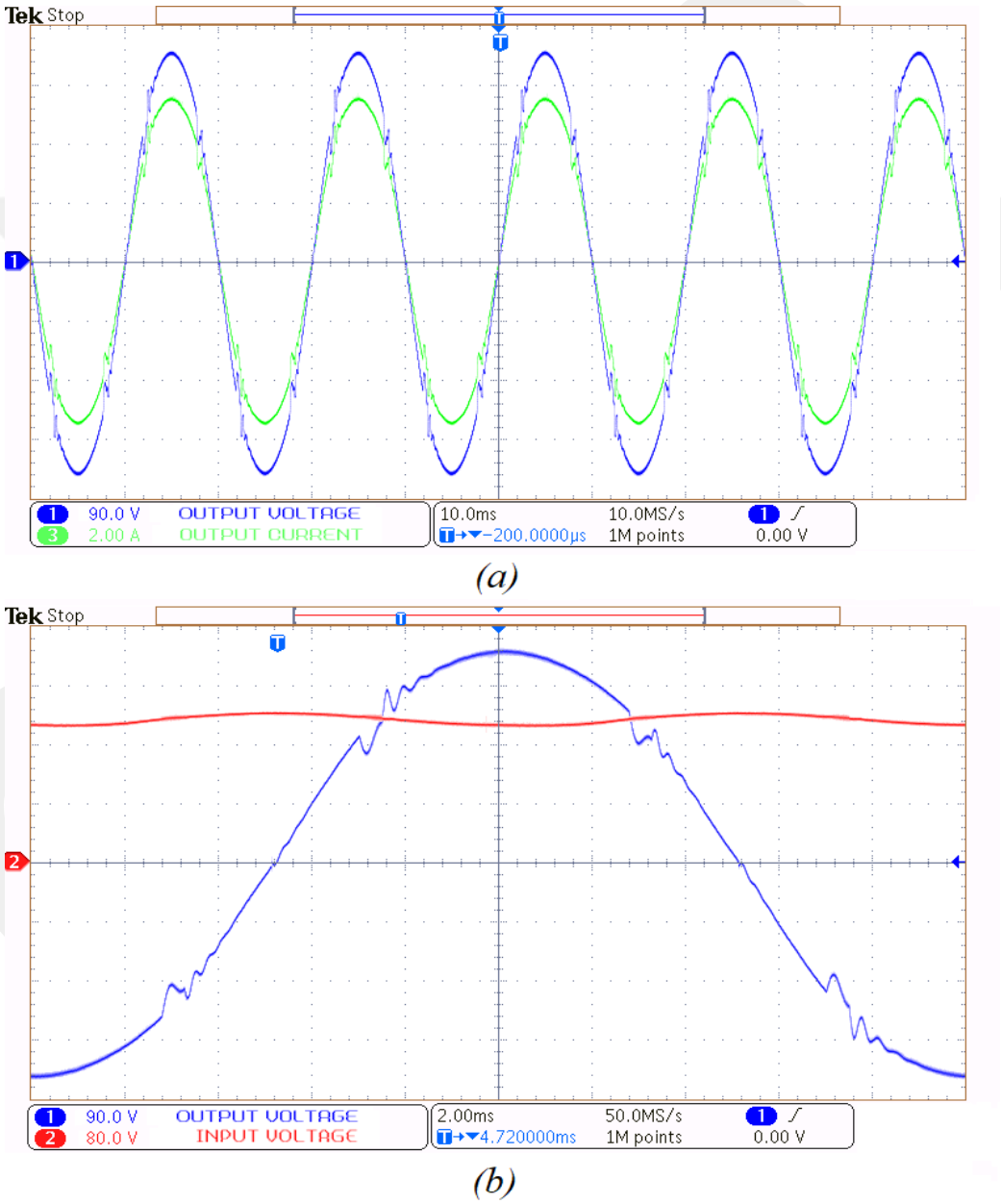

Figure 5.21Three-mode modulation (a) The output voltage and current (b) Zoomed output and input voltage

The waveforms of the output voltage and current when utilizing the inverter in buck, modified-buck, modified-boost, and boost operations are depicted in Fig. 5.22. Pure buck and boost modes are activated when the output voltage is adequately lower or higher than the input, respectively. Modified-buck and modified-boost modes come into play when the output voltage approaches the input and are situated between the buck and boost operations. By avoiding the four-switch operation in the buck-boost mode, improved power conversion efficiency can be achieved. It is evident that this approach effectively mitigates the dead zone. By enhancing transient and applying closed-loop control that minimizes errors during processing, a near-perfect sine wave can be achieved.

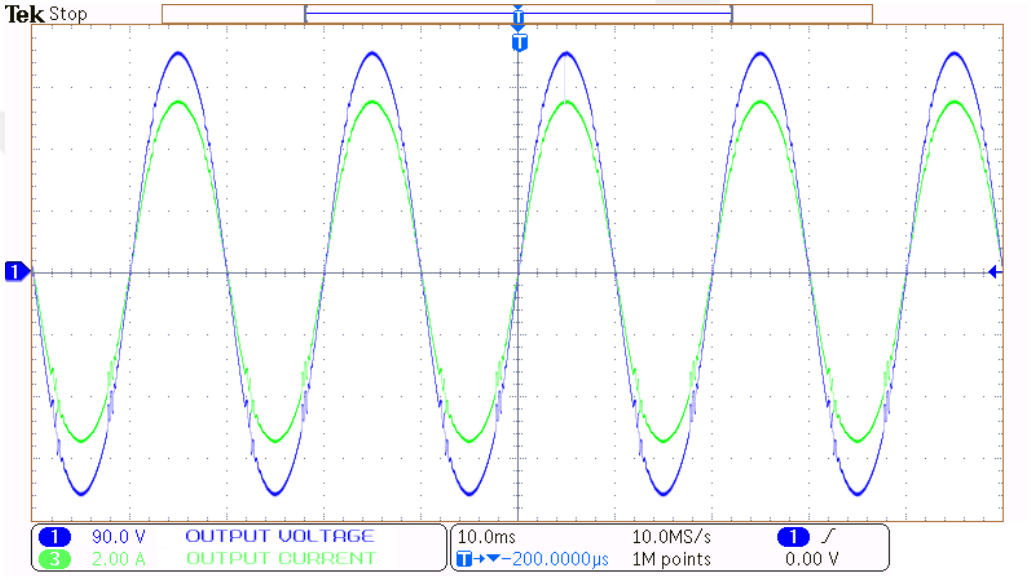

(a)

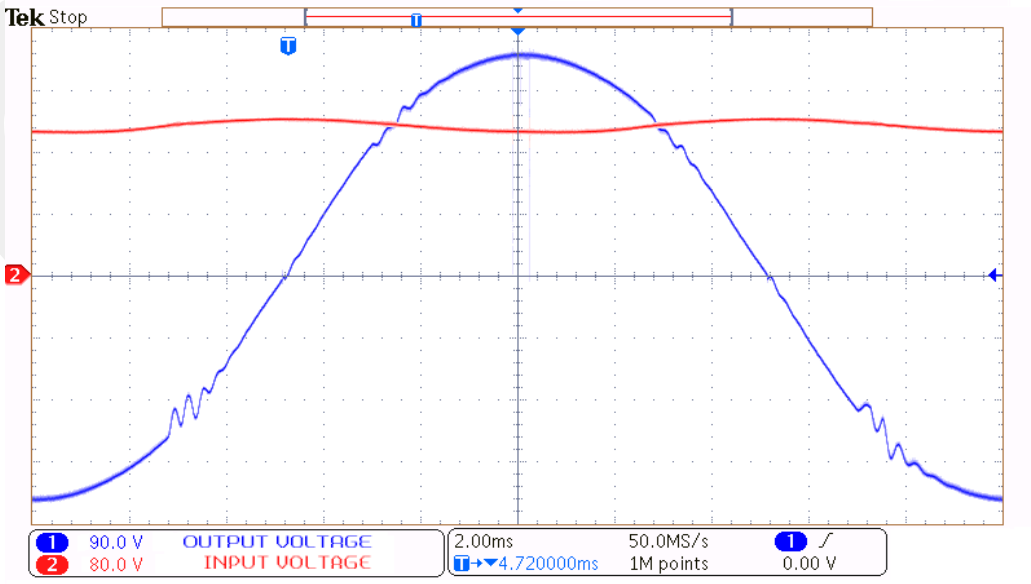

(b)

Figure 5.22 Four-mode modulation (a) The output voltage and current (b) Zoomed output and input voltage

Figure 5.23 illustrates the power conversion efficiency of five different modes under various loading conditions. The traditional two-mode modulation technique does not achieve the highest level of conversion efficiency as shown in simulation results. Additionally, it exhibits a drawback in the output voltage and current graphs due to the dead zone created during mode transitions. The single-mode technique successfully eliminates discontinuity and produces smooth signals, but its power conversion efficiency drops below 88% at full load. The modified two-mode control offers slightly better efficiency than single-mode but still lacks overall satisfaction in efficiency and switching performance. The three-mode control technique performs well with a reduction in the discontinuity region and a smoother transition. However, the overall power efficiency decreases due to the buck-boost operation used in the maximum limitation regions where switching cannot be performed. On the other hand, the four-mode modulation technique achieves the highest efficiency in the range of 95% - 96% for almost all loading scenarios.

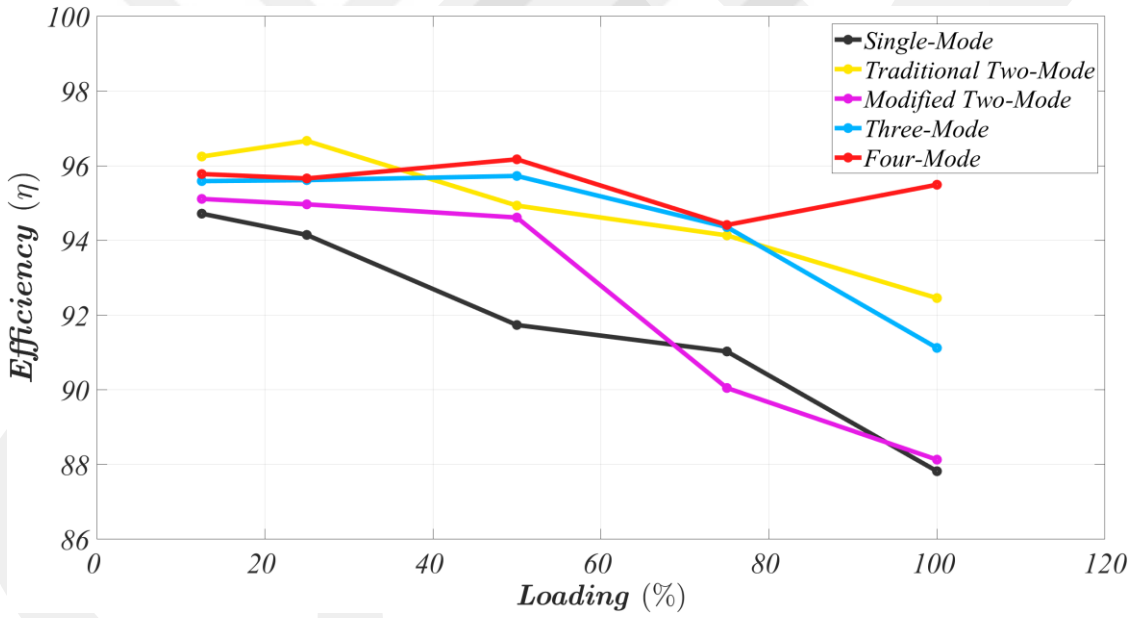

Figure 5.23 Measured efficiency comparison of five dead zone elimination techniques

Figure 5.24 depicts the Fast Fourier Transform (FFT) analysis of the output AC voltage under 100% loading. It can be observed from the figure that, regardless of how smooth the shape appears, it may still contain harmonics. In addition, Figure 5.25 compares the THD of an FSBB inverter under different load conditions, employing five different modulation schemes.

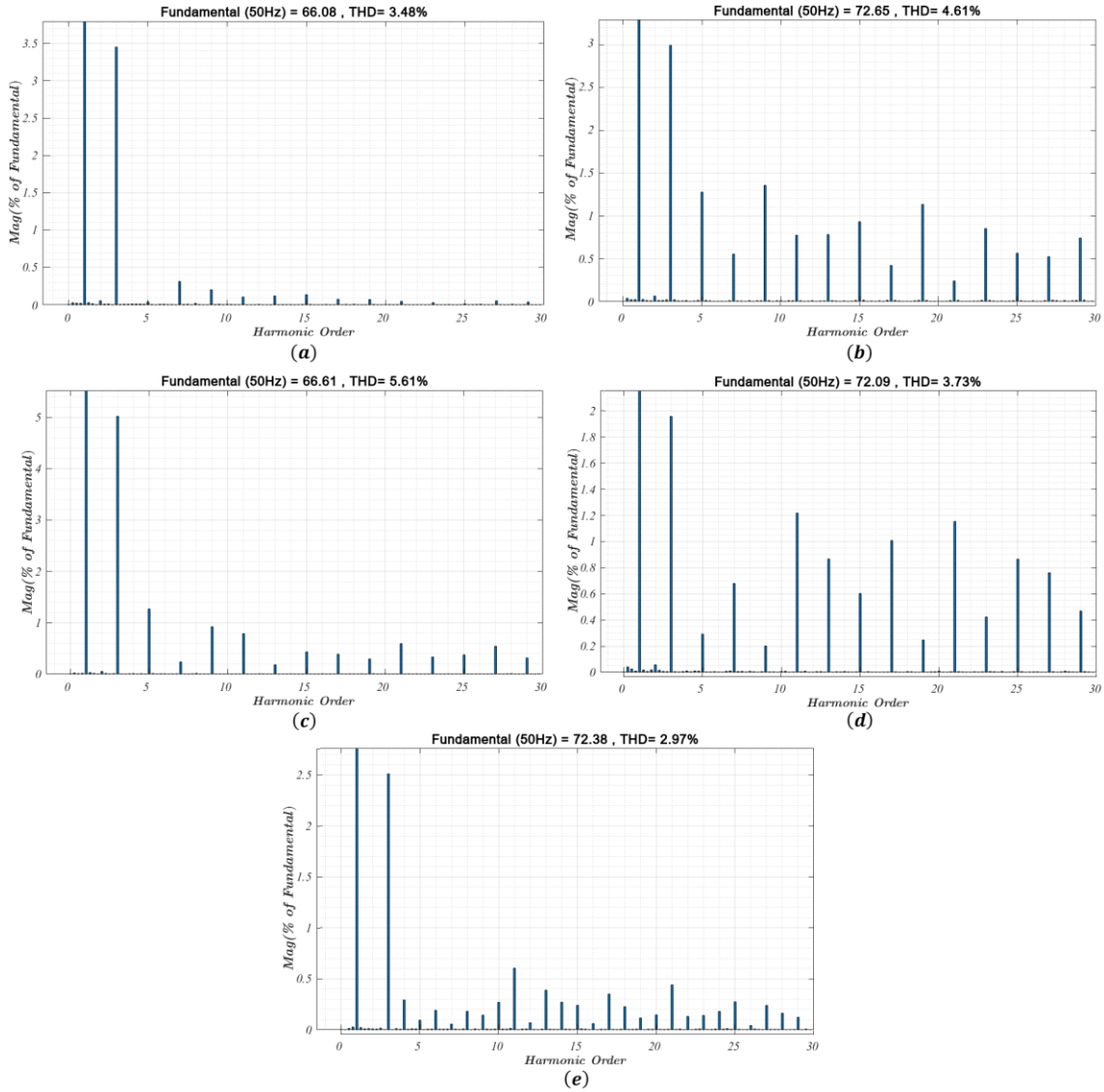

Figure 5.24 FFT analysis of output voltage under full load condition (a) Single-mode (b) Traditional Two-mode (c) Modified Two-mode (d) Three-mode (e) Four-mode

Although the single-mode visually displays a pure sinusoidal waveform, its THD reaches 3.48% due to dominant third harmonics. The two-mode modulation exhibits significant distortion above 4% as expected. Surprisingly, the modified two-mode technique becomes the worst-performing scheme, producing a distortion of over 5% at full load. The three-mode modulation generates high harmonics at low loads but performs close to single-mode distortion levels at nearly full loads. Lastly, the four-mode modulation demonstrates the best performance, achieving a THD of 2.97% under increasing loading conditions and the lowest THD of 1.2%.

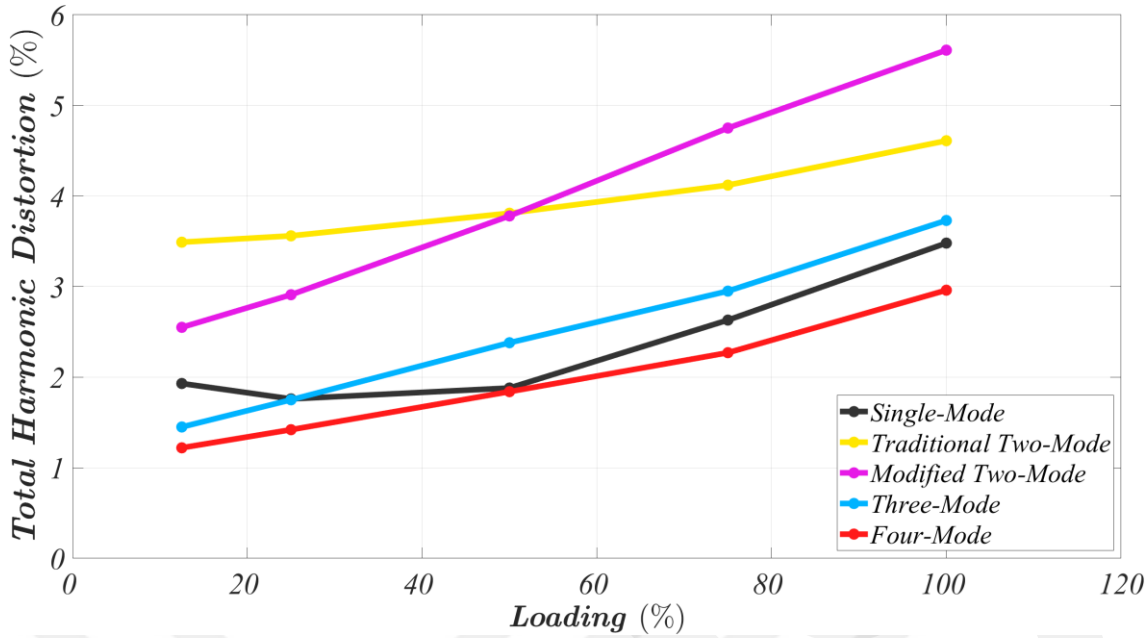

Figure 5.25 Measured THD comparison of FSBB inverter under dead zone elimination techniques

When examining the mode transitions on the graphs, it is observed that the dead zone problem, which occurs when the input voltage approaches the output voltage, has been significantly reduced, despite being controlled by open-loop control. As a result, comparisons of all general converter performance parameters are made for a four-switch buck-boost inverter under various loading conditions described in Table 5.3. The four-mode modulation technique, a dead zone elimination method, shows satisfactory efficiency and low harmonic distortion under all load conditions. In addition, while providing all these, it provides smooth mode transitions when the input and output voltages, which is its main purpose, are close to each other.

Table 5.3 Summary of results

Modulation Technique	Efficiency at 100% Loading	THD Value at 100% Loading	Dead Zone Elimination
Single-Mode	87.82%	3.48%	Yes
Traditional Two-Mode	92.46%	4.61%	No
Modified Two-Mode	88.13%	5.61%	Yes
Three-Mode	91.12%	3.73%	Yes
Four-Mode	95.49%	2.97%	Yes

5.5 Conclusions

The four-switch buck-boost inverter prototype design specifications such as input and output voltage, maximum converter power, and switching frequency are determined. According to the selection criteria and theoretical analysis for the inductor, input and output capacitor, and power MOSFETs are selected. The parameter list is included in the table and the design criteria for the FSBB inverter are presented in Section 5.2. The aforementioned single, traditional, and modified two, three, and four-mode dead zone elimination techniques simulation results are discussed with the instantaneous efficiency comparison result during the entire half period of the output signal and the THD comparison of all modulation techniques is depicted in Section 5.3. In addition, the experimental implementation of the FSBB inverter is built and the control techniques from the previous sections are applied to compare their figure of merits in Section 5.4. Additionally, the production process of the real-time model of the circuit and the names of the materials required for the measurement are explained. The performance of a four-switch buck-boost inverter was extensively compared under different loading conditions, considering all general converter performance parameters. The adopted four-mode modulation technique, aimed at eliminating the dead zone, exhibited satisfactory efficiency and minimal harmonic distortion across all load conditions. Notably, this scheme achieved its primary goal of providing smooth mode transitions when the input and output voltages were in proximity to each other. Consequently, both computer simulations and laboratory tests highlighted the outstanding performance of the four-mode modulation scheme in terms of dead zone avoidance and power conversion efficiency.

Chapter 6

Conclusions and Future Prospects

6.1 Conclusions

This thesis aims to investigate the effects of the “dead zone” in the buck-boost DC-rectified AC-AC inverter, also known as the four-switch buck-boost inverter. This inverter consists of an FSBB converter coupled with an unfolding operated H-bridge inverter. While the FSBB converters have commonly opted for power converter applications, they are not without limitations, which arise from various unavoidable disturbances and constraints. The objective is to reveal the origin of the dead zone and determine the most efficient and effective modulation scheme for completely eliminating it during the transition between the buck and boost operations. Additionally, the study aims to present an optimum control method for optimizing efficiency and minimizing distortion in current-controlled systems capable of generating reference voltages for current production through open-loop voltage control.

Chapter 2 discussed numerous existing methods related to avoiding the dead zone based on the FSBB converter application. The advantages and disadvantages of these methods were described with respect to efficiency, control complexity, and figure of merit. Among these methods, the most suitable topology was selected for use in the proposed FSBB inverter design.

Chapter 3 presented the circuit analysis and operation principle of the FSBB based inverter topology are given in order to understand and design appropriately a control system for an inverter. To comprehensively analyze the behavior of the inverter, the H-bridge part of the system which is responsible to convert DC-AC was also explained in detail, in addition to the FSBB converter analysis. At the end of this chapter, the selection of the inductor and capacitor was discussed, and the theoretical calculation of total loss for an inverter system was also presented.

Chapter 4 proposed a detailed explanation along with various methods to eliminate the origin of the dead zone, which occurs when the input and output voltages are quantitatively close to each other. Since the converter inherently allows for control in three different modes, various combinations that could provide reasonable outcomes and achieve the intended purpose were included in the comparison. In addition to getting rid of the dead zone, the inductor current behavior which encompasses current ripple and average value, is analyzed in the research, in order to decide the superiority of the modes.

Chapter 5 presented a simulation and experimental verification setup to demonstrate the result of the most suitable modulation method within the five different control schemes. This chapter aims to compare modulation schemes in terms of their superiority in effectiveness and THD levels in both a test bench and a computer environment. In the simulation results, single, two, modified two, three, and four-mode modulation techniques were adjusted according to the open-loop control principle, and the modes were executed sequentially on the inverter circuit without making any changes. According to the results, the single-mode technique exhibited the lowest THD performance at full load operation with 0.3%, closely followed by the four-mode technique with a small difference. The two-mode control showed the worst distortion performance. When it comes to efficiency, the modulation technique has been found to be effective for all load ranges, which is contrary to the THD comparison. The four-mode technique ranked second in terms of efficiency, while the single-mode modulation obtained the worst performance. In the experimental results, similar to the simulation comparison, five techniques were adjusted according to the open-loop control principle, and the modes were executed sequentially on the inverter circuit without any alterations. At full load operation, the four-mode modulation achieved the lowest THD performance with 2.96%, and it attained the highest efficiency with 95.6%. The single-mode ranked second-best in terms of THD performance, while the two-mode modulation emerged as the second-best mode in terms of efficiency. The three-mode technique performed moderately compared to the others. However, the modified two-mode could not demonstrate satisfactory performance in terms of THD and efficiency. Consequently, among the different modulation schemes, the four-mode scheme demonstrated superior performance in the elimination of the dead zones and converting power efficiently.

6.2 Societal Impact and Contribution to Global Sustainability

As the demand for renewable energy sources, such as photovoltaic, wind, and geothermal energy, continues to rise, power electronic systems have gained significant attention in various applications, including electric vehicles, renewable energy systems, and industrial automation, to name a few. However, these systems consume a substantial amount of energy, leading to high carbon emissions and posing a significant threat to the environment, especially given the depletion of energy resources. Therefore, the efficient operation of power electronic systems is crucial to ensuring sustainable development across all fields.

Specifically, inverters waste energy when converting DC power to AC power when used in renewable energy systems. When buck-boost type inverters are controlled with traditional two-mode inverter control techniques, they suffer from efficiency losses and poor transient response with discontinuity. The smooth mode transition technique in the four-switch buck-boost inverters created by adding a converter to the end provides an effective solution to address the issue which is exposed twice in each period.

The smooth mode transition technique in a four-switch buck-boost converter holds immense potential for contributing to global sustainability by increasing efficiency. The smooth mode transition technique can enable the integration of renewable energy sources into the grid, which is crucial for reducing carbon emissions and ensuring sustainable development. With the increasing use of renewable energy sources such as solar and wind, efficient and reliable power electronics systems are necessary to integrate these sources into the grid.

Furthermore, the use of the smooth mode transition technique in power electronics systems can help achieve this objective by providing efficient and reliable control of the systems. By eliminating the discontinuity and producing a pure sine signal, this technique reduces power losses with low ripple and increases the overall inverter performance. This improvement in efficiency has a direct impact on reducing carbon emissions and conserving energy resources. Furthermore, when this approach is applied to systems with other transition issues, heat loss is decreased, increasing system longevity, and lowering the need for cooling, both of which lead to additional energy savings.

In conclusion, the technique for smooth mode transition in a four-switch buck-boost converter has a substantial influence on power electronics systems and can help the world become more sustainably powered. This method offers enormous promise for tackling the problems of sustainable development by increasing the effectiveness of power electronics systems, decreasing carbon emissions, and facilitating the integration of renewable energy sources into the grid. In addition, this technique's application to the creation of inverters can boost the effectiveness and dependability of power electronics systems, contributing to a more sustainable future.

6.3 Future Prospects

Several investigation subjects for further research and examination can be identified based on the findings of this thesis.

1. Conducting component parameter design optimization for the adopted four-switch buck-boost inverter to minimize output voltage ripple while utilizing the discussed modulation schemes.
2. Investigating control algorithms such as voltage or current mode control methods, which have been studied in the literature, to improve the converter efficacy, transient response, and output voltage ripple.
3. Expansion of the dead zone analysis to include other types of power electronics converters, like dual active bridge topologies.
4. Development of a practical application of the proposed four-switch buck-boost inverter for electric vehicle applications with non-unity power factor operation.
5. Investigation of sophisticated control techniques such as adaptive or model predictive control for the proposed four-switch buck-boost inverter to further improve performance and efficiency.

BIBLIOGRAPHY

[1] IEA World Electricity Consumption, "World Electricity Consumption," . https://www.iea.org/fuels-and-technologies/electricity#data-browser (accessed Apr. 15, 2023).

[2] D. W. Hart, "Power Electronics," Pearson Education, (2010).

[3] P. Yang, J. Cao, Z. Shang, Y. Cai, and J. Xu, "Double-Line Frequency Ripple Suppression of a Quasi-Single Stage AC-DC Converter," *IEEE Trans. Circuits Syst. II Express Briefs*, vol. 67, no. 10, pp. 2074–2078 (2020).

[4] S. M. Dabour *et al.*, "Modeling and Control of Single-Stage Quadratic-Boost Split Source Inverters," *IEEE Access*, vol. 10pp. 24162–24180 (2022).

[5] S. V. Araújo, P. Zacharias, and R. Mallwitz, "Highly Efficient Single-Phase Transformerless Inverters for Grid-Connected Photovoltaic Systems," *IEEE Trans. Ind. Electron.*, vol. 57, no. 9, pp. 3118–3128 (2010).

[6] X. Guo *et al.*, "Overview of Recent Advanced Topologies for Transformerless Dual-Grounded Inverters," *IEEE Trans. Power Electron.*, vol. 37, no. 10, pp. 12679–12704 (2022).

[7] A. A. Khan *et al.*, "Single-Stage Bidirectional Buck-Boost Inverters Using a Single Inductor and Eliminating the Common-Mode Leakage Current," *IEEE Trans. Power Electron.*, vol. 35, no. 2, pp. 1269–1281 (2020).

[8] A. R. Boynuegri, "A Power Management Unit With a Polarity Changing Inverter For Fuel Cell/Ultra-Capacitor Hybrid Power Systems," *Int. J. Hydrogen Energy*, vol. 42, no. 43, pp. 26924–26932 (2017).

[9] B. Tekgun, D. Tekgun, I. Alan, and M. Badawy, "Design and Control of a Single Phase DC/Rectified AC/AC Inverter for low THD Applications," *7th Int. IEEE Conf. Renew. Energy Res. Appl. ICRERA 2018*, vol. 5pp. 424–430 (2018).

[10] Y. Chen, S. Member, Y. Liu, S. Hung, and C. Cheng, "Multi-Input Inverter for Grid-Connected Hybrid PV / Wind Power System," vol. 22, no. 3, pp. 1070–1077 (2007).

[11] B. Chandrasekar *et al.*, "Non-Isolated High-Gain Triple Port DC-DC Buck-Boost Converter with Positive Output Voltage for Photovoltaic Applications," *IEEE Access*, vol. 8pp. 113649–113666 (2020).

[12] S. M. Muyeen, R. Takahashi, T. Murata, and J. Tamura, "Integration of an Energy Capacitor System With a Variable-Speed Wind Generator," *IEEE Trans. Energy Convers.*, vol. 24, no. 3, pp. 740–749 (2009).

[13] Y. Chen and K. Smedley, "Three-Phase Boost-Type Grid-Connected Inverter," vol. 23, no. 5, pp. 2301–2309 (2008).

[14] T. Kerekes, R. Teodorescu, P. Rodríguez, G. Vázquez, and E. Aldabas, "A New High-Efficiency Single-Phase Transformerless PV Inverter Topology," *IEEE Trans. Ind. Electron.*, vol. 58, no. 1, pp. 184–191 (2011).

[15] J. Rodríguez, S. Bernet, B. Wu, J. O. Pontt, and S. Kouro, "Multilevel Voltage-Source-Converter Topologies for Industrial Medium-Voltage Drives," *IEEE Trans. Ind. Electron.*, vol. 54, no. 6, pp. 2930–2945 (2007).

[16] R. O. Cáceres and I. Barbi, "A Boost DC-AC Converter: Analysis, Design, and Experimentation," *IEEE Trans. Power Electron.*, vol. 14, no. 1, pp. 134–141 (1999).

[17] R. González, J. López, P. Sanchis, and L. Marroyo, “Transformerless Inverter For Single-Phase Photovoltaic Systems,” *IEEE Trans. Power Electron.*, vol. 22, no. 2, pp. 693–697 (2007).
[18] F. Zhang and C. Gong, “A New Control Strategy of Single-Stage Flyback Inverter,” *IEEE Trans. Ind. Electron.*, vol. 56, no. 8, pp. 3169–3173 (2009).
[19] F. Z. Peng, “Z-Source Inverter,” vol. 39, no. 2, pp. 504–510 (2003).
[20] U. A. Khan, A. A. Khan, F. Akbar, and J. W. Park, “Single-Stage Single-Phase H6 and H8 Non-Isolated Buck-Boost Photovoltaic Inverters,” *IEEE J. Emerg. Sel. Top. Power Electron.*, vol. 10, no. 4, pp. 4865–4878 (2022).
[21] M. Çelebi and I. Alan, “A Novel Approach for a Sinusoidal Output Inverter a Novel Approach for a Sinusoidal Output Inverter,” *Electr. Eng.*, vol. 92, no. 7–8, pp. 239–244 (2010).
[22] W. Kunrong, L. Fred C., and D. Wei, “A New Soft-Switched Quasi-Single-Stage (QSS) Bi-directional Inverter/charger,” *Conf. Rec. 1999 IEEE Ind. Appl. Conf. Thirty-Forth IAS Annu. Meet.*, vol. 3pp. 2031–2038 (1999).
[23] W. Wu, J. Ji, and F. Blaabjerg, “Aalborg Inverter — A New Type of ‘ Buck in Buck , Boost in Boost ’ Grid-Tied Inverter,” vol. 30, no. 9, pp. 4784–4793 (2015).
[24] O. Husev, O. Matiushkin, S. Member, D. Vinnikov, and S. Member, “Novel Family of Single-Stage Buck – Boost Inverters Based on Unfolding Circuit,” vol. 34, no. 8, pp. 7662–7676 (2019).
[25] M. Gaboriault and A. Notman, “A High Efficiency, Non-Inverting, Buck-Boost DC-DC Converter,” *Ninet. Annu. IEEE Appl. Power Electron. Conf. Expo.*, vol. 3pp. 1411–1415 (2004).
[26] A. Chakraborty, A. Khaligh, A. Emadi, and A. Pfaelzer, “Digital Combination of Buck and Boost Converters to Control a Positive Buck-Boost Converter,” *2006 37th IEEE Power Electron. Spec. Conf.*, pp. 1–6 (2006).
[27] R. Paul and D. Maksimovic, “Smooth Transition and Ripple Reduction in 4-Switch Non-Inverting Buck-Boost Power Converter for WCDMA RF Power Amplifier,” *Proc. - IEEE Int. Symp. Circuits Syst.*, pp. 3266–3269 (2008).
[28] R. Paul and D. Maksimovic, “Analysis of PWM Nonlinearity in Non-Inverting Buck-Boost Power Converters,” *PESC Rec. - IEEE Annu. Power Electron. Spec. Conf.*, vol. 3pp. 3741–3747 (2008).
[29] G. Zhang, J. Yuan, S. S. Yu, N. Zhang, Y. Wang, and Y. Zhang, “Advanced Four-Mode-Modulation-Based Four-Switch Non-Inverting Buck–Boost Converter with Extra Operation Zone,” *IET Power Electron.*, vol. 13, no. 10, pp. 2049–2059 (2020).
[30] C. Restrepo *et al.*, “Current-Mode Control of a Coupled-Inductor Buck – Boost DC – DC Switching Converter,” vol. 27, no. 5, pp. 2536–2549 (2012).
[31] R. Lin and R. Wang, “Non-inverting Buck-Boost Power-Factor-Correction Converter with Wide Input-Voltage-Range Applications,” vol. 4pp. 599–604 (2010).
[32] D. C. Jones and R. W. Erickson, “A Nonlinear State Machine For Dead Zone Avoidance And Mitigation in a Synchronous Noninverting Buck-Boost Converter,” *IEEE Trans. Power Electron.*, vol. 28, no. 1, pp. 467–480 (2013).
[33] X. E. Hong, J. F. Wu, and C. L. Wei, “98.1%-Efficiency Hysteretic-Current-Mode Noninverting Buck-Boost DC-DC Converter with Smooth Mode Transition,” *IEEE Trans. Power Electron.*, vol. 32, no. 3, pp. 2008–2017 (2017).
[34] J. You, W. Fan, N. Ghasemi, and M. Vilathgamuwa, “Modulation and Control Method for Double-Switch Buck-Boost Converter,” *IET Power Electron.*, vol. 12, no. 5, pp. 1160–1169 (2019).

[35] Y. Y. Chen, Y. C. Chang, and C. L. Wei, “Mixed-Ripple Adaptive On-Time Controlled Non-Inverting Buck-Boost DC-DC Converter with Adaptive-Window-Based Mode Selector,” *IEEE Trans. Circuits Syst. II Express Briefs*, vol. 69, no. 4, pp. 2196–2200 (2022).
[36] C. Restrepo, T. Konjedic, J. Calvente, and R. Giral, “Hysteretic Transition Method for Avoiding the Dead-Zone Effect and Subharmonics in a Noninverting Buck-Boost Converter,” *IEEE Trans. Power Electron.*, vol. 30, no. 6, pp. 3418–3430 (2015).
[37] Y. He, W. Chen, J. Deng, and M. Xu, “A Four-Phase Interleaved Four-Switch Buck-Boost Converter with Smooth Mode Transition Strategy for Fuel Cell System,” *Proc. - 2021 IEEE Sustain. Power Energy Conf. Energy Transit. Carbon Neutrality, iSPEC 2021*, pp. 3175–3181 (2021).
[38] L. Callegaro, M. Ciobotaru, D. J. Pagano, E. Turano, and J. E. Fletcher, “A Simple Smooth Transition Technique for the Noninverting Buck-Boost Converter,” *IEEE Trans. Power Electron.*, vol. 33, no. 6, pp. 4906–4915 (2018).
[39] X. Li, Y. Liu, and Y. Xue, “Four-Switch Buck-Boost Converter Based on Model Predictive Control with Smooth Mode Transition Capability,” *IEEE Trans. Ind. Electron.*, vol. 68, no. 10, pp. 9058–9069 (2021).
[40] N. Zhang, G. Zhang, and K. W. See, “Systematic Derivation of Dead-Zone Elimination Strategies for the Noninverting Synchronous Buck-Boost Converter,” *IEEE Trans. Power Electron.*, vol. 33, no. 4, pp. 3497–3508 (2018).
[41] J. Ma, M. Zhu, Y. Li, and X. Cai, “Dynamic Analysis of Multimode Buck-Boost Converter: An LPV System Model Point of View,” *IEEE Trans. Power Electron.*, vol. 36, no. 7, pp. 8539–8551 (2021).
[42] L. Jia, X. Sun, Z. Zheng, X. Ma, and L. Dai, “Multimode Smooth Switching Strategy for Eliminating the Operational Dead Zone in Noninverting Buck-Boost Converter,” *IEEE Trans. Power Electron.*, vol. 35, no. 3, pp. 3106–3113 (2020).
[43] J. Moon *et al.*, “60-V Non-Inverting Four-Mode Buck-Boost Converter with Bootstrap Sharing for Non-Switching Power Transistors,” *IEEE Access*, vol. 8pp. 208221–208231 (2020).
[44] R. W. Erickson and D. Maksimovic, “Fundamentals of Power Electronics, ” Kluwer Academic (2001).
[45] A. Nabae, I. Takahashi, and H. Akagi, “A New Neutral-Point-Clamped PWM Inverter,” *IEEE Trans. Ind. Appl.*, vol. IA-17, no. 5, pp. 518–523 (1981).
[46] M. H. Rashid, “Power Electronics Devices, Circuits & Applications” Pearson Education (2014).
[47] J. Hagedorn, “Basic Calculations of a 4 Switch Buck-Boost Power Stage (SLVA535B),” *TI Appl. Rep.*, no. July, pp. 1–13 (2018).
[48] PSIM, “Loss Calculation and Transient Analysis of SiC and GaN Devices,” *Altair PSIM Tutor.* (2022).
[49] G. Lakkas, “MOSFET Power Losses and How They Affect Power-Supply Efficiency,” *Analog Appl. J.*, no. April, pp. 22–26 (2016).
[50] D. Tekgun, B. Tekgun, and I. Alan, “A Modular Three-Phase Buck-Boost Motor Drive Topology,” *Proc. - 2020 6th Int. Conf. Electr. Power Energy Convers. Syst. EPECS 2020*, pp. 130–135 (2020).
[51] Y. J. Lee, A. Khaligh, and A. Emadi, “A Compensation Technique for Smooth Transitions in a Noninverting Buck-Boost Converter,” *IEEE Trans. Power Electron.*, vol. 24, no. 4, pp. 1002–1015 (2009).

[52] B. Hwang, B. Sheen, J. Chen, Y. Hwang, and C. Yu, “A Low-Voltage Positive Buck-Boost Converter Using Average-Current-Controlled Techniques,” pp. 23–26 (2012).
[53] R. Ridley and S. Kern, “Analysis and Design of a Wide Input Range Power Factor Correction Circuit for Three-Phase Applications,” pp. 299–305 (1993).
[54] Y. J. Lee, A. Khaligh, A. Chakraborty, and A. Emadi, “Digital Combination of Buck and Boost Converters to Control a Positive Buck-Boost Converter and Improve the Output Transients,” *IEEE Trans. Power Electron.*, vol. 24, no. 5, pp. 1267–1279 (2009).
[55] Q. Ullah, X. Wu, and U. Saleem, “Current Controlled Robust Four-Switch Buck-Boost DC-DC Converter,” *2021 Int. Conf. Comput. Electron. Electr. Eng. ICE Cube 2021 - Proc.*, pp. 1–6 (2021).
[56] H. B. B. Converter, P. Huang, S. Member, W. Wu, S. Member, and H. Ho, “Hybrid Buck – Boost Feedforward and Reduced Average Inductor Current Techniques in Fast Line,” vol. 25, no. 3, pp. 719–730 (2010).
[57] Y. Ma, S. Wang, S. Zhang, and X. Fan, “An Automatic Peak-Valley Current Mode Step-Up / Step-Down DC-DC Converter With Smooth Transition,” pp. 1–4 (2013).
[58] N. Zhang, S. Batternally, K. C. Lim, K. W. See, and F. Han, “Analysis of the non-inverting buck-boost converter with four-mode control method,” *Proc. IECON 2017 - 43rd Annu. Conf. IEEE Ind. Electron. Soc.*, pp. 876–881 (2017).
[59] N. Zhang, “On the Improvement of Boost and Buck-Boost Converters for Battery Applications”, Doctor of Philosophy thesis, Institute for Superconducting and Electronic Materials, University of Wollongong (2017).
[60] J. Fang, X. Ruan, X. Huang, R. Dong, X. Wu, and J. Lan, “A PWM Plus Phase-Shift Control for Four-Switch Buck-Boost Converter to Achieve ZVS in Full Input Voltage and Load Range,” *IEEE Trans. Ind. Electron.*, vol. 69, no. 12, pp. 12698–12709 (2022).
[61] Y. Wang, J. Lan, X. Huang, T. Fang, X. Ruan, and M. Dong, “An Improved Single-mode Control Strategy Based on Four-switch Buck-Boost Converter,” *Conf. Proc. - IEEE Appl. Power Electron. Conf. Expo. - APEC*, pp. 320–325 (2020).
[62] Y. Tsai, Y. Tsai, C. Tsai, and C. Tsai, “Digital Noninverting-Buck – Boost Converter With Enhanced Duty-Cycle-Overlap Control,” vol. 64, no. 1, pp. 41–45 (2017).
[63] A. Hilal and B. Cougo, “Optimal Inductor Design and Material Selection for High Power Density Inverters Used in Aircraft Applications,” pp. 0–5 (2016).
[64] J. Arrigo, “Input and Output Capacitor Selection,” *TI Appl. Rep.*, pp. 1–11 (2006).
[65] Toshiba Electronic Devices & Storage Corporation, “Power MOSFET Selecting MOSFFETs and Consideration for Circuit Design,” *Appl. Note*, pp. 1–18 (2018).
[66] PSIM, “IGBT and MOSFET Loss Calculation in the Thermal Module,” *Altair PSIM Tutor.* (2022).
[67] Texas Instruments, “TMS320F2837xD Dual-Core Delfino Microcontrollers Data Sheet SPRS880O,” *Dallas, TX, USA.* (2021).

CURRICULUM VITAE

2014 – 2019	B.Sc., Electrical Engineering Yıldız Technical University, İstanbul
2020 – Present	M.Sc., Electrical and Computer Engineering Abdullah Gul University, Kayseri
2021-06 – 2021-10	Electric-Electronics Engineer Kayseri Ulaşım A.Ş., Kayseri
2021-11 – Present	Research Assistant Abdullah Gul University, Kayseri